



A groundwater-flow model and effective nitrate calculator for Waupaca, Wisconsin

Technical Report 007 • April 5, 2022



 **Wisconsin Geological and Natural History Survey**
DIVISION OF EXTENSION
UNIVERSITY OF WISCONSIN-MADISON

Stephanie L. DeVries
University of Tennessee at Chattanooga

Kenneth R. Bradbury
Wisconsin Geological and Natural History Survey, Division of Extension,
University of Wisconsin-Madison

Michael Cardiff
University of Wisconsin-Madison

Suggested citation:

DeVries, S.L., Bradbury, K.R., Cardiff, M., 2022, A groundwater-flow model and effective nitrate calculator for Waupaca, Wisconsin: Wisconsin Geological and Natural History Survey Technical Report 007, 88 p., <https://doi.org/10.54915/xdis1726>.



**Wisconsin Geological
and Natural History Survey**
DIVISION OF EXTENSION
UNIVERSITY OF WISCONSIN-MADISON

3817 Mineral Point Road ■ Madison, Wisconsin 53705-5100
608.263.7389 ■ www.WisconsinGeologicalSurvey.org
Kenneth R. Bradbury, Director and State Geologist

ISSN: 2159-9351

Photo credits

Front: Monitoring well 8, Stephanie DeVries
All other photos by Stephanie DeVries

Acknowledgments

We thank the following: Bruce Rheineck and Brian Austin (Wisconsin Department of Natural Resources) for suggesting this project and coordinating stakeholders; Justin Berrens (Director of Public Works, City of Waupaca, Wisc.) for historical water-quality and well-pumping data; Dr. Dave Hart, Mike Parsen, and Pete Chase (Wisconsin Geological and Natural History Survey) for advice and training needed to complete field activities; Steve Mael (Wisconsin Geological and Natural History Survey) for technical assistance with ArcMap; Paul Juckem (U.S. Geological Survey) for comments on the GFLOW and MODFLOW models described in this report and for extracting the boundary-flow data from the GFLOW model; and the peer reviewers for the constructive feedback they provided.

Contents

Executive summary	1	Section 2:		Estimating nitrate concentrations	
Introduction	2	Land cover and water quality	30	in high-capacity wells	56
Motivation for study	2	Objectives	30	Results	57
Background	2	Land cover	30	Monitoring-well approach	59
Purpose and goals	4	Water use	30	Land-cover approach	59
Study approach	4	Water quality	30	Application of the model	60
Model domain	5	Monitoring wells	33	Evaluating the effects of a	
Section 1:		Study wells	38	concentrated source of nitrates	60
Hydrogeologic setting	6	Section 3:		Evaluating the effects of	
Objectives	6	Groundwater-flow model	41	residential septic systems	60
Well construction reports	6	Objectives	41	Evaluating the effects of crops	60
Surficial geology	6	Simulation approaches	41	Evaluating the effect of pumping	
Bedrock geology	10	GFLOW model	41	rates	61
Estimates of depth to bedrock		MODFLOW	45	Model limitations	62
from well construction reports	10	Model grid	45	Nitrate-loading estimates	62
Estimates of depth to bedrock		Boundary conditions	45	Recharge estimates in the	
using passive-seismic analysis	10	Stratigraphic layer elevation		effective nitrate calculator	63
Interpolation of		data	45	Irrigation impacts	63
bedrock-elevation surface	10	Surface-water network	45	Summary	64
Surface hydrogeology	10	Recharge	45	Supplemental material	64
Surface-water features	14	Groundwater withdrawals	45	References	65
Streamflow measurements	14	Head calibration targets	47	Appendix A:	
Groundwater hydrogeology	15	Streamflow calibration targets	47	Water-table measurements	68
Monitoring wells and		Hydraulic conductivity	47	Appendix B:	
piezometers	15	Particle tracking	48	Historical land-cover maps	73
Water-table elevation	19	Section 4: Effective nitrate		Appendix C:	
Hydraulic conductivity	23	calculator	52	Streamflow data	83
Results	24	Overview	52	Appendix D:	
Hydrostratigraphy	24	General approach	52	Input data for monitoring-well	
Climate and recharge	26	Estimating nitrate concentrations in		method	84
Soil-water-balance model	27	recharge (1994–2018)	52	Appendix E:	
		Monitoring-well approach	54	Input data for land-cover method	85
		Land-use approach	55		

Figures

1. Study area location near Waupaca, Wisconsin 3
2. Historical map of water-table elevation and groundwater-flow direction . . 5
3. Locations of wells with well construction reports 7
4. Surface elevation of study area . . . 8
5. Generalized surficial geology 9
6. Bedrock geology of study area . . . 11
7. Point data used to interpolate elevation of bedrock and water-table surfaces 12
8. Elevation of bedrock surface 13
9. Watersheds within the model domain 14
10. Elevation in the model domain . . . 15
11. Major surface-water features 16
12. Thickness of unconsolidated sediments 17
13. Municipal, nested monitoring, and water-table wells 18
14. Water-table elevation estimated from well construction reports 19
15. Water-table elevation surface estimated from monitoring wells. . 20
16. Weekly average head at monitoring wells from July 2018 to June 2019 . 21
17. Water-table elevation, snowpack, and daily precipitation at monitoring wells from March to May, 2019 22
18. Water-table elevation and snowpack at monitoring wells in March, 2019 23
19. Hydraulic conductivity estimates from well tests 24
20. Lithologic maps from smoothed Thiessen polygons 27
21. Estimated recharge potential for 2018 29
22. Land cover in 2018 31
23. Land parcels of interest with respect to elevated nitrate 32
24. Observed nitrate in monitoring wells MW 1–MW 4 from 1993 to 2018 . . 34
25. Observed nitrate in monitoring wells MW 5–MW 8 from 1993 to 2018 . . 35

26. Schematic of groundwater-recharge capture zones for monitoring wells MW 1A and MW 1B 36
27. Schematic of groundwater-recharge capture zones for monitoring wells MW 8A and MW 8B 37
28. Nitrate in study well #5 from 1993 to 2019 38
29. Nitrate in study well #6 from 1993 to 2019 39
30. Seasonal trends of nitrate in study well #5 from 1993 to 2019. . 40
31. Seasonal trends of nitrate in study well #6 from 1993 to 2019. 40
32. Analytic elements included in the GFLOW model 42
33. Near-field area in the GFLOW model 43
34. GFLOW model results showing direction of groundwater flow . . 44
35. Streams, lakes, drains, and wells included in the MODFLOW simulation 46
36. Hydraulic conductivity values from PEST parameterization and pilot points 48
37. Calibration data for the MODFLOW simulation 49
38. Calibration data corresponding to streamflow targets 49
39. Example of starting points corresponding to 25-year capture zones 50
40. Example of time-of-travel capture zones 51
41. Time-of-travel capture zones delineated from steady-state MODFLOW models from 2014 to 2019 53
42. Conceptual flow of groundwater recharge and its age distribution at a pumping well in 2018. 54
43. Land-cover data from 2017 used to calculate nitrate-loading rate for land parcels of interest. 57
44. Effective nitrate calculator results for study well #5 from 2014 to 2019. . 59
45. Effective nitrate calculator results for study well #6 from 2014 to 2019. . 59

46. Land-cover-based effective nitrate calculator results for study well #5 by crop type on parcel 1 from 2014 to 2019 60
47. Land-cover-based effective nitrate calculator results as a function of the percentage of a well’s capture zone that is actively cultivated . . 61
48. Percentage of study well #5’s capture zone under cultivation versus its pumping rate. 61
49. Percentage of study well #6’s capture zone under cultivation versus its pumping rate. 62
50. Pumping rate of study well #6 versus the percentage of its capture zone within parcel 2. 62

Tables

1. City of Waupaca’s municipal wells . . 2
2. Streamflow measurements from 2018 14
3. Observed head values in monitoring wells from March 2019 23
4. Horizontal hydraulic conductivity measurements 23
5. Hydraulic conductivity measurements by test type 24
6. Monitoring well characteristics . . 25
7. Sediment types and groups used to model hydraulic conductivity zones 26
8. Mean potential recharge estimated by soil-water-balance model for 2011 to 2018 28
9. High-capacity-well withdrawals from 2013 to 2018 33
10. Values used for PEST optimization of hydraulic conductivity 47
11. Average nitrate concentrations in soil leachate under different land covers. 55
12. Sample calculation of area-weighted nitrate concentrations for parcel 1 in 2018 56
13. Sample calculation of effective nitrate concentration in study well #5 in 2019 58
14. Recharge for full capture zones compared to well discharge in study wells #5 and #6 from 2014 to 2019 63

Executive summary

This report investigates the potential causes of and solutions for rising levels of dissolved nitrate ($\text{NO}_3\text{-N}$, also known as nitrate-nitrogen) in two municipal wells serving the City of Waupaca, Wisc. Waupaca (population 6,069) is located within the Central Sands region of Wisconsin, a largely agricultural area served by a shallow sand-and-gravel aquifer. Groundwater extracted from a network of seven high-capacity municipal wells provides 100 percent of the city's municipal water supply for domestic, commercial, and public use. Due to their high productivity, the city relies heavily upon two wells located south of the city limits (municipal wells #5 and #6). Historically, water pumped from these two wells accounted for 40 to 60 percent of the city's total municipal water use. In recent years, an increase in nitrate concentrations in these wells has raised concerns that changing land- and water-use patterns may be negatively impacting groundwater quality and could potentially exceed the water-quality standard for nitrate in drinking water.

In 2018, the City of Waupaca, the Wisconsin Department of Natural Resources, and the Wisconsin Geological and Natural History Survey initiated a study designed to better understand the local groundwater system and to examine the potential influence of land and water management on groundwater quality. A groundwater-flow model developed as part of this study was used to delineate well capture zones and to create an effective nitrate calculator that estimates the impacts of land cover and groundwater-extraction rates on nitrate concentrations in municipal well water. The four primary components of this study correspond to the sections in this report.

1. **Hydrogeologic setting.** Inventory and interpretation of existing and newly obtained geologic data in the model domain assembled into a spatial database. Results include the distribution of physical and hydraulic aquifer properties.
2. **Land cover and water quality.** Inventory and interpretation of existing and newly obtained land-cover, water-use, and water-quality data.
3. **Groundwater-flow model.** Construction of a groundwater-flow model, which is used in conjunction with MODPATH particle-tracking models to delineate the capture zone for wells inside the model domain.
4. **Effective nitrogen calculator.** Construction of a tool that uses land- and water-use data in conjunction with well capture zones to model and predict the effective nitrate concentration at the study wells.

Hydrogeologic data sources included well construction reports, high-capacity-well pumping rates, groundwater-level measurements, slug tests, well pumping tests, and passive-seismic measurements of depth to bedrock, all assembled into a geodatabase. These data were analyzed to produce maps of bedrock elevation, depth to bedrock, saturated aquifer thickness, and estimates of hydraulic conductivity. The data are consistent with previous studies of the region, which show that the surficial aquifer consists of unlithified glacial sediments that overlie Precambrian crystalline bedrock. The spatial analysis suggests that the surficial sand-and-gravel deposits form a shallow (60–275 feet thick) but highly productive aquifer. This shallow aquifer is referred to as the “glacial aquifer” in the remainder of this report. The horizontal-hydraulic-conductivity estimates for this aquifer ranged from 0.08 to 1,432 feet per day and have a mean



of 68 feet per day. The shallow aquifer supports high-capacity wells at yields as high as 2,200 gallons per minute.

The techniques used to develop the groundwater-flow model presented in this report may help guide the design of future well-head-protection studies in hydrogeologically similar areas of Wisconsin by providing recommendations for collecting data, establishing boundary conditions, and representing heterogeneous aquifer properties. The effective nitrate calculator presented in this report may apply to any hydrogeologically similar region in which the area of the capture zone is known and can be subdivided into discrete land-cover parcels. The results of the inventory, modeling, and analysis described in this report are available in an electronic database for public use (see “Supplemental material”).

Introduction

Motivation for study

Nonpoint-source nitrogen (N) pollution is a pervasive environmental health issue. A combination of well-draining sandy soils, a humid climate, and irrigated agriculture renders many parts of the north-central United States, including Wisconsin, especially vulnerable to dissolved nitrate ($\text{NO}_3\text{-N}$, also known as nitrate-nitrogen) contamination of groundwater. In some watersheds, nitrate may be appreciably attenuated by denitrification, a microbial process that reduces nitrate to inert nitrogen gas (N_2), which is then diffused to the atmosphere. However, evidence suggests that denitrification in shallow, well-oxygenated aquifers—such as the one underlying Wisconsin’s Central Sands region—is limited by low concentrations of dissolved carbon (Kraft and others, 1999). Under these conditions, nitrate may persist indefinitely, penetrate deep aquifers, and migrate farther from its original source areas (Kraft and others, 2008), where it has the potential to impact drinking-water supplies.

The U.S. Environmental Protection Agency recognizes several human health risks linked to acute nitrate toxicity, including methemoglobinemia (blue-baby syndrome), colon cancer, and reproductive disorders (Ward and others, 2018). To prevent negative health outcomes, nitrate in municipal drinking water is regulated, and its maximum contaminant level is 10 milligrams per liter (mg/L). Surveys conducted in 1999 and 2012 indicated that many of Wisconsin’s public-supply wells are at risk of exceeding this limit; others already have. In 1999, 14 systems had raw water samples that exceeded the maximum contaminant level; by 2012, the number of impacted systems had increased more than three-fold to 47 (Wisconsin Groundwater Coordinating Council, 2018). Many other municipalities where drinking-water supplies are still below the maximum contaminant level have reported rises in nitrate. The need to develop tools that predict nitrate transport and well contamination arose during coordinated efforts to protect public-supply wells in shallow, sandy aquifers from nitrate contamination. This study addresses this need for the City of Waupaca, Wisc., and the tools developed can be adapted for application to other municipal wells supplied by shallow, sandy aquifers.

Background

The City of Waupaca is in southwestern Waupaca County, Wisc., within a region known as the Central Sands. The Central Sands (fig. 1, inset) spans several counties in central Wisconsin and is characterized by surficial deposits of sand and gravel more than 50 ft deep (Wisconsin Department of Natural Resources, 2018). Throughout the Central Sands, sandy outwash and lake sediment form an important and highly productive shallow aquifer. In the area of interest near Waupaca, the aquifer averages 100 ft in thickness and supplies water for irrigated agriculture, industry, and domestic use (municipal and private wells). The City of Waupaca’s domestic supply system consists of seven high-capacity wells (table 1).

Five of the municipal wells are located within the principal municipal boundaries. Two of these wells, municipal wells #5 and #6 (defined for this report as study wells #5 and #6), are located outside of the municipal boundaries, east of the Crystal River along County Highway E (fig. 1). The two study wells, constructed in 1970 and 1980, respectively, contribute as much as 60 percent of the City of Waupaca’s domestic water supply. According to water-use data collected by the Wisconsin Department

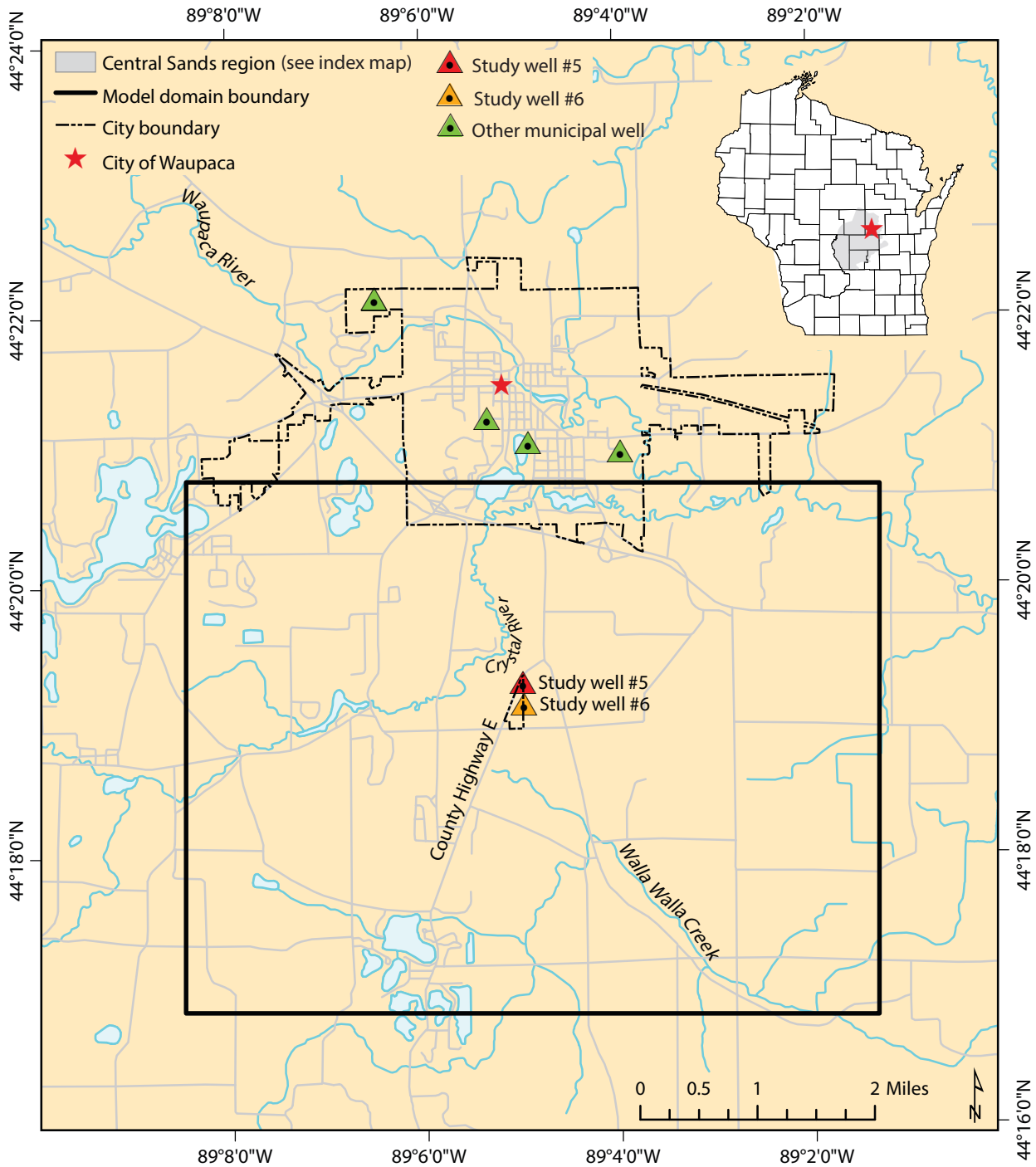
Table 1. The City of Waupaca’s municipal wells.

Unique well number	High-capacity well number	Local (city) well number
BH466	88257	2
BH477	88258	3
BH468	88259	4
*BH469	88260	5
*BH470	88261	6
†ND302	2327	7
†NG621	2328	8

*Study wells for this report. BH469 is study well #5 and BH470 is study well #6.

†Wells ND302 and NG621 overlap and appear as a single well on figures.

Figure 1. Location of the study area near Waupaca, Wisc. The model domain includes municipal wells #5 and #6, known in this report as study wells #5 and #6. The remaining five municipal wells are outside the boundaries of the model domain; these include two wells located inside the northwestern corner of the city boundary that overlap at the scale of this map. Inset map shows the extent of the Central Sands region (gray) and location of the City of Waupaca (star).



Political boundaries from Wisconsin Department of Natural Resources, 2011. Roads from U.S. Census Bureau, 2015. Hydrography from U.S. Geological Survey National Hydrography Dataset, 2016. Wisconsin Transverse Mercator projection, 1991 Adjustment to the North American Datum of 1983 (NAD 83/91); EPSG 3071.

of Natural Resources (WDNR), which is updated annually, the city used an average of 620 million gallons of groundwater per year from 2010 to 2018 (Wisconsin Department of Natural Resources, 2019). Since 2010, groundwater pumped from study wells #5 and #6 has accounted for 44 and 16 percent, respectively, of that demand. Elevated and increasing concentrations of nitrate in study wells #5 and #6 are some of the prime motivations for this study. Routine testing (described below and detailed later in this report) shows that nitrate levels in study well #5 have steadily increased from less than 4 mg/L in 1993 to nearly 10 mg/L in 2018. In study well #6, nitrate concentrations have fluctuated between about 5 mg/L and nearly 10 mg/L over the same period. If nitrate exceeds the Federal limit of 10 mg/L for two consecutive measurements, the affected wells are at risk of being taken out of service by the WDNR.

Under the State of Wisconsin's administrative code NR 809 for Safe Drinking Water, public drinking-water supplies in Wisconsin are subject to routine water-quality testing. Nitrate is among the potential drinking-water contaminants that are monitored annually, with more frequent testing required if the measured concentration exceeds 5 mg/L as dissolved nitrogen (NR 809.11(4)). Nitrate, which is recognized as one of Wisconsin's most widespread groundwater contaminants (Wisconsin Groundwater Coordinating Council, 2018), is increasingly reported at concentrations above the Federal limit (10 mg/L). Although low levels of nitrate occur naturally, nitrate levels in groundwater above 2 mg/L indicate an anthropogenic source such as synthetic fertilizers, animal waste, or septic systems (U.S. Geological Survey, 1999).

In response to concerns over rising nitrate levels in the study wells, the City of Waupaca and the WDNR requested that the Wisconsin Geological and Natural History Survey investigate

the regional contributions of water to the study wells to better understand the potential sources of nitrate and determine whether there is a relation between well-pumping rates and observed nitrate. Data collected during this investigation formed the basis for a groundwater-flow model of the Waupaca area. Groundwater-flow models can be used to simulate groundwater flow using estimated hydrogeologic properties and recharge. These models can also be used to predict the path of a particle, such as a single water molecule, as it moves through an aquifer from the surface of the water table to a discharge point such as a river or pumping well. The resulting particle traces provide a scientific basis to delineate the most probable capture zone. The University of Wisconsin Water Resources Institute and the WDNR provided funding for the project, which was undertaken by the WGNHS and formally began in June 2018.

Purpose and goals

The purpose of this study is to investigate the causes of elevated nitrate concentrations in water produced by study wells #5 and #6. The study integrates local hydrogeologic data into a three-dimensional groundwater-flow model of the groundwater that contributes recharge to these wells. The steady-state model is intended to achieve the following goals:

- Provide guidance on representing discontinuous geologic deposits common to the surficial aquifer in a high-resolution, three-dimensional groundwater-flow model.
- Delineate capture zones for study wells #5 and #6 that correspond to current and historical water-use data.
- Provide input for a simple spreadsheet-based model that simulates the effective nitrate concentration at each well on the basis of the different types of land cover within the capture zone.
- Provide a basis to recommend land- or water-management approaches to help reduce the effective nitrate concentration in the study wells.
- More broadly, this study provides examples of techniques that can be used to understand and predict nitrate concentrations in groundwater in shallow, sandy aquifers in agricultural settings.

Study approach

This project developed a three-dimensional, steady-state groundwater-flow model of the groundwater located between the Crystal River and Walla Walla Creek. This groundwater is the source of groundwater for study wells #5 and #6. The model used the USGS MODFLOW code (Harbaugh, 2005), the MODFLOW-NWT solver (Niswonger and others, 2011), and a related groundwater-model optimization code (Ahlfeld and others, 2009). Particle tracking was performed using MODPATH (Pollock, 2012). Recharge for the model was estimated using the soil-water-balance (SWB) modeling technique developed by WGNHS and USGS in Wisconsin, which is now commonly used for regional modeling studies (Westenbroek and others, 2010).

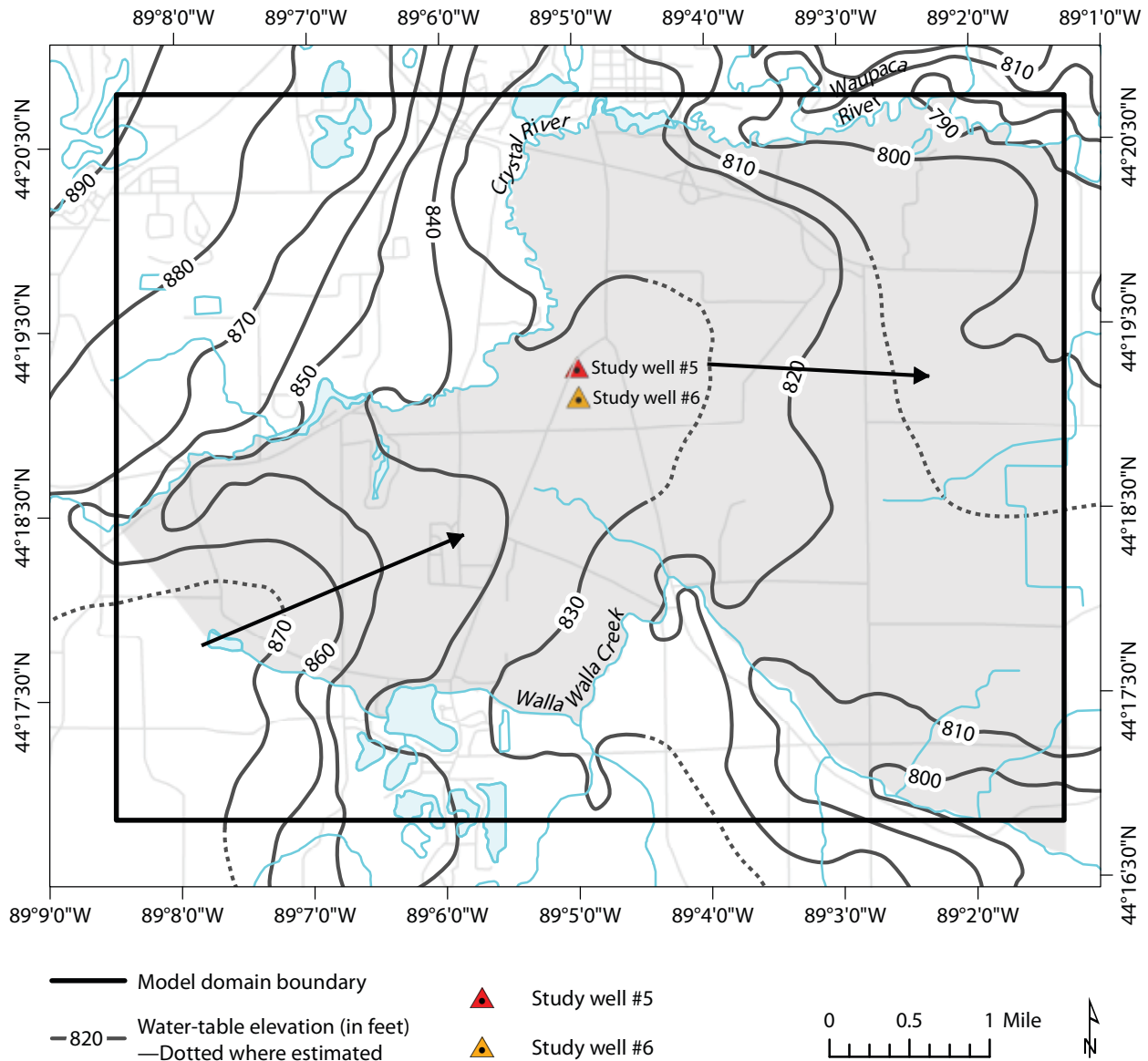
The MODFLOW model was developed using modern, field-measured boundary conditions. After running the optimization code, the model was calibrated using water-table measurements collected in the field during the same time frame. The calibrated model was used to simulate steady-state groundwater flow for the years 2011 to 2019 on the basis of estimated annual recharge and municipal well-pumping rates in each of those years. Capture zones delineated from these models were subsequently applied to the effective nitrate calculator to investigate relations between water use, land use, and the concentration of nitrate observed at each of the study wells.

Model domain

Study wells #5 and #6 are in the south-eastern corner of Waupaca County, Wisc., approximately 1 mile south of the City of Waupaca and a few miles north of the Town of Lind. The primary focus of this study is the land surface contributing recharge that flows as groundwater to these wells. According to a historical water-table map of Waupaca County

(Lippelt, 1981), the study area includes the land area bounded by the Crystal River to the west, the Waupaca River to the north, and Walla Walla Creek to the south (fig. 2). The model domain, also shown in figure 2, encloses these hydrologic features and represents the extent of the active groundwater model presented in this report.

Figure 2. Map of the model domain showing historical water-table-elevation contours and groundwater-flow directions modified from Lippelt (1981). Water-table-elevation contour interval is 10 ft; direction of groundwater flow is indicated by arrows. The land surface bounded by the Crystal River, the Waupaca River, and Walla Walla Creek (gray) is the most likely area to contribute recharge to study wells #5 and #6.



Roads from U.S. Census Bureau, 2015. Hydrography from U.S. Geological Survey National Hydrography Dataset, 2016. Wisconsin Transverse Mercator projection, 1991 Adjustment to the North American Datum of 1983 (NAD 83/91); EPSG 3071.

Section 1: Hydrogeologic setting

Objectives

Hydrogeologic data (dataset 1) were compiled and analyzed in the beginning of the study with the goal of developing a conceptual model of the hydrogeologic setting within the model domain. The sources of these data included publicly available well construction reports, geologic maps, and light detection and ranging (lidar)-derived surface elevations. These resources were supplemented by field measurements performed between July 2018 and June 2019 to estimate the water-table elevation, hydraulic conductivity of aquifer materials, stream discharge, and depth to bedrock; and to model estimates of annual recharge to groundwater.

Well construction reports

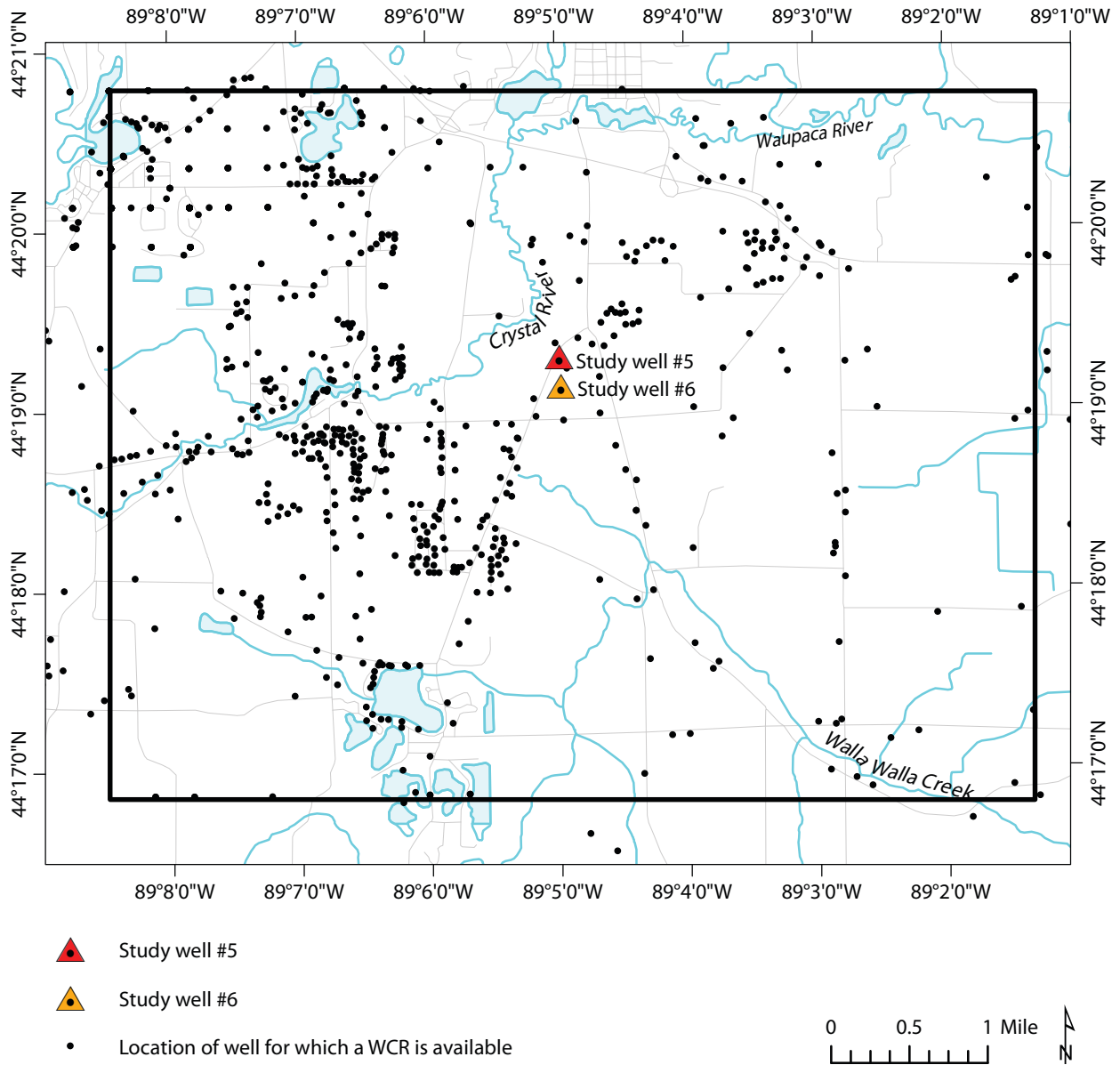
Well construction reports (WCRs) are one-page reports that are completed by well drillers following the construction of a new residential or high-capacity groundwater well in Wisconsin. Each WCR contains information about its location, owner, the date it was drilled, the depth of the well casing, screen length, a description of subsurface materials, and the results of a specific-capacity test. These data can be used as an aid in characterizing the subsurface lithology, depth to bedrock, and saturated thickness of the aquifer; they can also be used to estimate hydraulic conductivity at different locations and depths.

The WCR data used in this study are a subset of a digital database maintained by the WDNR (Wisconsin Department of Natural Resources, 2020c). Wells installed from 1988 to the present are identified with a Wisconsin Unique Well Number (WUWN). WCRs located within a 0.25-mile buffer zone outside the model domain boundaries were included in the geospatial dataset retained for this study. The well locations in the source dataset are only accurate to either quarter-quarter sections or a lot number, so individual records were moved to more precise locations using a method called geolocation. Geolocation involves the use of aerial photography, land-ownership records, plat maps, and location descriptions provided by the well drillers to identify the most likely location of a well with respect to visible buildings and other infrastructure identified on satellite imagery in the Esri World Imagery base layer (Esri, Redlands, Calif.). Although more than 1,000 WCRs were originally included in this study, records that were incomplete or could not be geolocated were discarded. After evaluating all records, 861 were retained for use in this project (fig. 3). The WDNR database (Wisconsin Department of Natural Resources, 2020c) provided detailed descriptions of the lithology corresponding to each WCR and was also used to characterize the subsurface properties of the glacial aquifer contained within the model domain.

Surficial geology

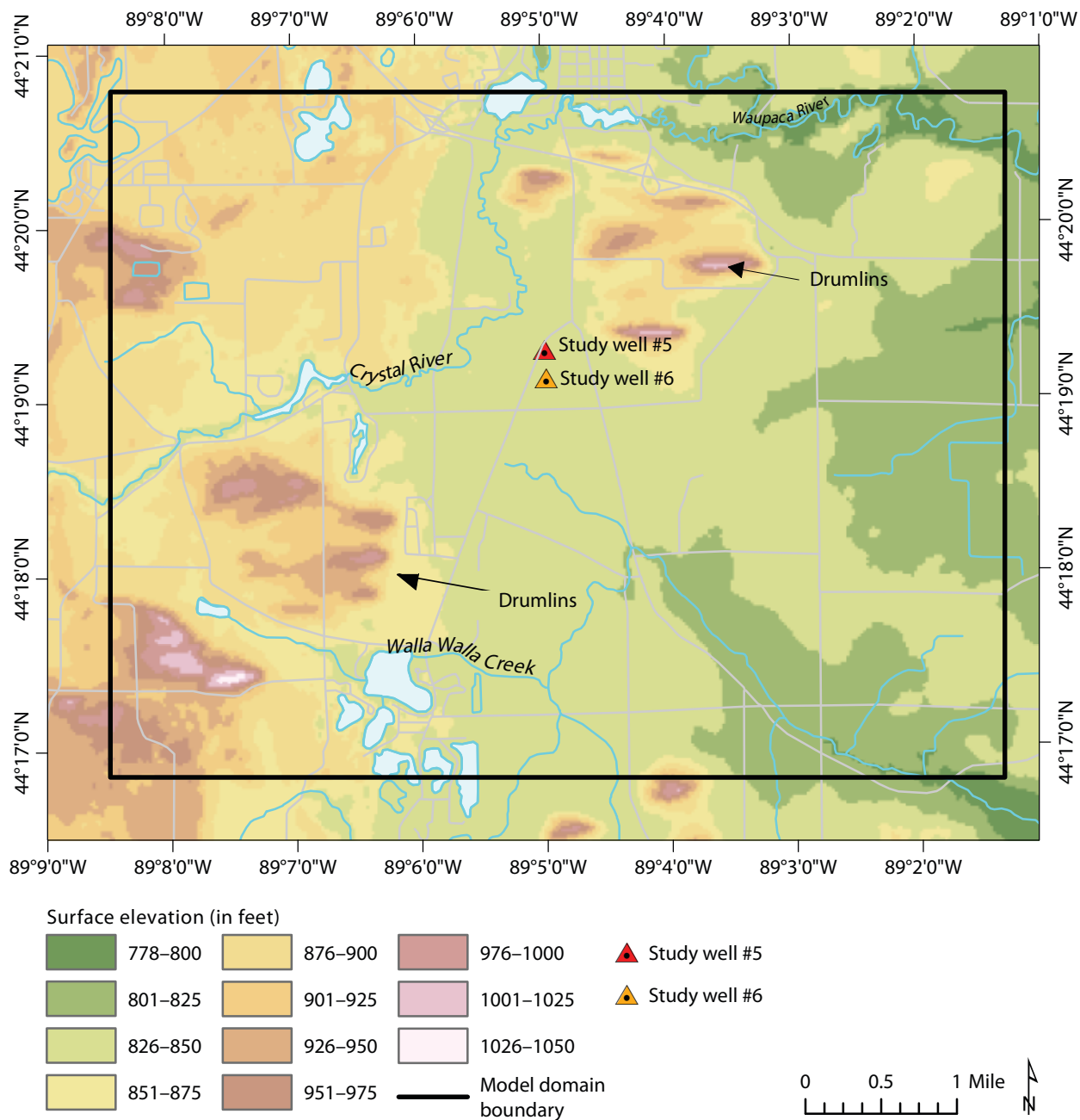
The model domain is located approximately 15 miles east of terminal moraines that were deposited by the Green Bay Lobe, an outlet glacier of the Southern Laurentide Ice Sheet that advanced across northern Wisconsin between 95,000 and 20,000 years ago (Dyke and Prest, 1987). As the ice sheet retreated to the east, meltwater streams flowing east to west fed into a proglacial lake depositing thick layers of sand into the region presently known as the Central Sands. The model domain is located near the easternmost boundary of the Central Sands (fig. 1), where lacustrine sands are interbedded with meltwater stream deposits of gravel, sand, silt, and clay and form a low, flat valley that slopes gently to the east between small clusters of elevated, east-west-trending glacial drumlins (fig. 4). Along modern stream channels, including the Crystal River, Walla Walla Creek, and the Waupaca River, the Quaternary deposits of meltwater-stream sediment have been eroded and overlain by postglacial stream deposits of sand, silt, and—in some wetland areas—peat (fig. 5).

Figure 3. Map showing the locations of 861 wells for which a well construction report (WCR) exists. Included are wells within a 0.25-mile perimeter outside of the model domain. Each WCR was geolocated and its data were used to characterize subsurface lithologies, hydraulic properties, and water-table elevations.



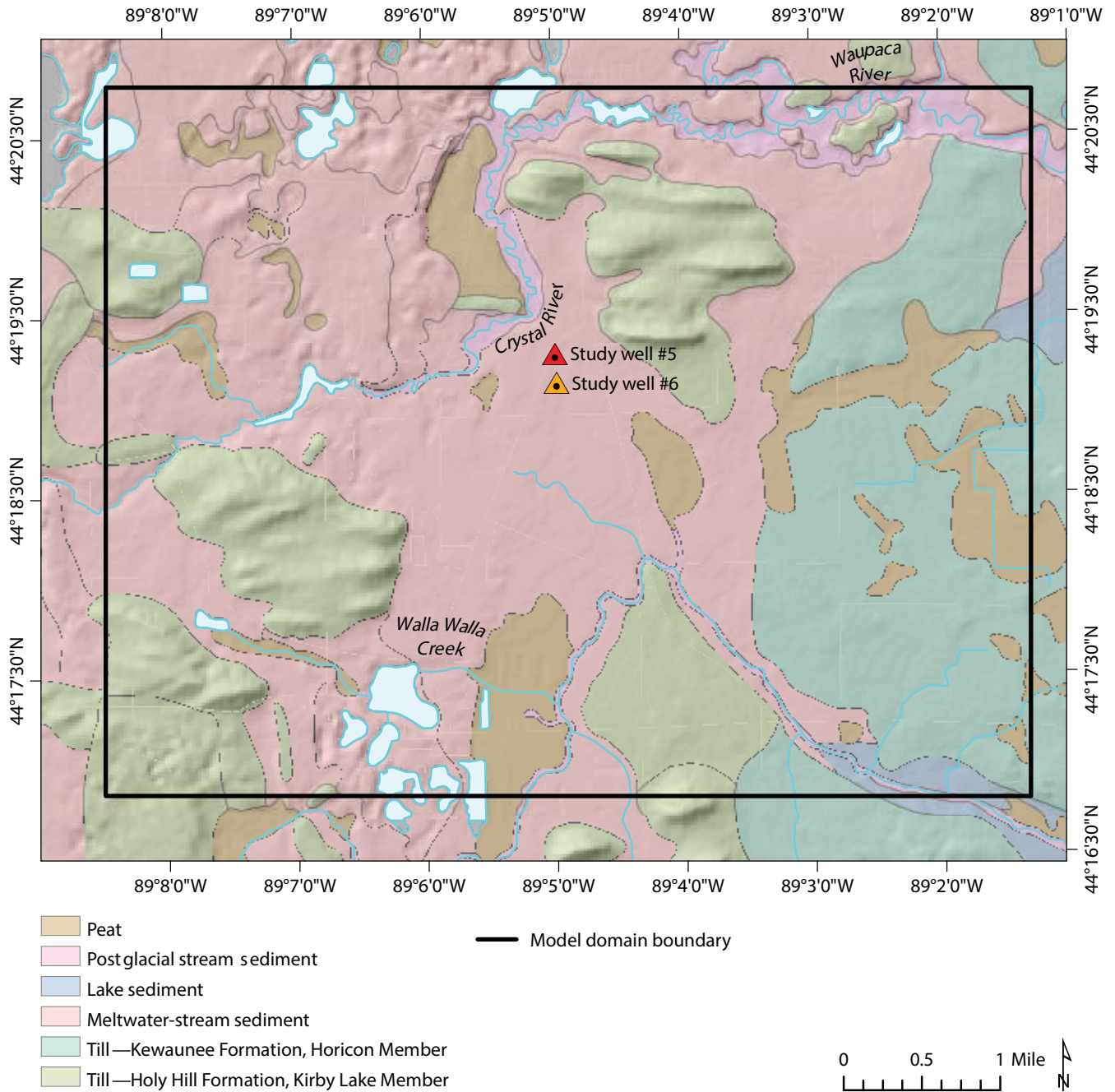
Roads from U.S. Census Bureau, 2015. Hydrography from U.S. Geological Survey National Hydrography Dataset, 2016. Wisconsin Transverse Mercator projection, 1991 Adjustment to the North American Datum of 1983 (NAD 83/91); EPSG 3071.

Figure 4. Map of the model domain derived from digital elevation model (DEM) data (U.S. Geological Survey, 2017).



Elevation from U.S. Geological Survey National Elevation Dataset, 2017. Roads from U.S. Census Bureau, 2015. Hydrography from U.S. Geological Survey National Hydrography Dataset, 2016. Wisconsin Transverse Mercator projection, 1991 Adjustment to the North American Datum of 1983 (NAD 83/91); EPSG 3071.

Figure 5. Generalized surficial geologic map. Data from Mode and others (2015). Base map from digital elevation model (DEM) data (U.S. Geological Survey, 2017).



Elevation from U.S. Geological Survey National Elevation Dataset, 2017. Roads from U.S. Census Bureau, 2015. Hydrography from U.S. Geological Survey National Hydrography Dataset, 2016. Wisconsin Transverse Mercator projection, 1991 Adjustment to the North American Datum of 1983 (NAD 83/91); EPSG 3071.

Bedrock geology

In east-central Wisconsin, Quaternary deposits overlie a bedrock surface composed of Precambrian granite that is regionally overlain by Cambrian sandstone. Mudrey and others (1982) estimated that the sandstone above the crystalline bedrock is prevalent to the south of an east-to-west-trending arc through the center of the domain, which is consistent with lithologic descriptions taken from wells drilled to bedrock (fig. 6). The thin and discontinuous sandstone deposits are highly weathered and are not considered a major barrier to vertical groundwater flow. In contrast, the Precambrian granites common to this region transmit water only through interconnected fracture networks that are often sparse and poorly characterized. For this reason, the Precambrian bedrock surface is regarded as impermeable and taken to represent the lower boundary of the groundwater system of the model domain. For the remainder of this report, this boundary is called the crystalline bedrock surface. An elevation map of the crystalline bedrock surface was estimated using a combination of (1) depth-to-bedrock values reported or estimated from WCRs and (2) passive-seismic recordings.

Estimates of depth to bedrock from well construction reports

The depths to the crystalline bedrock surface were reported in just 22 of the 861 WCRs that were geolocated for this study and ranged from 66 to 248 ft. The poor distribution of these data across the model domain (fig. 7) led us to develop a qualitative measure of the depth based on the knowledge that drill operators often cease drilling when the well first encounters hard crystalline bedrock. First, all wells drilled deeper than 100 ft were identified ($n = 327$); next, those wells were clustered on the basis of the distance from one another using a grouping function in ArcMap software (Esri, Redlands, Calif.). Within each cluster, the depth

to the crystalline bedrock surface was assumed to be the depth at which the deepest well in each cluster terminated. In some instances, this assumption resulted in a depth-to-bedrock estimate in a region of the model domain where more accurate measurements were already available (for example, from a direct report in a WCR or a passive-seismic analysis). When the more accurate measurement was available, estimates obtained from the cluster method were discarded. This clustering method resulted in an additional 79 depth-to-bedrock estimates (fig. 7).

Estimates of depth to bedrock using passive-seismic analysis

To further refine depth-to-bedrock estimates across the model domain, passive-seismic analysis was used to generate single-point estimates of bedrock depth at selected locations. Passive-seismic analysis is a geophysical technique that discerns geologic structures from recordings of natural low-frequency movements beneath the land surface. A digital tromograph was used to record these movements at 28 locations in and around the model domain in October and November of 2018 (fig. 7). The resulting recordings (also called traces) were imported into GRILLA (MoHo s.r.l., Venice, Italy), a software package that archives and analyzes seismic data. The resonance frequency (in hertz) of each trace was evaluated and converted to a depth-to-bedrock estimate using a fitting parameter described by Chandler (2011).

Interpolation of bedrock-elevation surface

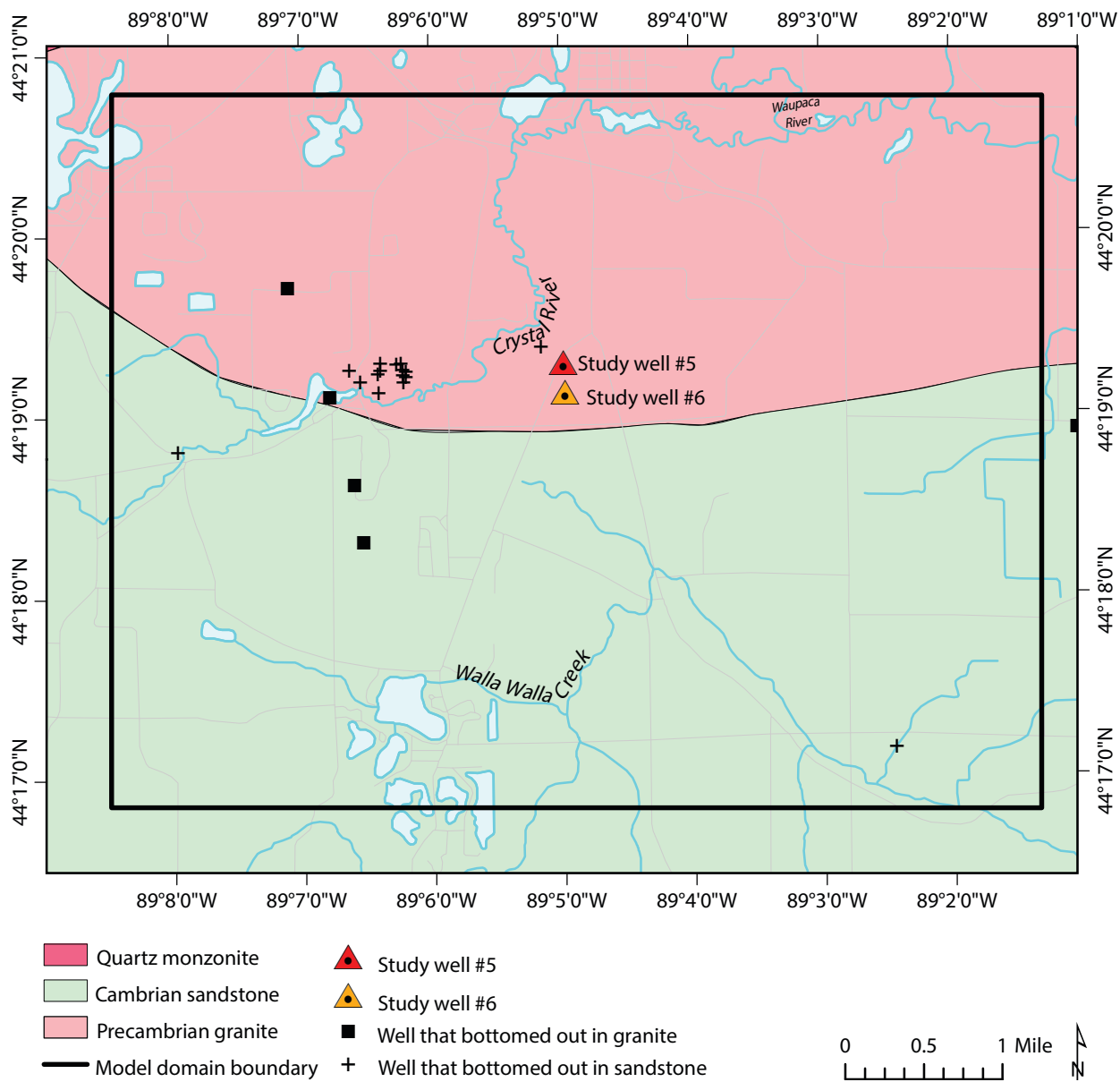
Each of the 129 depth-to-bedrock values obtained from WCRs and passive-seismic analyses was subtracted from the land-surface elevation to estimate the elevation of the crystalline bedrock surface at that point. The resulting data were interpolated to produce a raster grid representing the elevation of the crystalline bedrock surface. The interpolation was performed using the

inverse-weighted-distance technique (power = 2) in ArcMap software. This method was based on the assumption that near points are more alike than far points, which is an advantage when data are sparse or unevenly distributed; where there are isolated data points, this method can lead to “bull’s-eyes,” which are concentric areas of the same value around a known data point. To smooth the interpolated surface and eliminate any resulting “bull’s-eyes,” the interpolated raster grid was aggregated to a coarser resolution grid by assigning the median value of high-resolution (10 ft × 10 ft) input cells to a coarse resolution (1,500 ft × 1,500 ft) output cell. The aggregated-elevation raster grid was contoured in ArcMap software (fig. 8). The resulting elevation contours ranged from 660 to 760 ft above mean sea level and indicated that the crystalline bedrock surface generally sloped from northwest to southeast across the model domain.

Surface hydrogeology

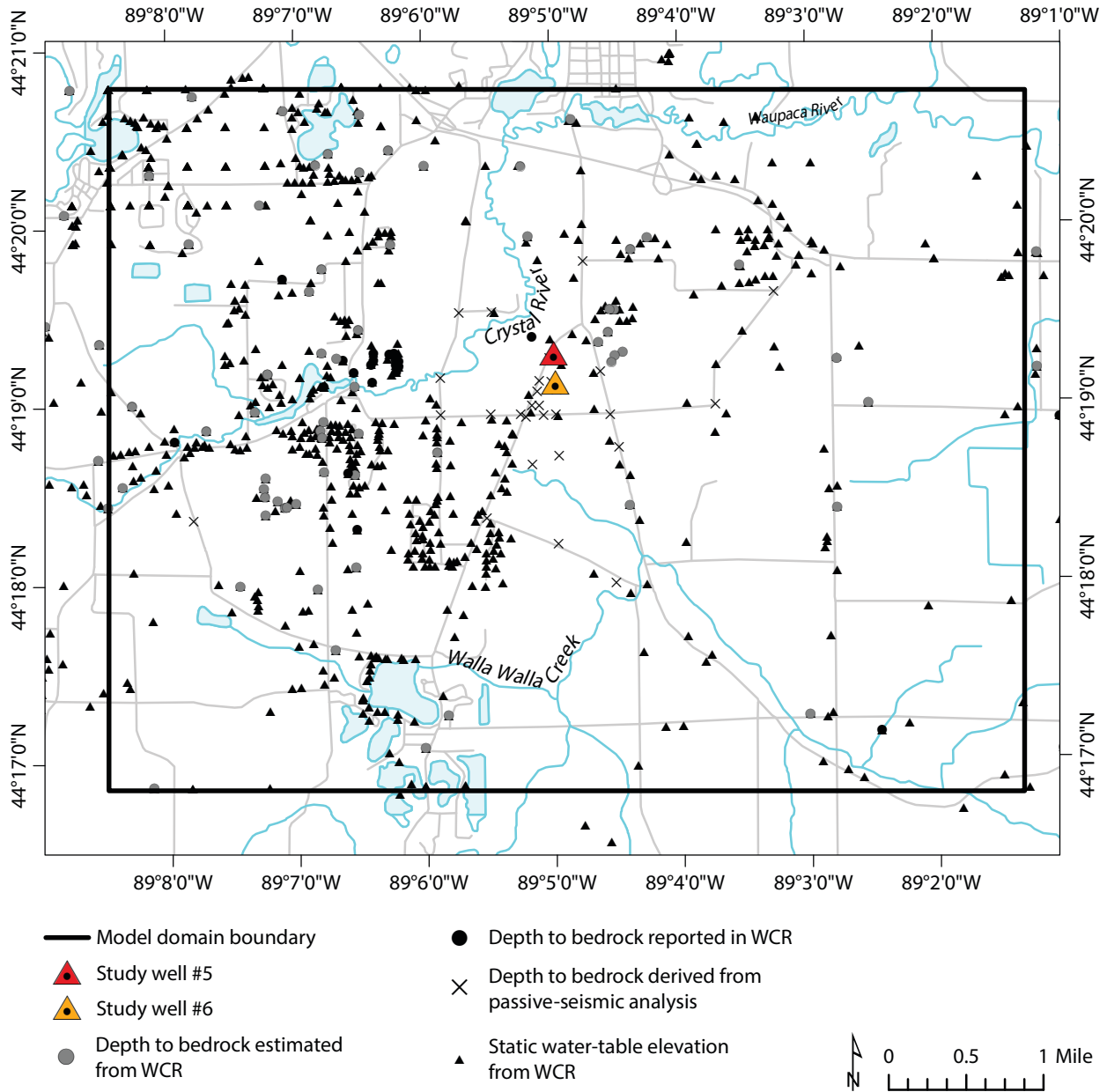
The model domain contains a portion of the boundary between the Waupaca River watershed and the combined Walla Walla and Alder Creeks watershed (fig. 9); Alder Creek is outside of the model domain area, so the watershed is referred to in this report as the Walla Walla Creek watershed for simplicity. The two watersheds have a combined surface area of 403 square miles and drain portions of Portage, Waushara, Waupaca, and Winnebago Counties into the lower reaches of the Wolf River. As seen in an east-to-west topographic profile drawn across the model domain (see fig. 9, line A–A'), the local topography is hummocky with an overall slope to the east (fig. 10).

Figure 6. Bedrock geology of the model domain. The extent of Precambrian granite shown on the original map by Mudrey and others (1982) was extended southward on this map on the basis of lithological descriptions provided in well construction reports (WCRs). A very small area of quartz monzonite is located in the upper left corner of the map area.



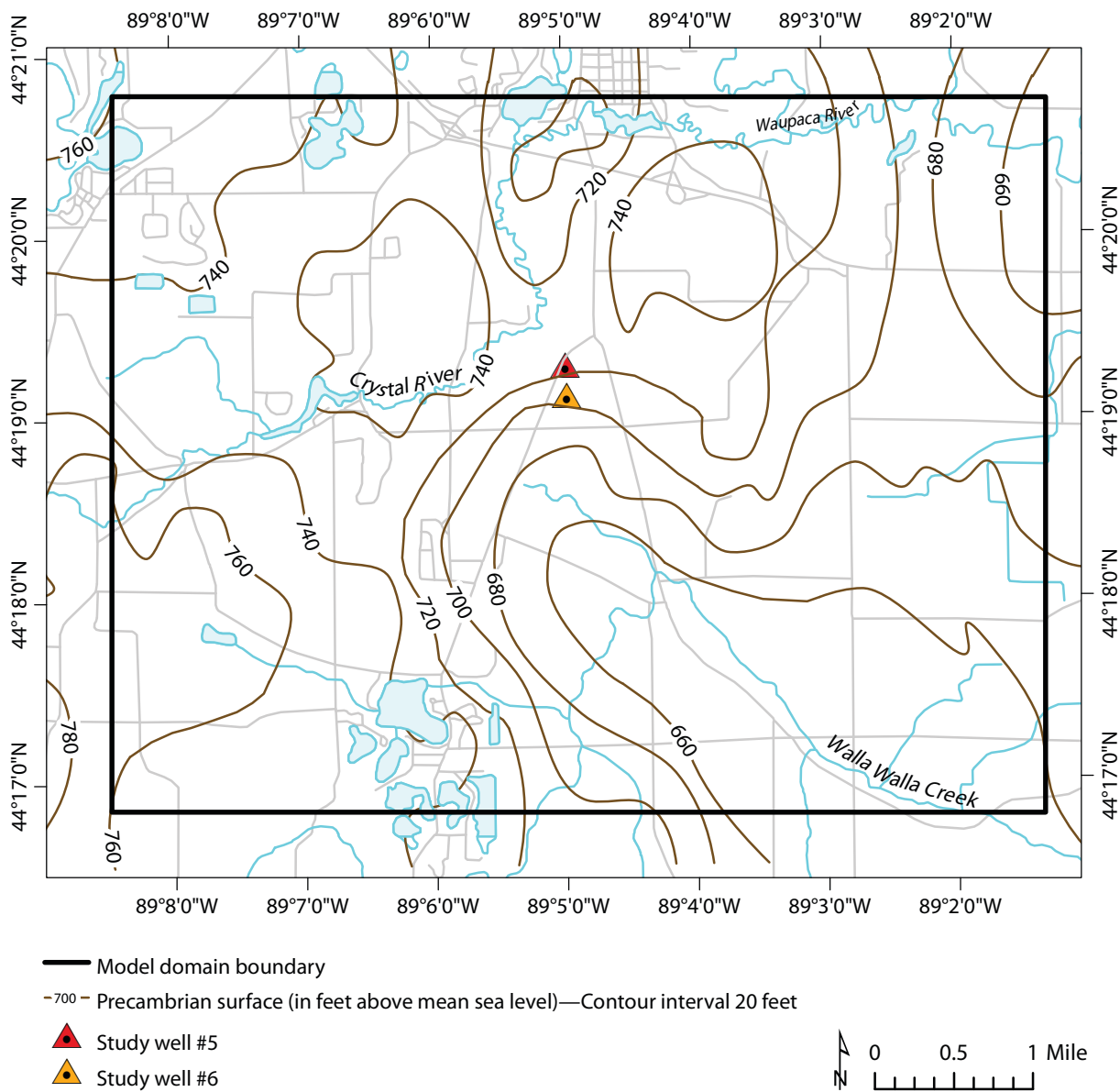
Roads from U.S. Census Bureau, 2015. Hydrography from U.S. Geological Survey National Hydrography Dataset, 2016. Wisconsin Transverse Mercator projection, 1991 Adjustment to the North American Datum of 1983 (NAD 83/91); EPSG 3071.

Figure 7. Point data used to interpolate elevation surfaces of the crystalline bedrock and the water table.



Roads from U.S. Census Bureau, 2015. Hydrography from U.S. Geological Survey National Hydrography Dataset, 2016. Wisconsin Transverse Mercator projection, 1991 Adjustment to the North American Datum of 1983 (NAD 83/91); EPSG 3071.

Figure 8. Elevation of the crystalline bedrock surface.



Roads from U.S. Census Bureau, 2015. Hydrography from U.S. Geological Survey National Hydrography Dataset, 2016. Wisconsin Transverse Mercator projection, 1991 Adjustment to the North American Datum of 1983 (NAD 83/91); EPSG 3071.

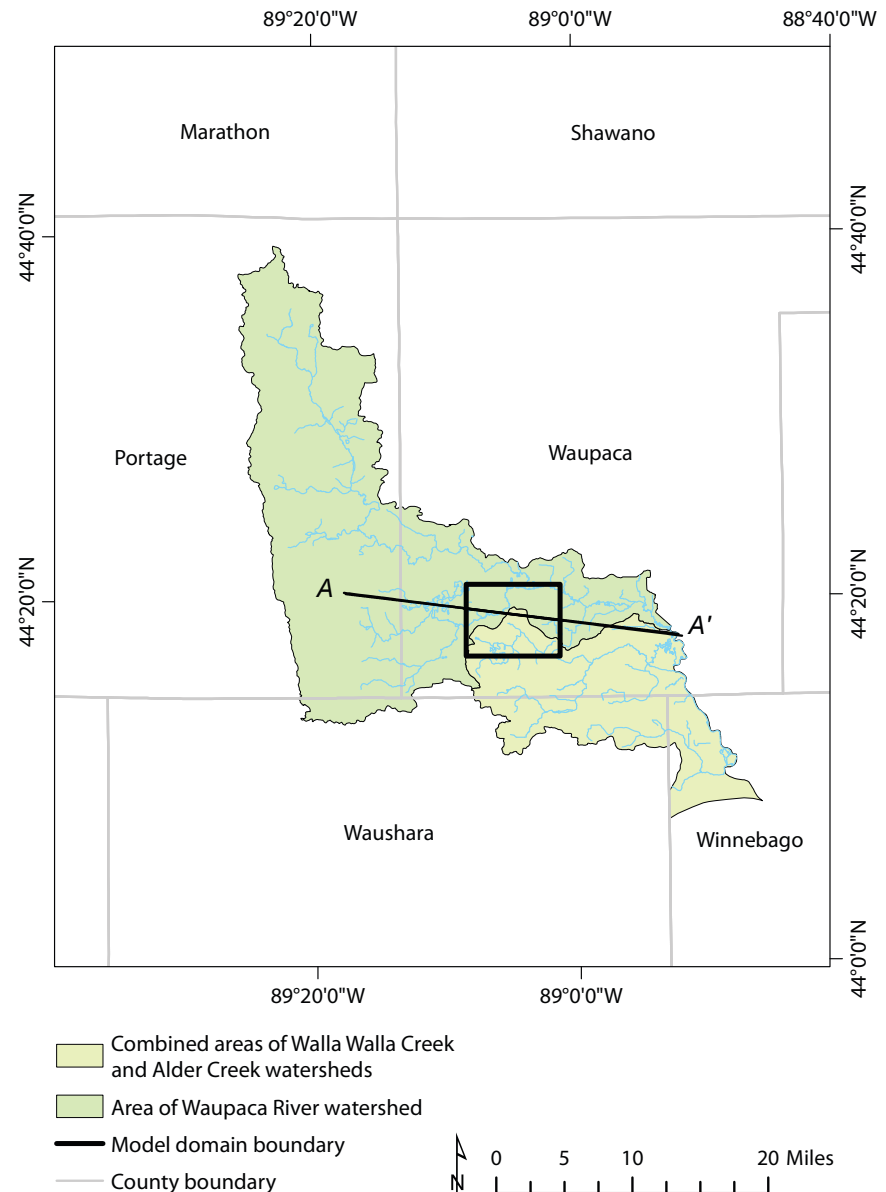
Surface-water features

The major surface-water features included in this study are labeled in figure 11. The Crystal River is dominant in the northern part of the model domain and flows from west to east across the western boundary of the model domain. Near Little Hope (see feature 2, fig. 11), the Crystal River is joined by a small tributary and then continues to flow north and east until it drains into the Waupaca River and exits the model, flowing eastward. Walla Walla Creek is the dominant water feature in the southern portion of the model domain. This stream originates as a drain from Jenson Lake and flows through Spencer Lake (features 6 and 7, fig. 11). As the stream flows to the east, it is joined by several tributaries and drainage ditches before changing course and flowing out through the southeastern corner of the model domain. There are 12 other named surface-water bodies in the model domain. These include six seepage lakes (features 1, 3, 8, 10–12, fig. 11) and one drained lake (feature 6, fig. 11) where the main water sources are precipitation and groundwater. The remaining five bodies (2, 4, 5, 7, 9, fig. 11) are drainage lakes where the main water sources are stream drainage.

Streamflow measurements

Streamflow measurements were collected at two locations each on the Crystal River and on Walla Walla Creek (fig. 11). The results (table 2) suggest that both the Crystal River and Walla Walla Creek are gaining streams, meaning that groundwater discharge into the stream channel sustains flow between water input events, and the volumetric discharge (in cubic feet per second) increases in the direction of streamflow. Additional streamflow is gained from small ephemeral streams and drainage ditches that are classified as losing streams. The gain in streamflow observed in the Crystal River is within the 5-percent margin of error for field measurements of streamflow ranked as “good” (Sauer and Meyer, 1992).

Figure 9. Watersheds enclosed by the model domain. Cross-section line A–A’ is the extent of a topographic profile presented in figure 10.



Political boundaries from Wisconsin Department of Natural Resources, 2011. Hydrography from U.S. Geological Survey National Hydrography Dataset, 2016. Wisconsin Transverse Mercator projection, 1991 Adjustment to the North American Datum of 1983 (NAD 83/91); EPSG 3071.

Table 2. Streamflow measurements collected on October 18, 2018, south of Waupaca, Wisc.

Stream	Location	Source	Streamflow (ft ³ /s)
Crystal River #1	Shadow Road (south)	Field-measured	120
Crystal River #2	Shadow Road (north)	Field-measured	126
Walla Walla Creek #1	Spencer Lake	Field-measured	1.8
Walla Walla Creek #2	Lind Center Road	Field-measured	16.7

Groundwater hydrogeology

Above the buried crystalline bedrock surface, weathered sandstones and unconsolidated deposits of sand, clay, and gravel constitute a shallow, unconfined aquifer. The thickness of these deposits ranges from more than 200 ft beneath drumlins (see east-to-west-trending, high-elevation topographic features labeled as “till” in fig. 5) to less than 100 ft in outwash plains, with an average thickness of 146 ft (fig. 12). These deposits are quite thin relative to the areal extent of the aquifer. The shallowness of the aquifer and the hummocky topography each favor the development of local groundwater-flow systems in which water moves from a recharge area to the next adjacent discharge area (Toth, 1963; Winter, 2001). Surface-water features such as lakes and streams are therefore assumed to be hydraulic barriers to groundwater flow.

Monitoring wells and piezometers

In 1994, the USGS and the City of Waupaca installed nested monitoring wells at eight locations near study wells #5 and #6 to investigate water quality and determine the horizontal and vertical hydraulic gradients near the municipal well field (fig. 13). Each of these sites originally contained one monitoring well screened across the water table (17–22 ft screen depth), one intermediate-depth piezometer (41–46 ft screen depth), and one deep piezometer (65–75 ft screen depth). For the remainder of this report, the shallow monitoring wells (MWs) are identified using the suffix “A” (for example, MW 1A), the intermediate-depth piezometers are identified using the suffix “B” (for example, MW 1B), and the deep piezometers are identified using the suffix “C” (for example, MW 1C). Each well and piezometer was constructed from 2-inch-diameter polyvinyl chloride casing with slotted screens that are 5 ft long (A and B) and

10 ft long (C) and completed at depth. In 2018, the WGNHS installed four additional water-table wells at locations south and east of the well field. These wells, intended for water-table monitoring only, were constructed of 1-inch-diameter polyvinyl chloride casing with 5-ft-long slotted screens (5–22 ft screen depth) and are also identified with the suffix “A” (MWs 9A–12A).

Figure 10. Elevation profile corresponding to cross-section line A–A’ (fig. 9). The position of the western and eastern boundaries of the domain are marked by black squares. Arrows indicating the general direction of regional and local groundwater flow are based on the hydrologic landscape model for hummocky terrain (Winter, 2001).

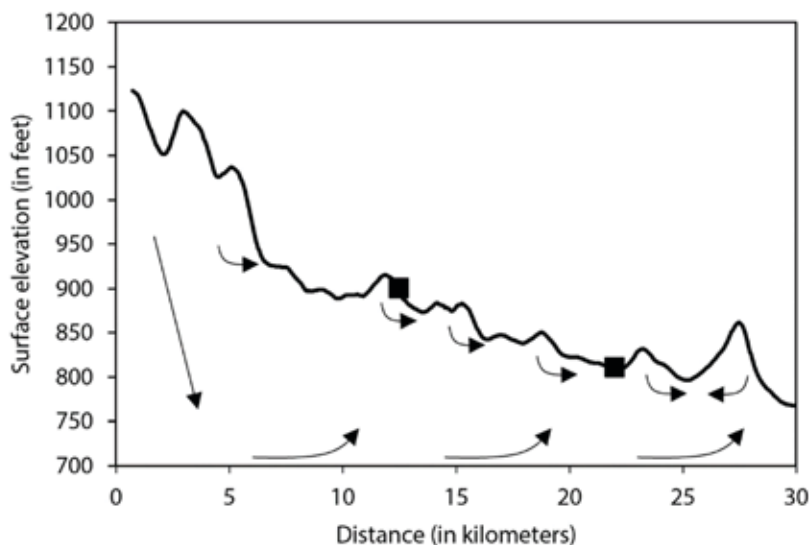
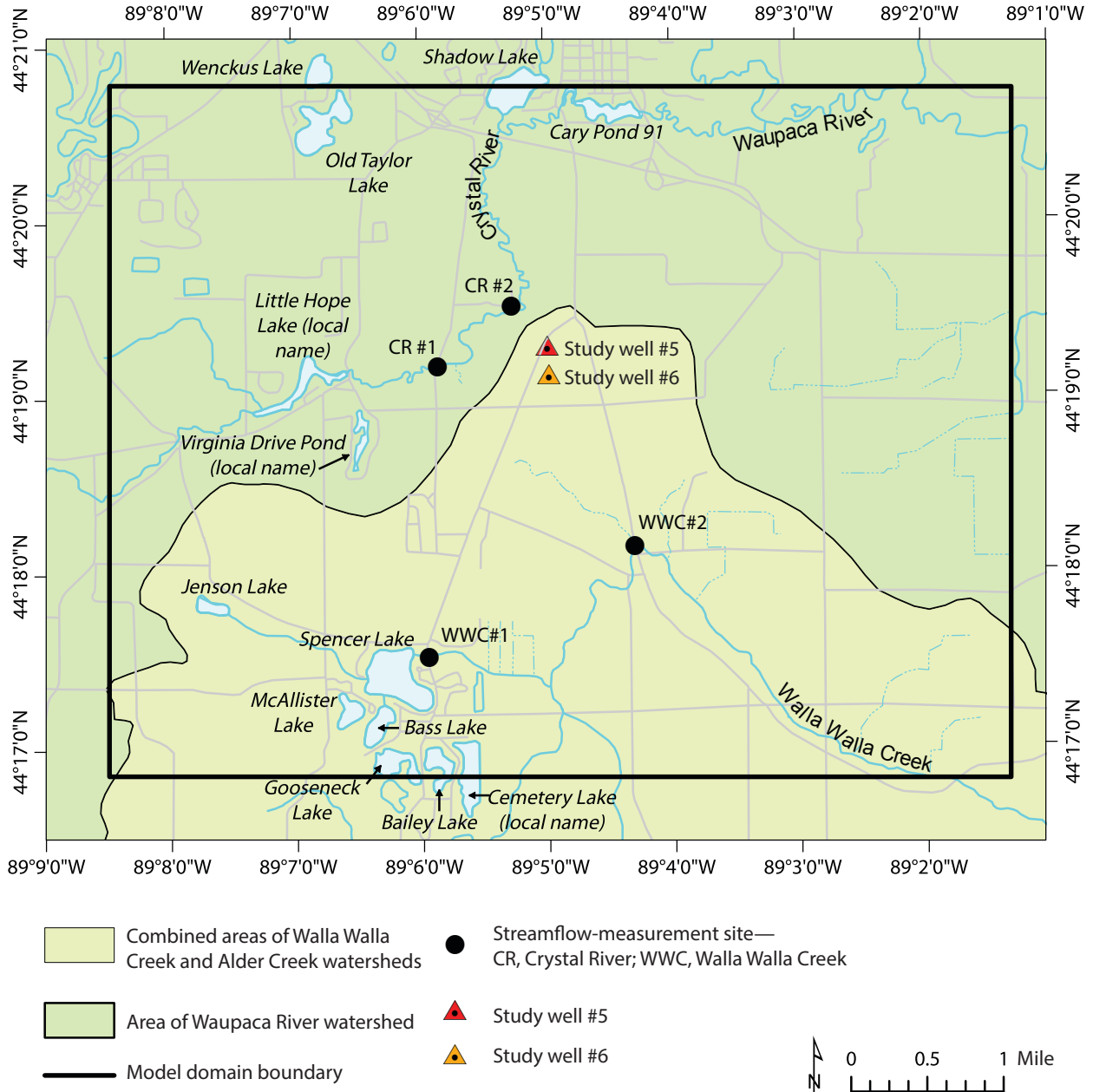
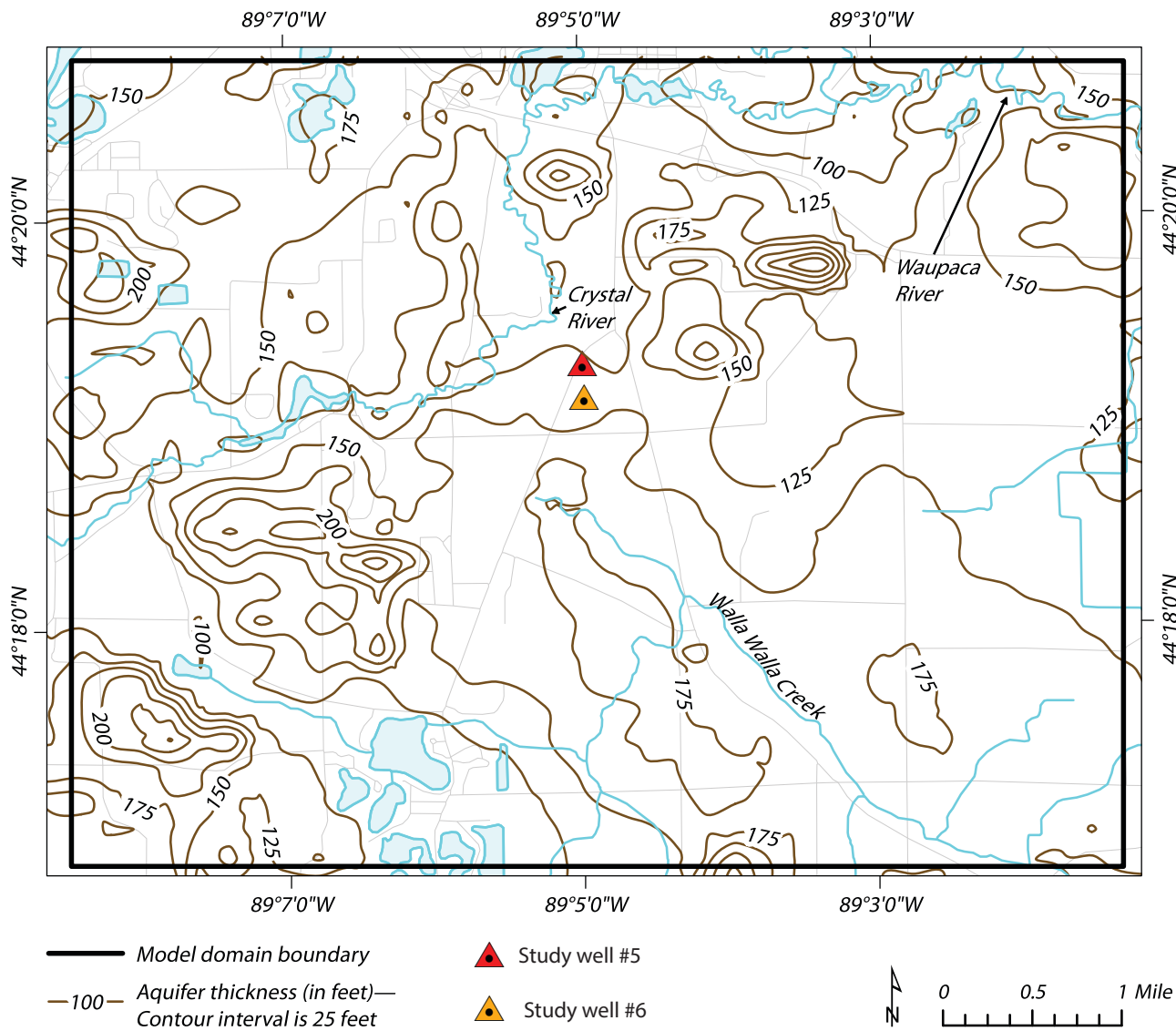


Figure 11. Major surface-water features in the model domain include the Crystal River, the Waupaca River, Walla Walla Creek, and the following lakes or ponds: (1) Virginia Drive Pond (local name), (2) Little Hope Lake (local name), (3) Old Taylor Lake, (4) Wenckus Lake, (5) Shadow Lake, (6) Cary Pond 91, (7) Jenson Lake, (8) Spencer Lake, (9) McAllister Lake, (10) Bass Lake, (11) Gooseneck Lake, (12) Bailey Lake, and (13) Cemetery Lake (local name). Also shown are locations of four streamflow-measuring sites (see table 2).



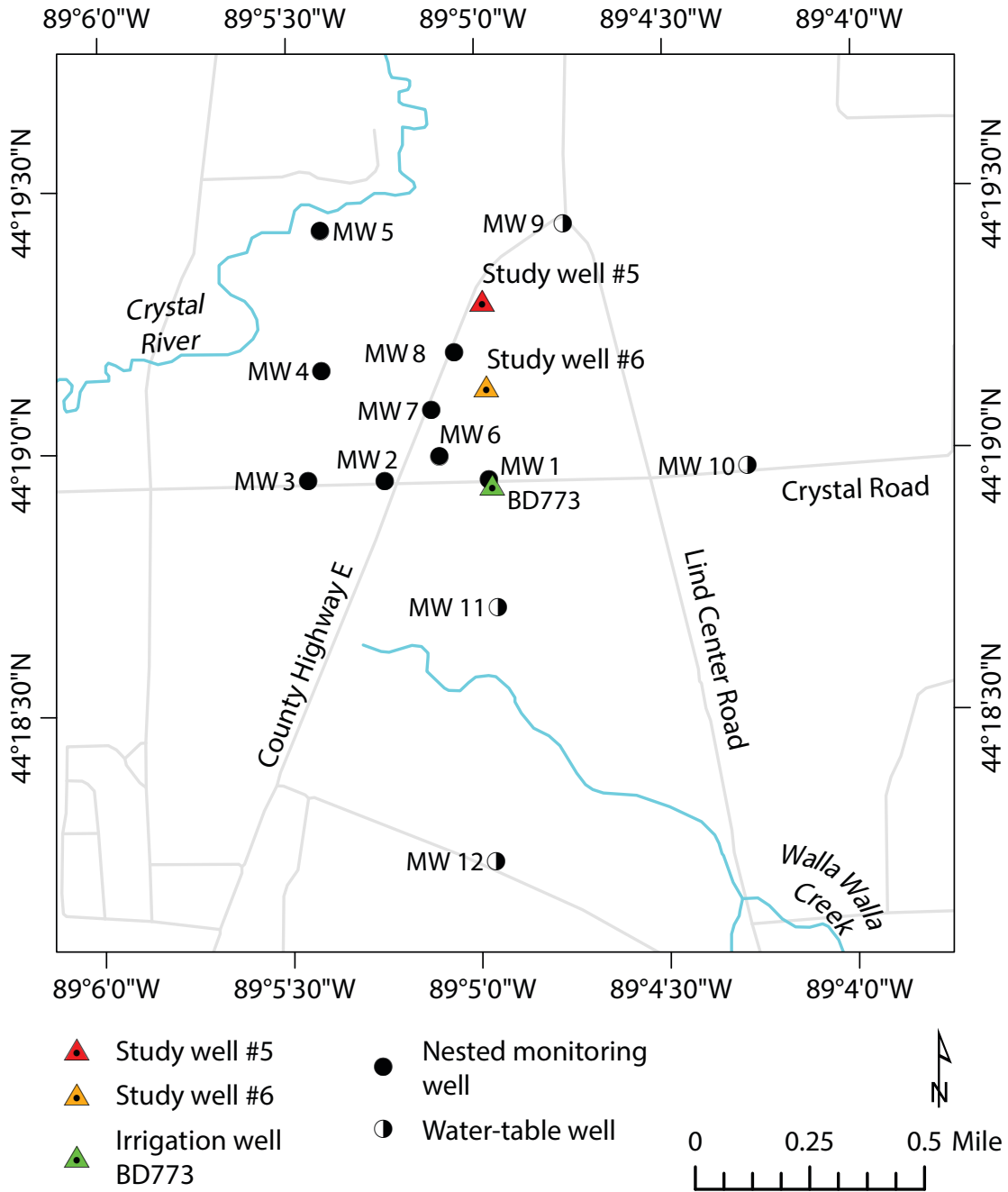
Roads from U.S. Census Bureau, 2015. Hydrography from U.S. Geological Survey National Hydrography Dataset, 2016. Wisconsin Transverse Mercator projection, 1991 Adjustment to the North American Datum of 1983 (NAD 83/91); EPSG 3071.

Figure 12. Isopach map showing thickness of unconsolidated deposits (including sandstone) above crystalline bedrock surface.



Roads from U.S. Census Bureau, 2015. Hydrography from U.S. Geological Survey National Hydrography Dataset, 2016. Wisconsin Transverse Mercator projection, 1991 Adjustment to the North American Datum of 1983 (NAD 83/91); EPSG 3071.

Figure 13. Location of the two municipal wells (study wells #5 and #6) and the nested monitoring wells and water-table wells installed by the U.S. Geological Survey and Wisconsin Geological and Natural History Survey.



Roads from U.S. Census Bureau, 2015. Hydrography from U.S. Geological Survey National Hydrography Dataset, 2016. Wisconsin Transverse Mercator projection, 1991 Adjustment to the North American Datum of 1983 (NAD 83/91); EPSG 3071.

Water-table elevation

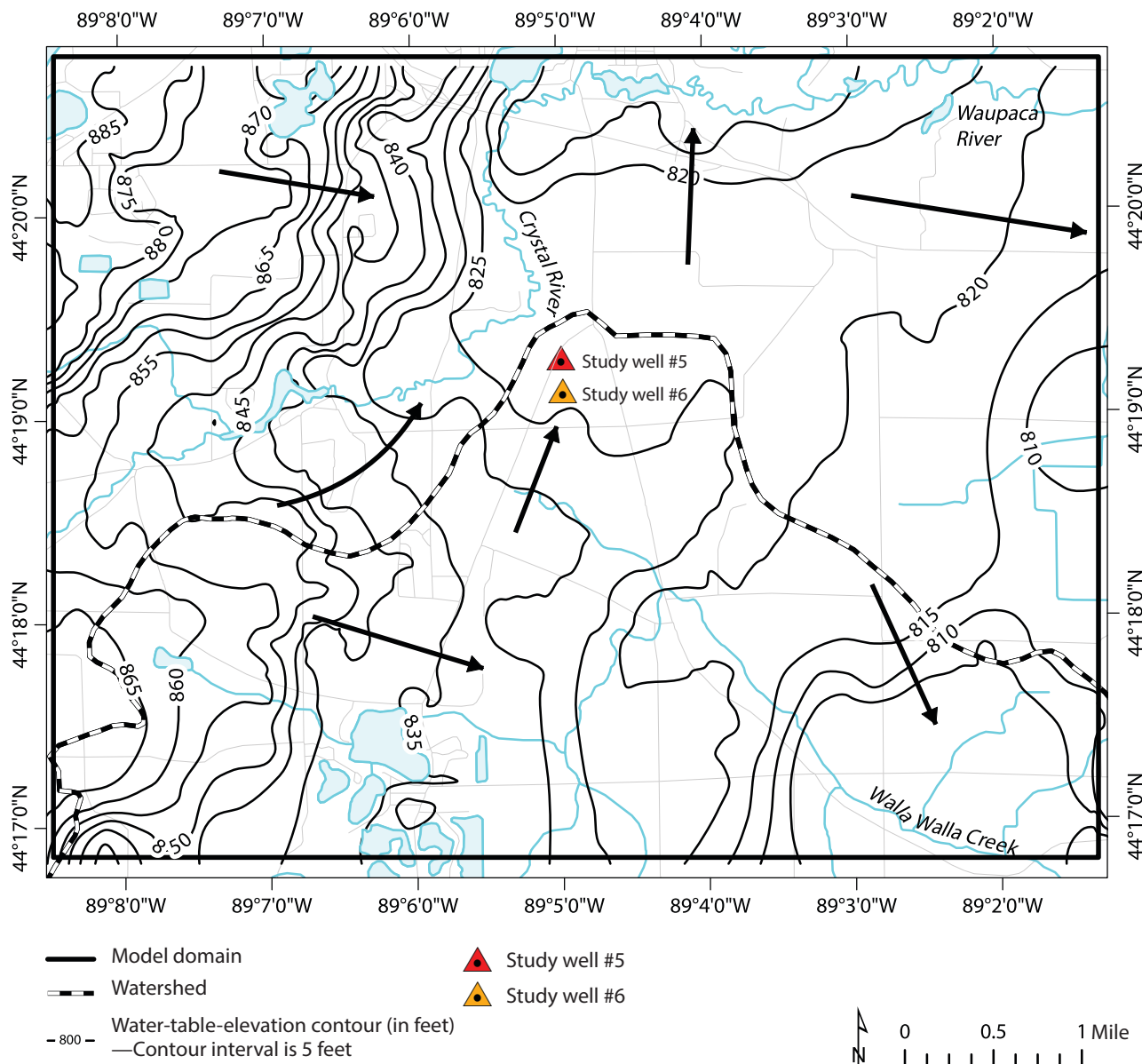
Static water levels were reported in WCRs as depth-to-water measurements. After extracting the surface elevation for each well from a lidar elevation dataset, the water-table elevation was calculated for each point by subtracting the depth-to-water value from the surface elevation. These data ($n = 751$) were combined with field-measured depth-to-water values ($n = 20$) and interpolated to a raster grid using the

inverse-weighted-distance technique (power = 2). The surface was edited using the aggregation technique described in a previous section (see “Interpolation of bedrock elevation surface”) and contoured to produce a generalized water-table-elevation map (fig. 14).

The water-table elevation ranges from 770 to 890 ft above mean sea level. Like the historical water-table map presented earlier (fig. 2), the interpo-

lated surface indicates that the general direction of groundwater flow in the model domain is west to east with local groundwater-flow systems that discharge into the Crystal River, the Waupaca River, and Walla Walla Creek. To better resolve the direction of groundwater flow in the portion of the model domain nearest the study wells, measurements were manually collected using a water level sensor from MWs 1A–4A and MWs 6A–12A on November

Figure 14. Contour map of water-table elevation estimated from measurements in well construction reports of depth to water. The approximate direction of groundwater flow is indicated by heavy arrows.



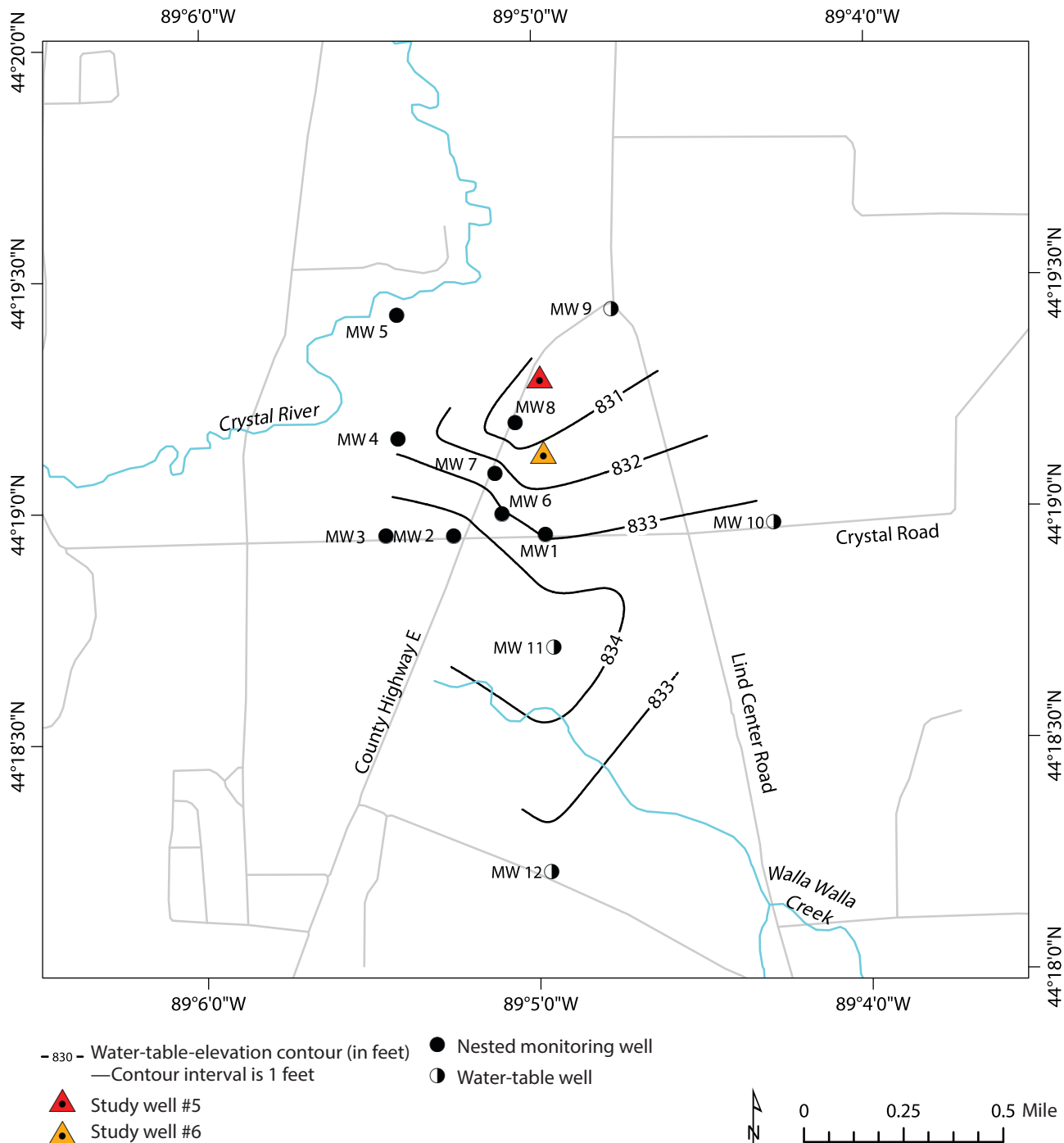
Roads from U.S. Census Bureau, 2015. Hydrography from U.S. Geological Survey National Hydrography Dataset, 2016. Wisconsin Transverse Mercator projection, 1991 Adjustment to the North American Datum of 1983 (NAD 83/91); EPSG 3071.

18, 2018. The measurements were then interpolated to 1-ft contours. The results imply that the primary direction of groundwater flow to study well #6 is southwest to northeast. Study well #5 is

located closer to the topographic divide between the Waupaca River and Walla Walla Creek watersheds. Groundwater flow from the divide (fig. 14) toward study well #5 may originate from the

west or the north. The interpolated contours are not conclusive north of study well #5 because of a lack of data

Figure 15. Water-table-elevation contours interpolated from water-table-elevation measurements manually collected in shallow monitoring wells MW 1A–4A and MW 6A–12A on November 18, 2018.



Projection: NAD83(HARN)/Wisconsin Transverse Mercator. Hydrography from National Hydrography Dataset (U.S. Geological Survey, 2016).

points, but the available data suggest that the groundwater flow is west to east (fig. 15).

Short- and long-term fluctuations in the water table were evaluated by monitoring the water-table elevation for 1 year. Measurements were collected using pressure transducers deployed below the water table in MWs 1A–4A and 6A–8A (MW 5A was not accessible during the study period) and a barometric pressure transducer deployed above the water table in MW 8A. Additional pressure transducers were installed in the water-table wells (MWs 9A–12A) on November 11, 2018. Measurements of the water-table elevations were collected every 15 minutes after installation. Pressure transducer measurements were matched to measurements manually collected with a water level sensor every 3 to 4 months and adjusted to account for barometric pressure fluctuations. The resulting time-series from

July 11, 2018, to July 10, 2019, is shown in figure 16. The maximum water-table elevation was measured in the first week of June 2019, following several large recharge events corresponding to snowmelt and spring rain in March through June (fig. 17). A more detailed view of the water-table response to snowmelt shows that the water table responded quickly to water input events and indicates that locally variable lithologies may have influenced the magnitude or duration of the response (fig. 18). For example, several piezometers recorded an increase in the water-table elevation on March 12, 2019, just 1 day before the first measurable reduction in the snowpack. After the snowmelt terminated, the water-table elevation rose from 0.7 to 3.7 ft (table 3). At MWs 7A, 8A, and 10A, the recharge resulting from the snowmelt occurred as a pulse rather than a steady increase, indicating the presence of a low-permeability heterogeneity upon which recharge was

temporarily perched. This conclusion is consistent with slug tests performed at MWs 6A–6B, 7A–7C, and 8A–8C (described in a later section).

Major recharge events also affected the slope of the water table. Between October and March, the water table was relatively flat close to the well fields (MWs 1A, 6A, 7A, 8A). During and after March recharge, stronger gradients developed near MWs 7A, 8A, and 10A and even changed direction for a time (fig. 18). The most evident and persistent change was observed in MW 1A, where the water-table elevation was much lower than in nearby MWs 6A and 7A in the late summer and fall. Between August and September, the water table at this location rose nearly 4 ft and remained steady for the remainder of the winter (fig. 16). The pressure-transducer data showed greater drawdown at MW 1A when the nearby high-ca-

Figure 16. Weekly average head measured at shallow monitoring wells 1A–4A and 6A–12A. Measurements shown from July 2018 to July 2019.

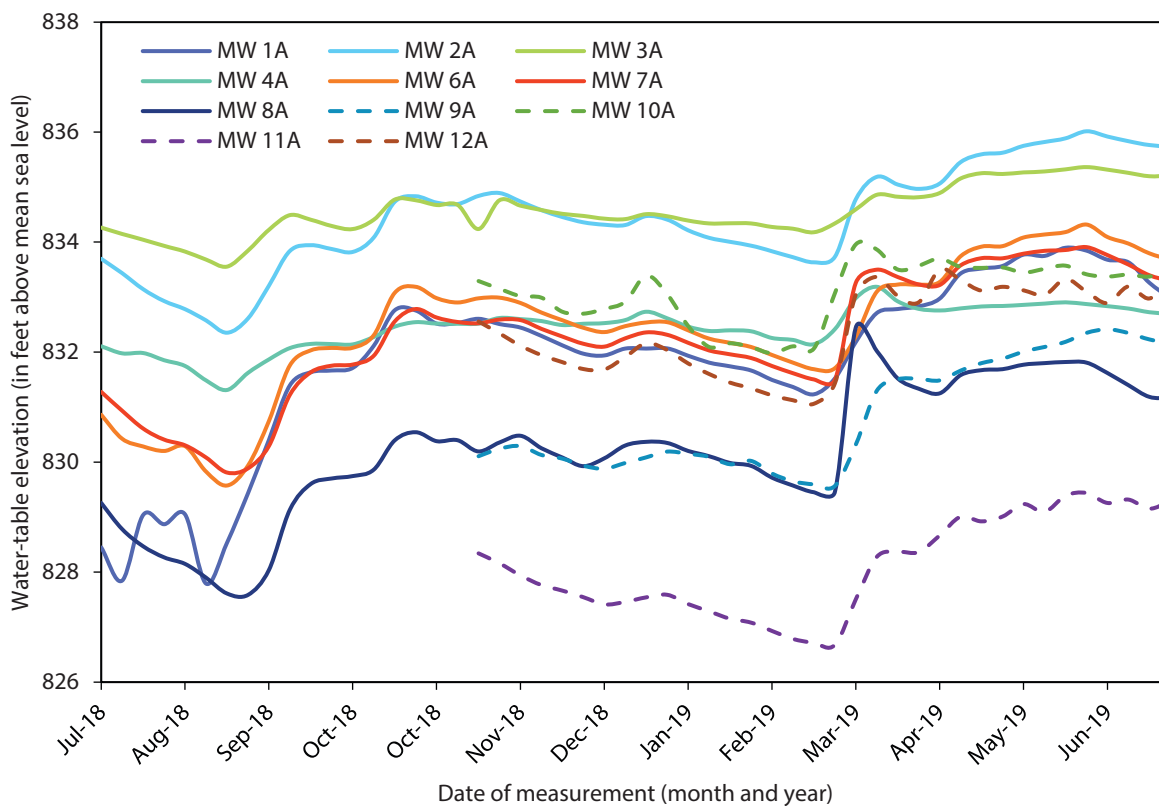


Figure 17. Water-table elevations in shallow monitoring wells 1A–4A and 6A–12A from March 1, 2019, to May 30, 2019, are illustrated alongside depth of snowpack and daily precipitation totals.

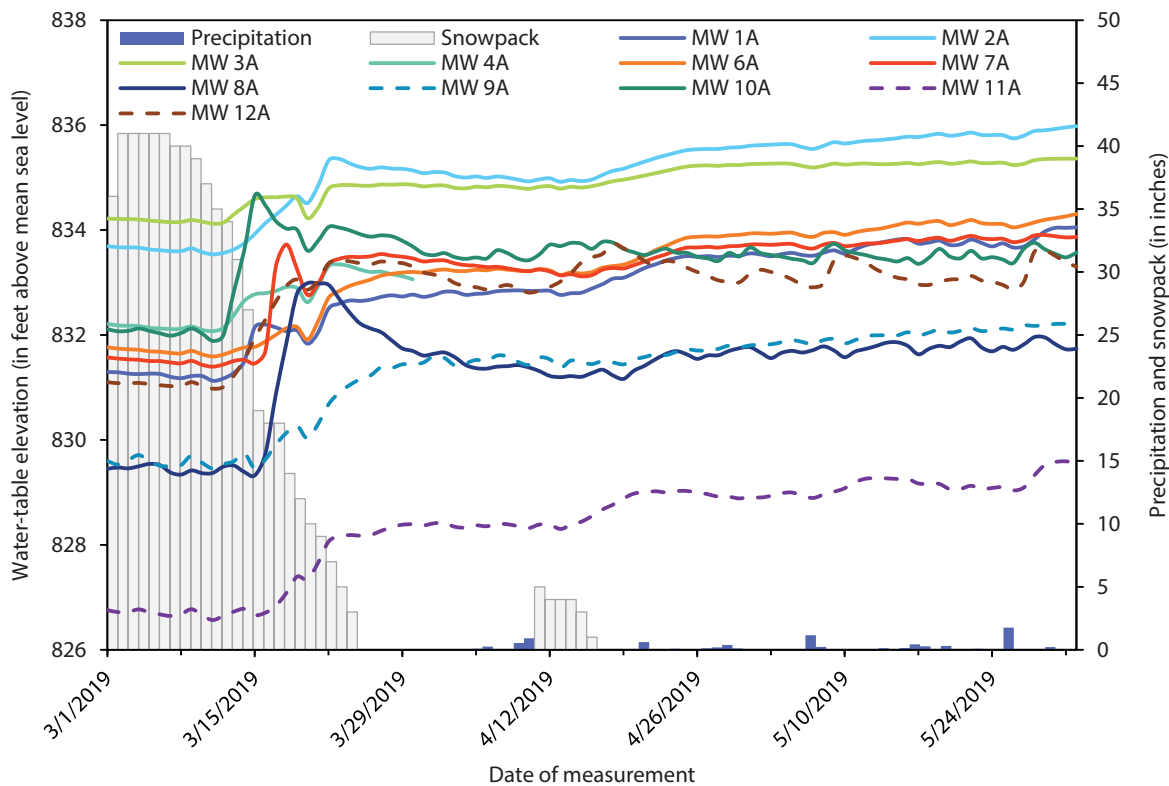
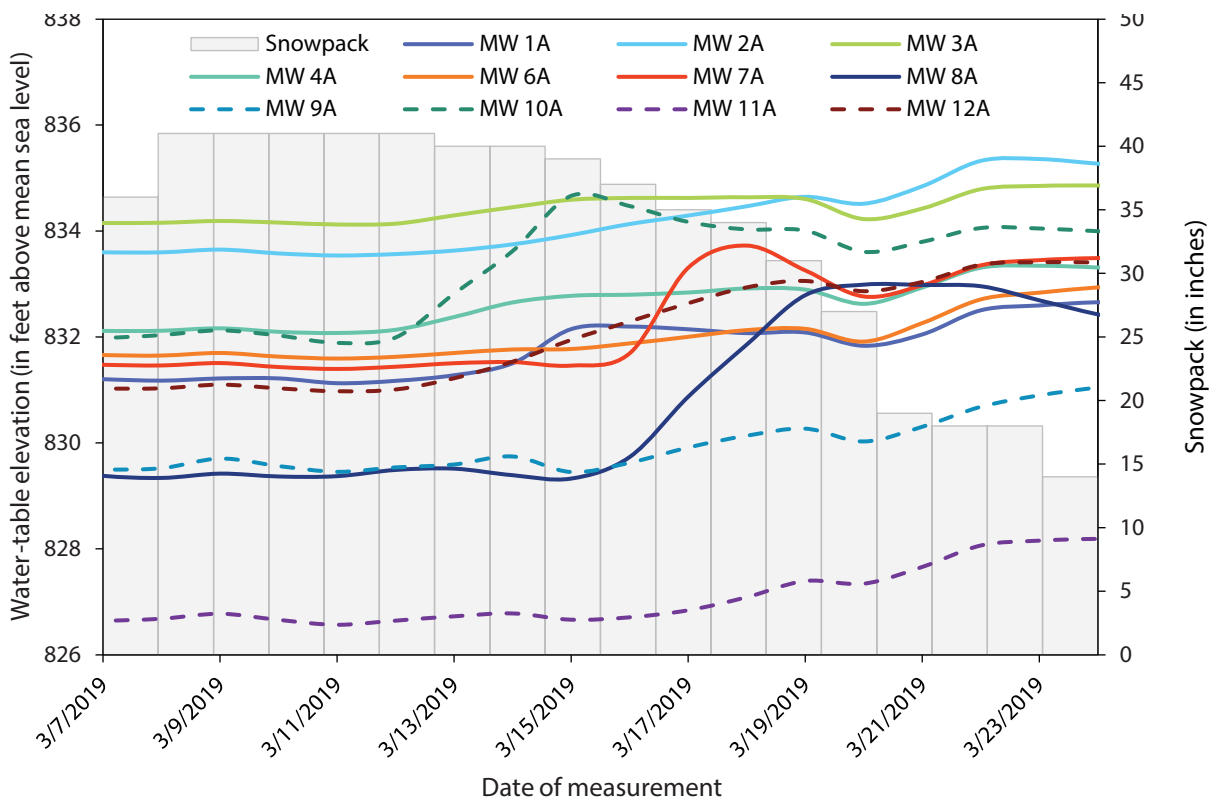


Figure 18. Water-table elevations in shallow monitoring wells 1A–4A and 6A–12A from March 7, 2019, to March 24, 2019, are illustrated alongside the depth of snowpack.



capacity irrigation well (BD773) was activated; withdrawals from that well may explain this temporal trend.

Hydraulic conductivity

Hydraulic conductivity (K) is a measure of how easily fluid moves through porous media. Hydraulic conductivity often ranges from a few inches per day in fine-grained or clay deposits to hundreds of feet per day in coarse sand and gravel. In heterogeneous aquifers, which consist of more than one lithology, hydraulic conductivity can vary greatly among deposits of differing textures. In this study, hydraulic conductivity was estimated using the specific-capacity tests performed during well construction and from slug tests and multi-well pumping tests performed in the field.

Specific-capacity tests

Specific-capacity tests are performed during well construction and the results are reported in WCRs. This process measures the depth to water in a newly drilled well before any pumping is initiated and again after pumping begins. When the rate and duration of pumping are known, the specific capacity (drawdown in cubic feet per day per foot) is calculated as the yield (in cubic feet per day) divided by the drawdown (in feet) and can be used to estimate transmissivity and horizontal hydraulic conductivity. For this study, 751 estimates of hydraulic conductivity were calculated using TGUSS software (Bradbury and Rothschild, 1985) with inputs of drawdown data from WCRs, screen length, screen depth, and the saturated thickness of the aquifer at the well location.

Field measurements

Additional hydraulic conductivity data were acquired through multi-well pumping tests and slug tests performed on August 27, 2018. Multi-well pumping data were collected for study well #6 (WUWN BH470) and a neighboring irrigation well (WUWN BD773). Drawdown in monitoring wells 6A, 7A, and 8A was measured by pressure transducers that were deployed before the onset of pumping at each well. The Theis model for an unconfined aquifer (Theis, 1935) was used to calculate horizontal hydraulic conductivity at each location. Slug tests were performed at nested monitoring wells 6A–6B, 7A–7C, and 8A–8C by lowering a pressure transducer 15 ft below the water surface and then dropping a slug (a cylindrical piece of composite material with a known volume) into the well. The pressure transducers recorded the total displacement and the time required for the water level to return to equilibrium. The Kansas Geological Survey's model (Hyder and others, 1993) was used to calculate horizontal hydraulic conductivity from these data (table 4).

Table 3. Maximum, minimum, and range of observed head values from March 7, 2019, to March 24, 2019.

Monitoring well	Maximum head (ft)	Minimum head (ft)	Range (ft)
1	832.7	831.1	1.5
2	835.4	833.5	1.8
3	834.9	834.1	0.7
4	833.3	832.1	1.3
6	832.9	831.6	1.3
7	833.7	831.4	2.3
8	833.0	829.3	3.7
9	831.0	829.5	1.6
10	834.7	831.9	2.8
11	828.2	826.6	1.6
12	833.4	831.0	2.4

Table 4. Field measurements of horizontal hydraulic conductivity.

Test well	Type of test	Estimated conductivity, K (ft per day)
BH470 (study well #6)	Multi-well pumping test	490
BD773	Multi-well pumping test	2.2
MW 6A	Slug test	43
MW 6B	Slug test	0.78
MW 7A	Slug test	2.8
MW 7B	Slug test	0.78
MW 7C	Slug test	1.0
MW 8A	Slug test	1.7
MW 8B	Slug test	0.88
MW 8C	Slug test	2.3

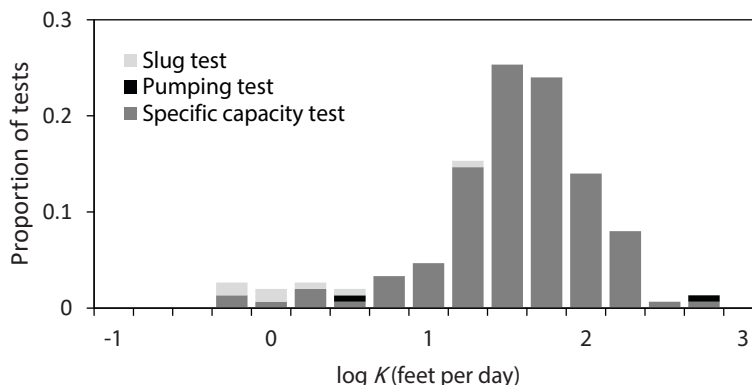
Results

The combined results of hydraulic conductivity estimates obtained through these methods are summarized in table 5 and figure 19. The geometric mean of hydraulic conductivity estimates in the glacial aquifer is 36 ft/d with a range of 0.09 to 1,432 ft/d. The observed range of hydraulic conductivity underscores the degree of heterogeneity observed in this aquifer.

Vertical groundwater flow

In typical unconfined groundwater-flow systems, downward vertical gradients develop in recharge areas and upward gradients develop in discharge areas. Vertical gradients can also be induced by pumping (Börner and Berthold, 2009). For this study, the piezometers installed at intermediate and deep screen depths relative to the monitoring wells allowed for the determination of vertical hydraulic gradients that developed in local groundwater-flow systems. An example of hydraulic-head measurements for each of the nested monitoring wells and piezometers is provided in table 6. Additional measurements are provided in appendix A. The hydraulic heads recorded on November 28, 2018 (table 6), indicate that vertical hydraulic gradients are present at several nested monitoring-well locations. Strong downward gradients observed between MW 4A and piezometers MW 4B and MW 4C correspond to a local topographic high, so this gradient is most likely driven by recharge. This conclusion is consistent with the result of an SWB model (Westenbroek and others, 2010)

Figure 19. Distribution of hydraulic conductivity estimated from specific-capacity tests, multi-well pumping tests, and slug tests. Abbreviations: K = conductivity.



used to estimate potential recharge, where recharge at this site is higher than in the surrounding area (see “Climate and recharge,” below).

At three of the nested monitoring-well locations, upward vertical gradients were observed between the shallow monitoring wells (MWs 3A, 6A, and 8A), the intermediate-depth piezometers (MWs 3B, 6B, and 8B), and the deep piezometers (MWs 3C, 6C, and 8C). These gradients likely resulted from pumping at nearby municipal and (or) irrigation wells. Slug tests performed at MW 6A and 6B (table 4) show a greater decrease in hydraulic conductivity with depth (43 ft/d compared with 0.78 ft/d), indicating the presence of low-conductivity subsurface heterogeneity, such as a clay or silt lens in mainly sandy strata. Between MW 7A, 7B, and 7C, the vertical gradients were divergent with the highest hydraulic head recorded in the intermediate-depth piezometer (7B). Given the proximity of this nested monitoring

well to a high-capacity well (study well #6), this divergence may have been the result of the combined effects of nearby pumping with a local subsurface heterogeneity, such as a low-conductivity lens sandwiched between two layers of high-conductivity material.

Hydrostratigraphy

The WDNR database (Wisconsin Department of Natural Resources, 2020c) provided detailed descriptions of the lithology corresponding to each WCR and was also used to characterize the subsurface properties of the glacial aquifer contained within the model domain. These data were imported into borehole logs using the Rockworks 17 software package (Rockware, Golden, Colo.) and subsequently used to generate a three-dimensional solid model of the subsurface with dimensions equal to the model domain. The three-dimensional model is based on a proprietary lithology algorithm that extrapolates the lithology between boreholes and displays the interpolated space accordingly. The resulting model indicates that deposits of sand, gravel, clay, and other lithologies are discontinuous throughout the subsurface of the model domain and may lack clear or distinct boundaries. The thickness of individual deposits is small relative to the extent of the aquifer and is unlikely to greatly influence the overall direction of horizontal groundwater flow,

Table 5. Hydraulic conductivity data points, by type of test.

	Slug test	Specific-capacity test	Multi-well pumping test
Number of tests	8	751	2
Minimum (ft/day)	0.78	0.90	2.2
Maximum (ft/day)	43	897	490
Geometric mean (ft/day)	7.5	48	NA

NA = not available.

Table 6. Data from the U.S. Geological Survey's monitoring-well network for the City of Waupaca, Wisc.

Well number	Screen or piezometer ¹	Depth-to-water (feet) ²	TOC elevation (feet)	Total head (feet)	Screen elevation (top)	Screen elevation (bottom)	Vertical gradient ³
MW 1	A	9.29	843.9	834.61	828.9	818.9	
	B	NT	843.9	NT	802.9	797.9	
	C	NT	843.9	NT	778.9	768.9	
MW 2	A	10.38	847.1	836.72	833.1	822.1	
	B	10.38	847.1	836.72	812.1	797.1	0
	C	NT	847.1	NT	789.1	772.1	
MW 3	A	12.55	849.02	836.47	839.02	824.02	
	B	12.46	849.02	836.56	816.02	801.02	0.01125
	C	12.37	849.02	836.65	791.02	773.02	0.009
MW 4	A	11.4	846.08	834.68	836.08	821.08	
	B	11.4	846.08	834.68	814.08	799.08	0
	C	12.13	846.08	833.95	789.08	771.08	-0.073
MW 5	A	NT	846.09	NT	826.09	821.09	
	B	NT	846.09	NT	806.09	801.09	
	C	NT	846.09	NT	782.09	772.09	
MW 6	A	11.14	846.91	835.77	836.91	821.91	
	B	11.14	846.91	835.77	811.91	796.91	0
	C	10.5	846.91	836.41	788.91	771.91	0.08
MW 7	A	11.25	846.33	835.08	836.33	821.33	
	B	11.02	846.33	835.31	811.33	796.33	0.023
	C	11.03	846.33	835.3	788.33	771.33	-0.00125
MW 8	A	12.05	845.32	833.27	835.32	820.32	
	B	11.8	845.32	833.52	810.32	795.32	0.025
	C	11.4	845.32	833.92	787.32	770.32	0.05

Abbreviations: NT = not taken; TOC = top of casing.

¹A = screened shallow well; B = intermediate-depth piezometer; C = deep piezometer.

²Collected on November 14, 2018. Where value is listed as NT, depth-to-water measurement was not taken due to clogging (MW 1B and 1C) or inability to access the well (MW 2C and all of MW 5).

³Where values are positive, vertical gradients are upward.

but it may have small-scale effects on vertical groundwater flow. To account for these heterogeneous deposits in the groundwater-flow model (see Section 3), the subsurface was divided into three model layers and the spatial variation of hydraulic properties in each layer were represented as zones, as defined below.

Stratigraphic layers

Because the modeled area lacks distinct stratigraphic units, the three vertical layers discussed in the modeling section of this report were defined by thickness. The primary goal of defining these layers was to develop a groundwater-flow model that captured vertical transport variabilities that may have influenced the well-capture zone while also allowing deeper groundwater to pass below the well screens. From bottom to top, the boundaries of the three layers are defined as follows:

1. Layer 3 is a 50-ft-thick layer of unconsolidated sand and gravel deposits immediately above the crystalline bedrock surface. A raster grid of bedrock elevation served as the lower boundary for this layer and a raster grid of the upper boundary (layer 3's top) is equal to bedrock elevation plus 50 ft for each grid cell. The study wells were screened approximately 50 ft above the crystalline bedrock, so groundwater that penetrated this layer was not captured by the pumping well in groundwater-flow models.
2. Layer 2 is a 25-ft-thick layer of unconsolidated sand and gravel deposits that lies immediately above layer 3. The upper boundary is represented as a raster grid equal to bedrock elevation plus 75 ft (layer 2's top).
3. Layer 1 is the top layer. The upper boundary is a raster grid of surface elevation prepared from digital elevation model (DEM) data from U.S. Geological Survey (2017; see fig. 5). The thickness of layer 1 ranges from 1 to 15 ft in modern streambed channels to 150 ft thick beneath glacial drumlins composed of till.

For each of the three model layers, spatial variabilities in hydraulic properties were established by classifying lithologic deposits into hydraulic conductivity zones. At each WCR point in the model domain, lithologic descriptions were examined to determine the dominant sediment texture between the upper and lower boundaries of each model layer. An integer value corresponding to different sediment types was assigned to each point in the layer (table 7). These integer values served as the basis for constructing Thiessen polygons in each model layer using the "Create Thiessen Polygons" tool in ArcMap software. A Thiessen polygon is an irregular polygon that defines an area of influence around its sample point. Unlike methods that interpolate values between two points, Thiessen polygons allow for nonconsecutive values to occupy adjacent areas; for instance, a clay layer (value = 1) can be adjacent to a gravel layer (value = 6) without a transition through intermediate materials. Using editing tools in ArcMap software, the Thiessen polygons were reclassified into three hydraulic conductivity zones, where the hydraulic properties tended toward the same order of magnitude. Adjacent, same-value polygons were merged into a single feature. The result-

ing polygon features were "smoothed" to produce generalized maps of the hydraulic conductivity zones for each layer (fig. 20).

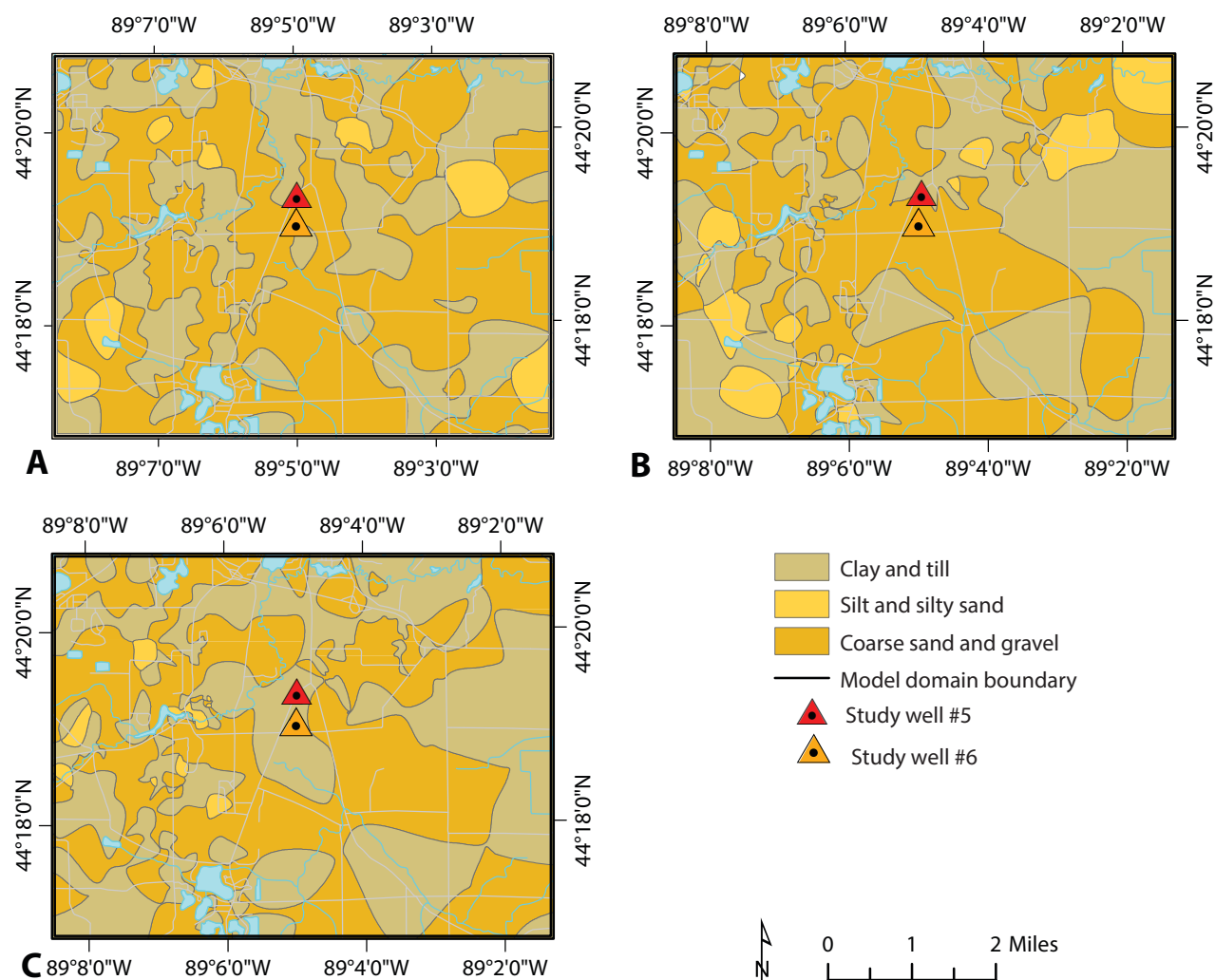
Climate and recharge

The mean temperature in this region is 44.6 °F and rainfall and snowfall average 33.5 and 44.3 inches per year (in./yr), respectively (National Centers for Environmental Information, 2019). Winters are characteristically cold and snowy and below-freezing temperatures are common; summers can be hot and humid. As seen in the pressure transducer data (fig. 16), most groundwater recharge in this area occurs in late spring and early summer. The total volume of recharge entering the groundwater system is an important part of the overall water balance and a required input for groundwater-flow models. Recharge is also the primary mechanism by which surface-derived contaminants are transported to groundwater. Because this study aims to better understand the relation between land cover and groundwater quality, a spatially variable estimate of groundwater recharge was prepared using an SWB model.

Table 7. Sediment groups and integer values used to define hydraulic conductivity zones in model layers 1 through 3.

Prime lithology derived from well construction report description	Sediment type	Integer value	Hydraulic conductivity zone
Clay	Clay	1	Clay and till
Hardpan	Clay	1	Clay and till
Mud or muck	Clay	1	Clay and till
Clay and gravel	Clay	2	Silt and silty sand
Gravel/cobbles/boulders/stones	Till	3	Clay and till
Till	Till	3	Clay and till
Sand	Sand	4	Sand and gravel
Sand and clay	Sand and clay	5	Clay and till
Sand and gravel	Sand and gravel	6	Sand and gravel
Silt	Silt	7	Silt and silty sand

Figure 20. Generalized lithologic maps created by smoothing Thiessen polygons. A, layer 1; B, layer 2; C, layer 3.



Roads from U.S. Census Bureau, 2015. Hydrography from U.S. Geological Survey National Hydrography Dataset, 2016. Wisconsin Transverse Mercator projection, 1991 Adjustment to the North American Datum of 1983 (NAD 83/91); EPSG 3071.

Soil-water-balance model

Groundwater potential recharge was estimated through the application of a soil-water-balance (SWB) model (Westenbroek and others, 2010) to the model domain. The SWB model used a modified Thornthwaite-Mather method to track the storage and flow of soil moisture across a grid over daily time steps to estimate the potential recharge beyond the root zone. The input data included land-surface topography, soil type, land use, available water storage, and climate. The output was a gridded dataset of mean daily potential recharge (in feet per day) for the specified time

period. A comprehensive description of this model is provided by Bradbury and others (2017).

Direction of overland flow

The SWB model uses a raster grid containing topographic data to determine surface-water flow direction and a route for surface runoff. For this study, a standard flow direction tool in ArcMap's software was applied to a 6-ft-resolution, lidar-based, surface-elevation dataset to calculate flow direction. Because many digital elevation datasets contain small imperfections that can lead to errors when calculating flow direction, a stan-

dard closed-depression fill routine was applied to the dataset before calculating the flow direction.

Hydrologic soil group and available water storage

The soil hydrologic groups were based on the soil's potential for infiltration by drainage runoff and ranged from low (A) to high (D). A digital soil map is publicly available in the Soil Survey Geographic Database (SSURGO; Natural Resources Conservation Service, 2018). A subset of these data for Waupaca County included coverage of the modeled area and was used in this study. Some units were classified with a dual designation such

as A/B, indicating artificial drainage. Because artificial drainage ultimately becomes runoff, these units were reclassified to the higher runoff category, B. The available water storage is a measure of a soil's ability to retain water and is measured in inches of water per foot of soil. For this study, the available water storage data were also obtained from SSURGO.

Land cover

The 2006 land-cover map from the National Land Cover Database (Multi-Resolution Land Characteristics Consortium, 2011) was selected to provide land-cover data for the modeled area. These data were used to estimate interception, runoff, evapotranspiration, and root-zone depth for different types of vegetation.

Daily temperature and precipitation

The SWB model uses a tabular dataset of observed daily temperature and precipitation, which is provided by the Global Historical Climatology Network (GHCN) and is publicly available at the National Oceanographic and Atmospheric Administration's Climate Data Online website (National Centers for Environmental Information, 2019). Data from station 478951 in the City of Waupaca, Wisc., were acquired for the years 2011 to 2018.

Running the SWB model

Data grids for the input maps (flow direction, hydrologic group, available water storage, and land cover) were prepared from the source datasets. Daily climate data for minimum, maximum, and average temperature and for total precipitation were tabulated. The model was run eight times to produce a recharge estimate for each of the modeled years (2011–2018).

Results

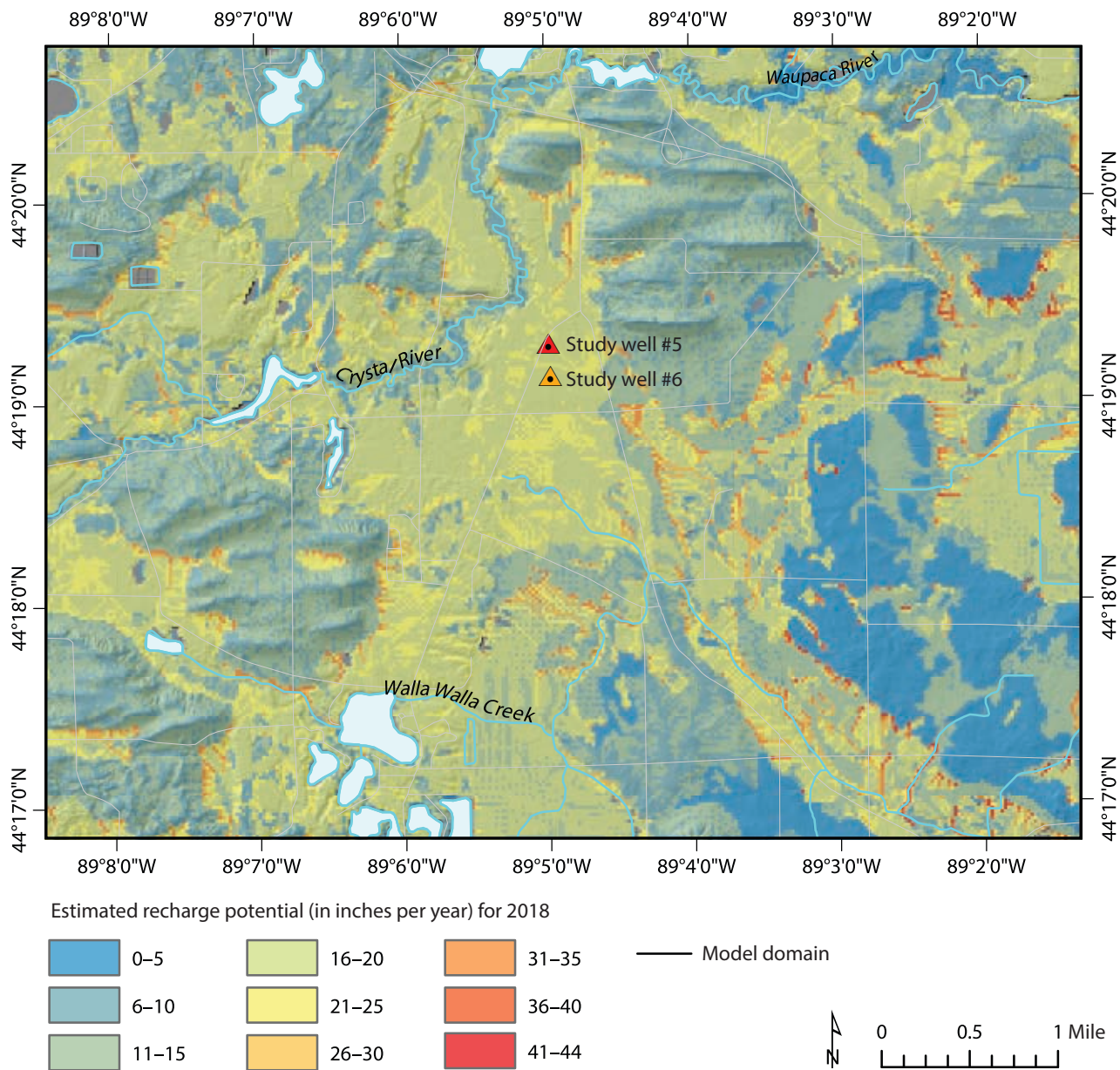
The SWB model simulated the annual soil-water budget for each year from 2011 to 2018, yielding eight results (table 8). The results from 2018 are shown in figure 21; the areal mean potential recharge in 2018 was 13.7 in. Each SWB model grid was manually edited to include the estimated recharge from irrigation. The irrigation rate was calculated by dividing the total annual water-use volume (in cubic feet) for each irrigation well by the irrigated land area (in square feet) corresponding to that well. The irrigation recharge was assumed to be 20 percent of the applied water (Bradbury and others, 2017).

Where applied, the average irrigation recharge in the modeled area is 0.63 in./yr, which is less than 5 percent of the annual mean recharge, so irrigation recharge is probably less important than the overall recharge rates. The spatial distribution of groundwater recharge strongly correlates to the surface geology. For instance, the lowest recharge is generally observed in areas dominated by the glacial till that forms the steep drumlins. However, high recharge is observed at the base of the drumlins where the runoff accumulates. Moderate recharge occurs across glacial-outwash plains, which are composed of sand and gravel. The lowest recharge rates are observed in highland areas, stream valleys, and areas where the surface is dominated by peat.

Table 8. Mean potential recharge within the model domain estimated by the soil-water-balance model for 2011 to 2018.

Year	Mean potential recharge (in./yr)
2011	10.8
2012	6.0
2013	7.8
2014	10.4
2015	6.9
2016	7.8
2017	6.9
2018	13.7

Figure 21. Estimated recharge potential for 2018.



Roads from U.S. Census Bureau, 2015. Hydrography from U.S. Geological Survey National Hydrography Dataset, 2016. Wisconsin Transverse Mercator projection, 1991 Adjustment to the North American Datum of 1983 (NAD 83/91); EPSG 3071.

Section 2: Land cover and water quality

Objectives

The second section of this study presents the historical land-cover, water-use, and water-quality data that were used to help develop a conceptual model of the relation between land cover and nitrate concentrations in groundwater in the model domain. The sources of these data included the U.S. Department of Agriculture's publicly available Cropland Data Layer (CDL) for land cover for each year from 2008 to 2018 (National Agricultural Statistics Service, 2020) and WDNR water-use data (Wisconsin Department of Natural Resources, 2020a). Water-quality data were provided by Justin Berrens (Director of Public Works, City of Waupaca, Wisc., 2019, written communication).

Land cover

The CDL for each year is a set of georeferenced, crop-specific, historical land-cover data that is derived from satellite imagery and onsite agricultural data. Inside the model domain, the current land-cover dataset includes low-density developed land, grasslands, mixed forest, wetlands, shrubs, and mixed agriculture (fig. 22). Data from previous crop years (see appendix B) show that the eastern half of the model domain has been dominated by agricultural activity since at least 2008. The primary crops grown include corn, alfalfa, and soybeans. Infrequent rotations of red beans, miscellaneous vegetables, and other grains were also reported. The western half of the model domain remains largely uncultivated, except for the region between Jenson Lake and the Crystal River near the western boundary of the model domain.

Four agricultural-use properties (parcels 1 through 4) in the model domain were selected as areas of interest with respect to the elevated nitrate concentrations in study wells #5 and #6 (fig. 23). These parcels were chosen on the basis of the general direction of groundwater flow, the effects of pumping, and the land-cover types most likely to contribute nitrate to the groundwater. The CDLs from 2008 to 2018 show that parcel 1 is used for pasture or grazing and the cultivation of alfalfa, soybeans, and corn. Although they are physically separated, parcels 2 and 3 are cultivated by a single operator who grows a rotation of alfalfa, soybeans, corn, and dry beans. Parcel 4, located adjacent to the northeastern corner of parcel 1 alongside County Highway E, is treated separately from parcel 1 because of its distinct land use. This parcel is less than half an acre in size, but it is occupied by an unlined manure lagoon serving more than 100 head of cattle. According to aerial photographs and land-ownership records, parcel 4 has been allocated for this use since at least 1994 (Justin Berrens, Director of Public Works, City of Waupaca, Wisc., 2019, written communication). Parcel 4 is a potentially distinct source of nitrate to the groundwater in study wells #5 and #6 because of their proximity.

Water use

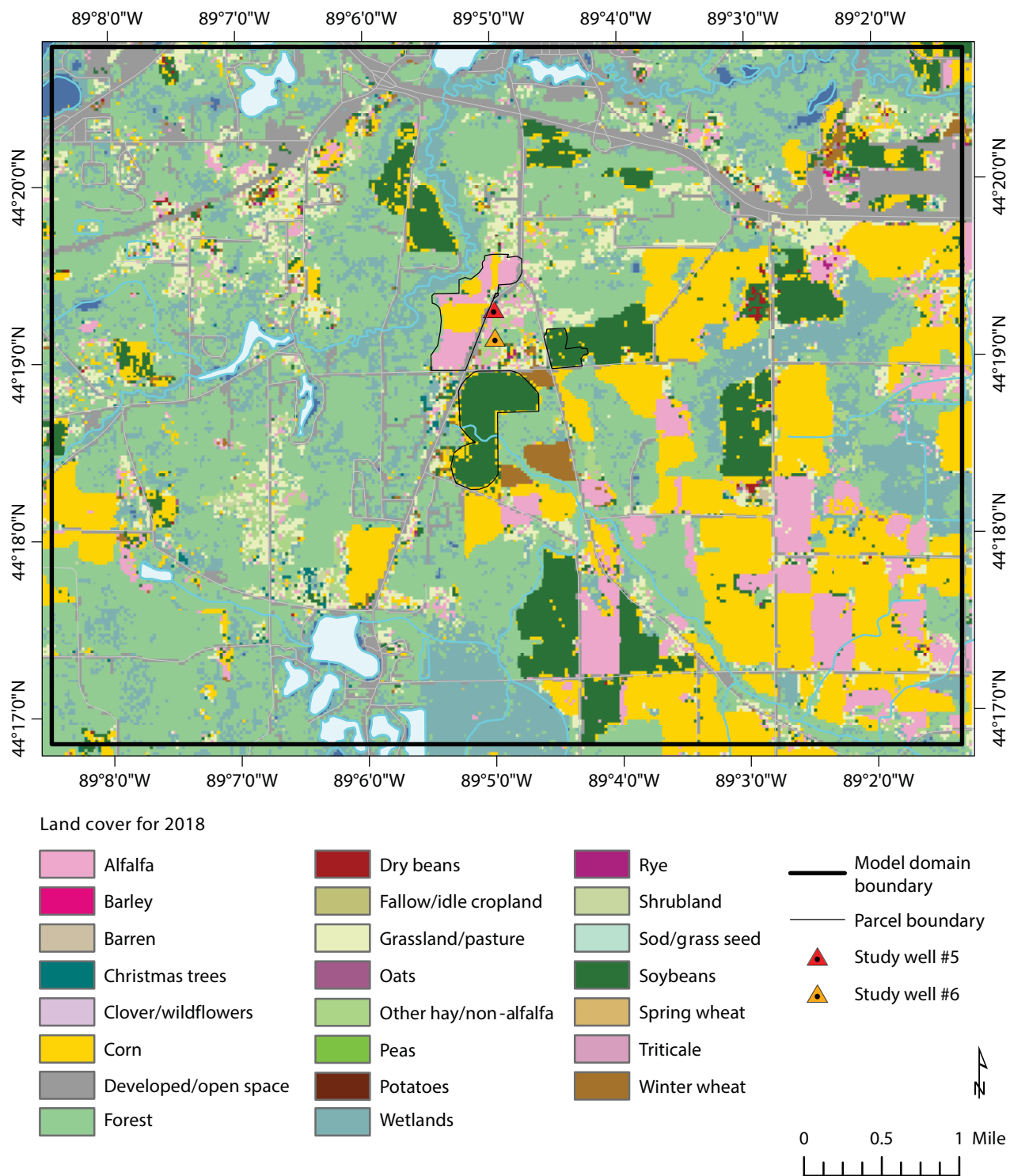
The WDNR maintains a public database of all high-capacity wells (capacity greater than 100,000 gallons per day) in Wisconsin (Wisconsin Department of Natural Resources, 2020b). As of 2019, this database contained records of 18 active high-capacity wells within the study area, including the two municipal wells (study wells #5 and #6) that are the subject of this study (table 9). These and the other high-capacity wells in the study area are screened at depths ranging from 75 to 170 ft below the land surface and extract water from the glacial aquifer.

Water quality

Records of nitrate concentrations in water from the City of Waupaca's municipal wells and in the USGS/WGNHS monitoring wells have been maintained by the City of Waupaca's Department of Public Works since 1994. These records were provided by Justin Berrens (Director of Public Works, City of Waupaca, Wisc. 2019, written communication) and were used to explore historical trends in nitrate concentrations that originated from different parts of the study area.

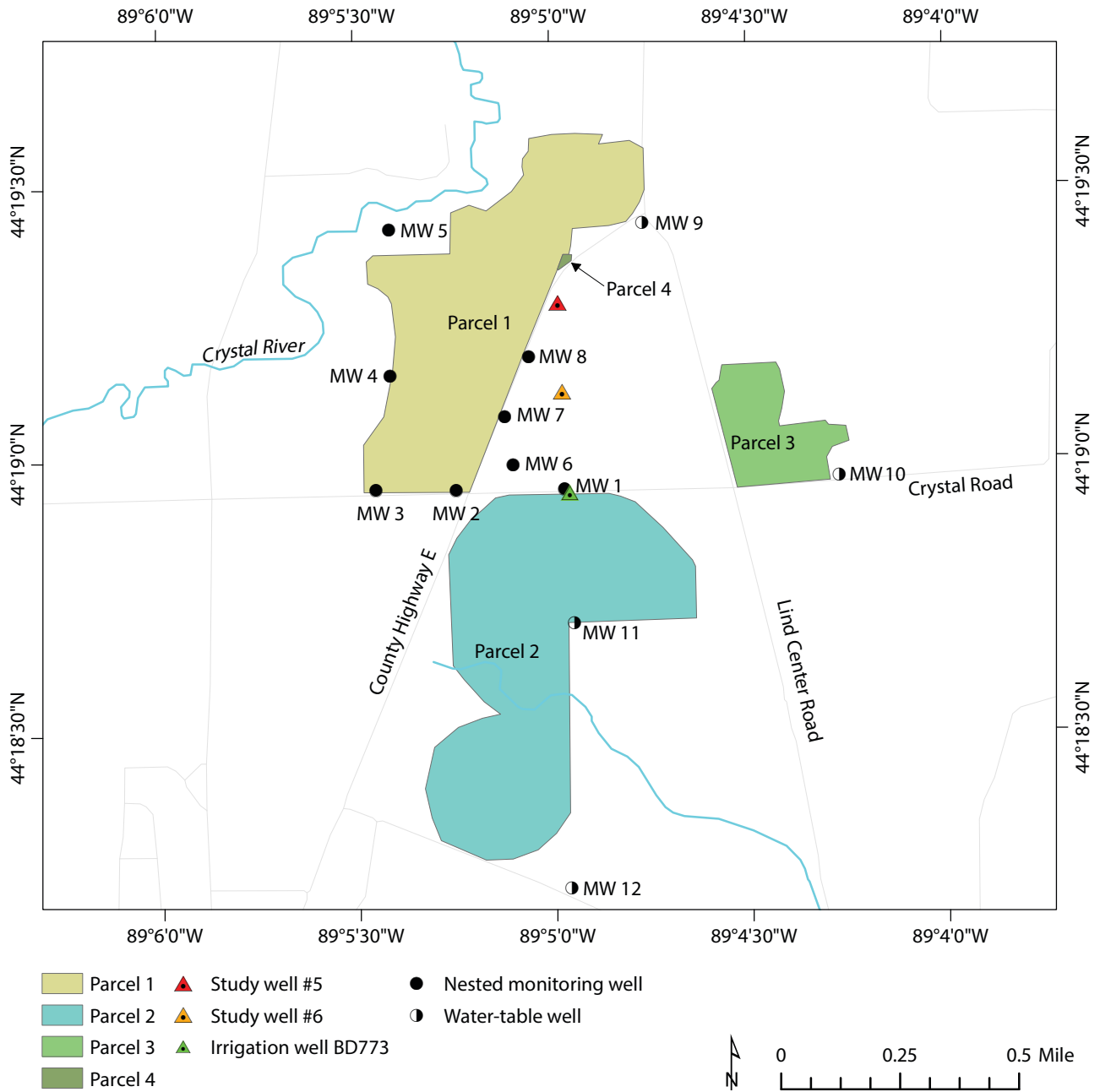


Figure 22. Cropland Data Layer (National Agricultural Statistics Service, 2020) for 2018. Parcels 1 through 4 (see figure 23) are considered potential contributors to elevated nitrate concentrations observed in study wells #5 and #6.



Roads from U.S. Census Bureau, 2015. Hydrography from U.S. Geological Survey National Hydrography Dataset, 2016. Wisconsin Transverse Mercator projection, 1991 Adjustment to the North American Datum of 1983 (NAD 83/91); EPSG 3071.

Figure 23. Parcels designated as areas of interest with respect to elevated nitrate concentrations in the study wells.



Roads from U.S. Census Bureau, 2015. Hydrography from U.S. Geological Survey National Hydrography Dataset, 2016. Wisconsin Transverse Mercator projection, 1991 Adjustment to the North American Datum of 1983 (NAD 83/91); EPSG 3071.

Table 9. High-capacity-well withdrawals in the vicinity of the modeled area.

Wisconsin unique well number ¹	Depth (in feet)	2013	2014	2015	2016	2017	2018
Public supply (in gallons per year)							
*BH469	84	279,530,000	327,312,000	357,497,000	229,041,000	170,844,000	177,803,000
*BH470	75	107,038,000	110,324,000	110,390,000	86,219,000	97,520,000	82,634,000
BH446	NA	570,920	660,625	618,555	485,520	370,270	480,345
SP831	168	2,106,000	2,196,000	2,106,000	2,556,000	1,980,000	2,556,000
IB475	144	67,550	67,550	62,790	61,565	60,555	76,055
MR762	141	3,071,658	3,346,730	3,817,454	3,040,290	1,769,141	2,898,369
BH447	NA	129,430	133,070	176,155	142,800	128,840	157,290
NO374	110	6,751,000	12,509,281	16,581,542	5,330,425	3,818,825	3,769,676
NO371	161	598,137	764,579	34,336	54,169	43,781	17,119
Irrigation (in gallons per year)							
BD773	75	22,275,000	13,027,500	9,900,000	12,420,000	13,590,000	9,740,000
YD748	87	NA	NA	NA	NA	7,995,000	5,109,000
BD751	NA	17,451,000	9,438,000	8,424,000	8,112,000	8,302,000	13,182,300
WM032	96	17,664,100	5,605,600	8,193,700	3,098,246	1,163,900	6,721,400
NO372	170	5,875,677	10,011,888	3,160,680	2,747,245	3,164,519	2,288,424
VC300	135	9,619,200	9,447,408	7,843,692	1,774,807	1,317,600	2,938,421
WM517	108	17,008,800	7,733,100	12,067,200	5,256,000	7,549,200	13,010,800
EO717	114	38,340,000	22,039,200	34,066,800	20,072,000	34,814,300	30,228,830
Non-irrigation agriculture (in gallons per year)							
FT375	68	NA	NA	NA	NA	571,100	589,500

¹Data available through the Drinking and Groundwater Use Information System (Wisconsin Department of Natural Resources, 2020a).

*Study wells #5 (BH469) and #6 (BH470). Abbreviation: NA = not available.

Monitoring wells

Beginning in May 1994, the city sampled each well two to four times per year for nitrate. The only exception was in 2015, when no samples were collected from any of the monitoring wells. From 2004 to 2018, only shallow well (A) samples were collected regularly. During this period, the B and C piezometers were sampled twice for nitrate in 2010 and once in 2018. The historical trends of nitrate concentrations in groundwater observed in the shallow monitoring wells and intermediate-depth and deep piezometers are presented in figures 24 and 25, respectively. These figures highlight several general conclusions regarding the occurrence of nitrate in the model domain: (1) nitrate in ground-

water is pervasive, (2) nitrate in groundwater has been elevated since at least 1994, (3) nitrate is most concentrated in shallow groundwater, and (4) nitrate in shallow groundwater is more temporally variable than in deeper groundwater.

The highest nitrate concentrations were most commonly observed in shallow monitoring wells MW 1A and MW 8A. The location of these two monitoring wells with respect to the projected groundwater-flow paths (fig. 15) from those parcels is a strong indication that agricultural activities were a major source of nitrate to groundwater in this region.

MW 1A is located on the northern side of Crystal Road, directly adjacent to parcel 2 (fig. 23). Historical and recently interpolated maps of the water table (figs. 2, 14, 15) indicate that groundwater at this location flows from the south or southwest. According to measurements collected between 2016 and 2018, the average depth to water at MW 1A was 13.7 ft. SWB model simulations for each of the years 2011 to 2018 estimated that the average potential recharge was around 9 in./yr. To reach the top of the MW 1A screen, recharge would have to have been displaced vertically downward approximately 3.3 ft and, assuming the porosity (θ) of the aquifer material is between 0.2 and 0.3, the necessary displacement could

Figure 24. Observed nitrate concentrations in nested monitoring wells MW 1 through MW 4 from 1993 to 2018.

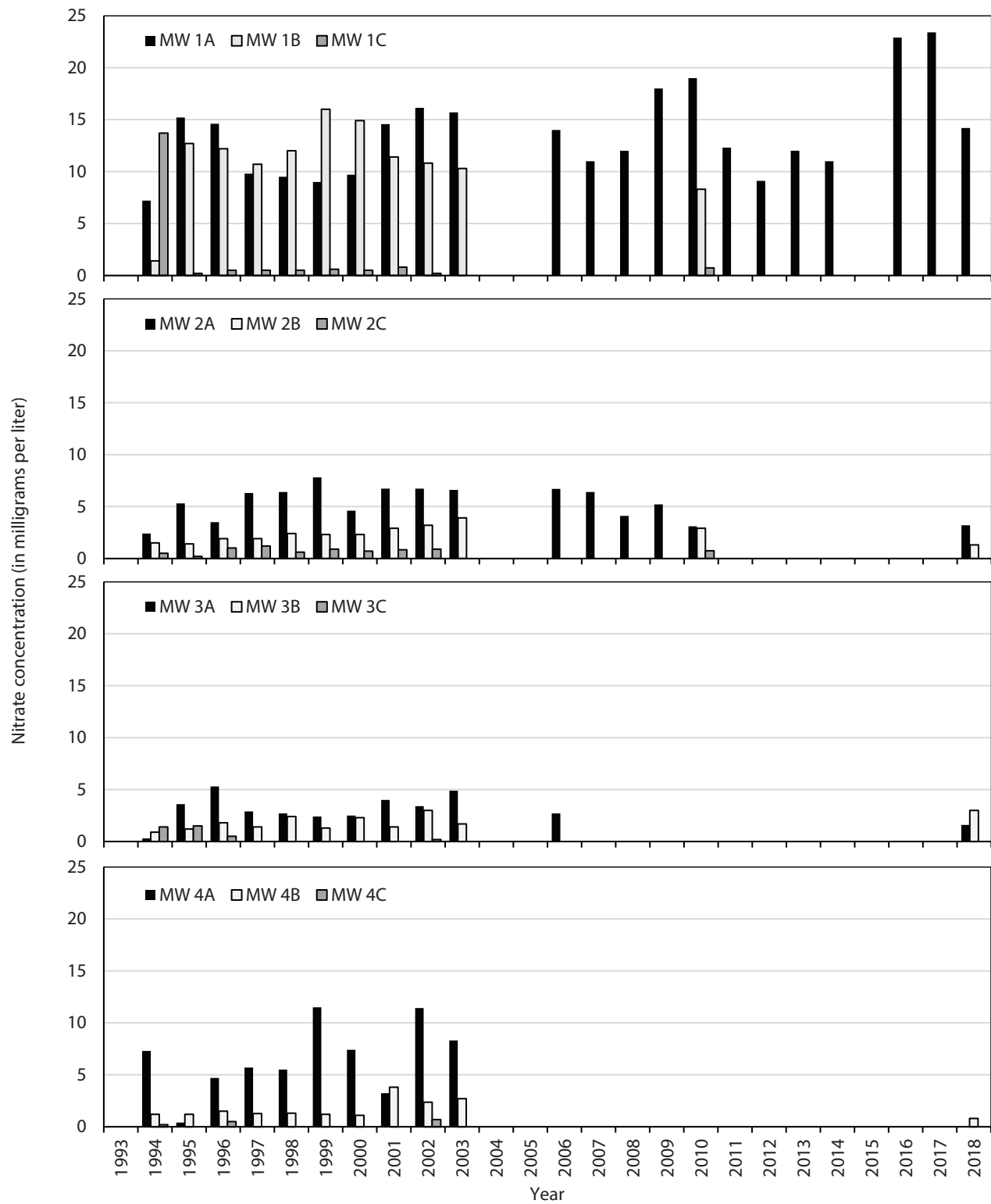
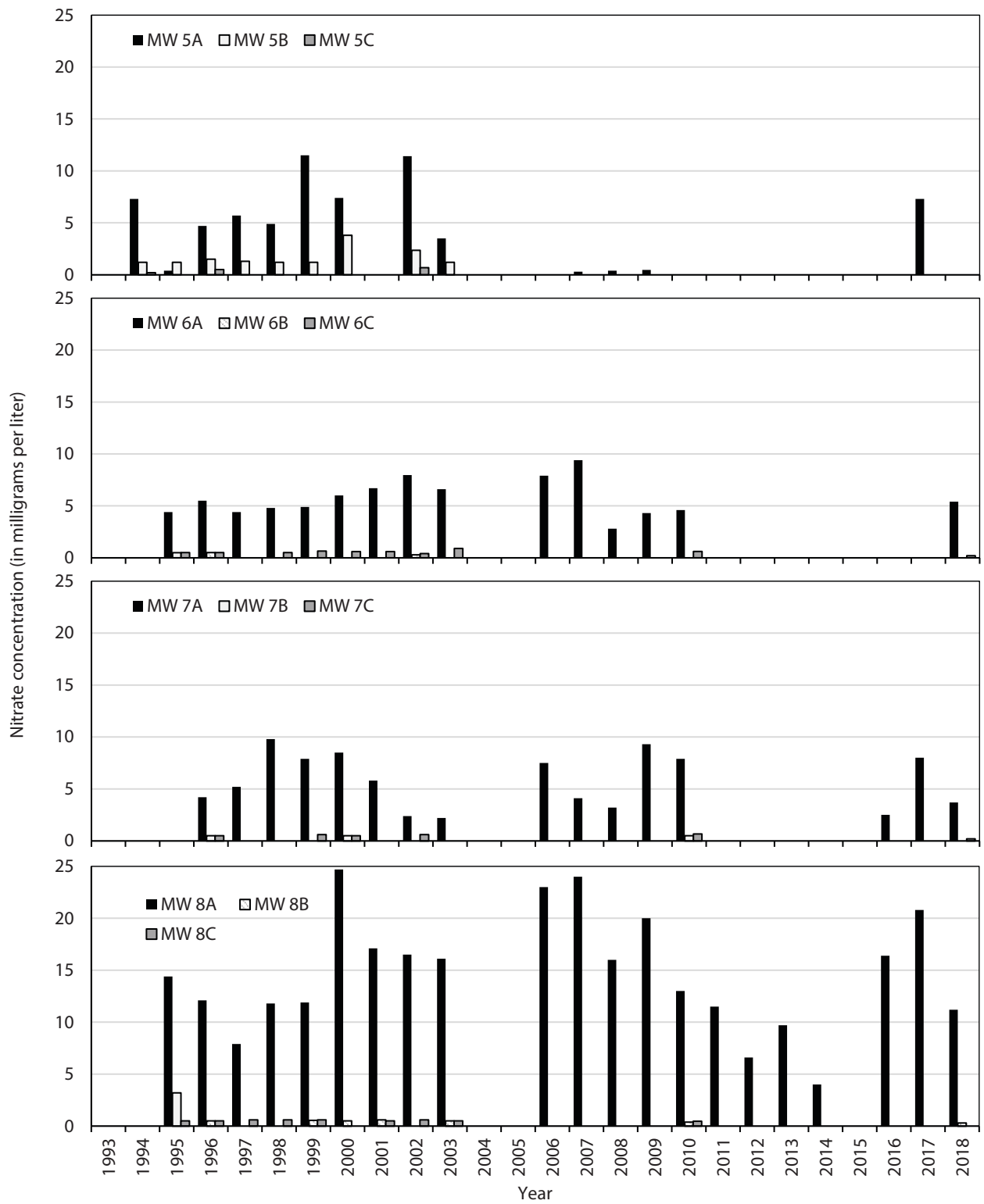


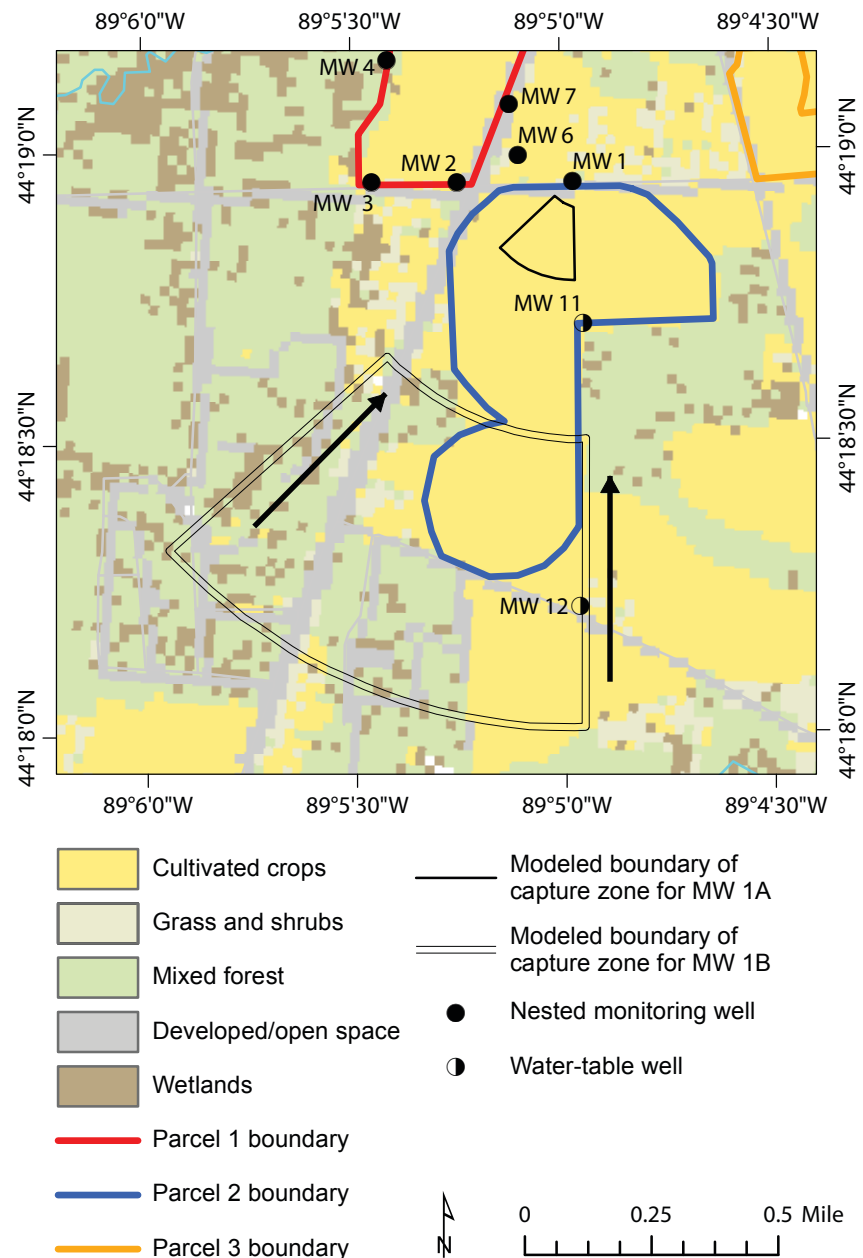
Figure 25. Observed nitrate concentrations in nested monitoring wells MW 5 through MW 8 from 1993 to 2018.



have occurred in 12 to 15 months. Local pumping tests and slug tests indicated that hydraulic conductivity near MW 1A was in the range of 1 to 2 ft/d, so water of that age would have traveled between 250 and 700 ft horizontally since recharge. Similarly, water passing through the 41- to 46-ft-deep piezometer screen at MW 1B probably recharged 7 to 8 yr earlier. When these assumptions are used to trace groundwater from well screens back to the surface along projected flow paths, the results indicate that groundwater sampled from MW 1A originated as recharge in the northeastern corner of parcel 2 (fig. 26). Similar calculations suggest that the origin of groundwater sampled from the intermediate piezometer (MW 1B) may include (1) groundwater that recharged over low-density residential developments and mixed forest west of County Highway E or groundwater that recharged over parcel 2 and adjacent cropland located south of Nelsen Road.

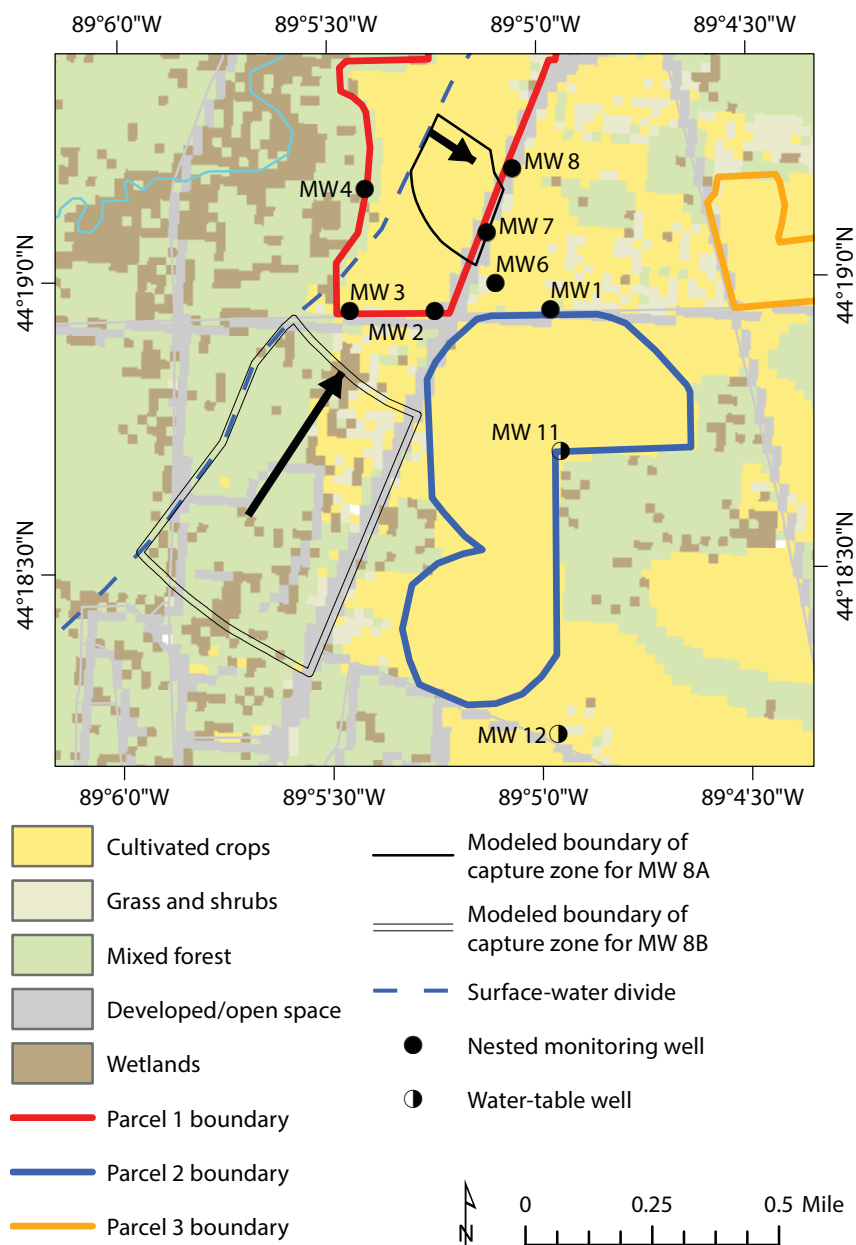
Because the groundwater samples collected at MW 1A most likely recharged over parcel 2, there is compelling evidence that cultivated crop production on this parcel has contributed to high concentrations of nitrate in the groundwater. In this monitoring well, nitrate concentrations have exceeded 15 mg/L at least once every 4 yr since 1993. Where the land-cover history was available (see appendix B), there was no simple interpretation that adequately accounted for the episodic peaks of high nitrate concentrations observed in 1995–1996, 2001–2003, 2009–2010, and 2016–2017; these peaks may simply be artifacts of sample density and timing. Over each calendar year, the highest nitrate concentrations in MW 1A were most commonly observed in November and December, but not enough historical data are available to reliably establish seasonal trends. Until 2016, samples were rarely collected more than 2 to 3 times per year and, notably, nitrate concentrations above 15 mg/L have only been observed in years when the November or December samples were reported.

Figure 26. Schematic illustration of the groundwater-recharge capture zones for MW 1A and MW 1B. The areas of these zones were estimated by assuming that the downward vertical displacement of recharge was 3.3 feet per year and the horizontal hydraulic conductivity was 1 to 2 feet per day. The direction of groundwater flow is indicated by heavy arrows. The actual area of the capture zone may vary over time in response to changes in recharge and high-capacity-well pumping rates, and it may be larger or smaller than these estimates.



Roads from U.S. Census Bureau, 2015. Hydrography from U.S. Geological Survey National Hydrography Dataset, 2016. Wisconsin Transverse Mercator projection, 1991 Adjustment to the North American Datum of 1983 (NAD 83/91); EPSG 3071.

Figure 27. Schematic illustration of the groundwater-recharge capture zones for MW 8A and MW 8B. The areas of these zones were estimated by assuming that the downward vertical displacement of recharge was 3.3 feet per year and the horizontal hydraulic conductivity was 1 to 2 feet per day. The direction of groundwater flow is indicated by heavy arrows. The surface-water divide between the Waupaca River and the Walla Walla Creek watersheds is presumed to coincide with the groundwater divide boundary.



Roads from U.S. Census Bureau, 2015. Hydrography from U.S. Geological Survey National Hydrography Dataset, 2016. Wisconsin Transverse Mercator projection, 1991 Adjustment to the North American Datum of 1983 (NAD 83/91); EPSG 3071.

Between 1994 and 2003, nitrate concentrations greater than 10 mg/L were also observed in the intermediate-depth piezometer screened at 41 to 46 ft (MW 1B). More recent data are not available for MW 1B because the piezometer screen was clogged by organic material. The contributing area estimated for MW 1B (fig. 26) includes three potential sources of nitrate: residential septic systems, lawn fertilizers, and agricultural activities. The nested monitoring wells MW 2A–2C and MW 3A–3B are most likely to contain groundwater that recharged in the residential and forested area west of County Highway E, a conclusion supported by a southwest-to-northeast groundwater-flow path. Nitrate in shallow wells MW 2A and MW 3A, which may also capture some recharge from parcel 1, has occasionally reached nitrate concentrations as high as 7.8 mg/L, but they are generally less than 5 mg/L. In deeper groundwater, sampled from intermediate-depth piezometers MW 2B and MW 3B and deep piezometer MW 2C, nitrate concentrations above 5 mg/L have never been observed. Within the model domain, residential septic systems and lawn fertilizers are therefore assumed to be a lesser contributor than farming to nitrate in groundwater.

The contributing area to MW 8A and MW 8B was estimated using the previously stated assumptions (θ between 0.2 and 0.3, K between 1 and 2 ft/d). Groundwater flow was traced backward to the topographic divide between the Waupaca River and Walla Walla Creek watersheds because this boundary was presumed to coincide with the groundwater divide. The results suggest that groundwater sampled at MW 8A may include a mix of (1) groundwater that recharged over parcel 1 and (2) groundwater that recharged in the residential and forested land east of County Highway E (fig. 27). In this monitoring well, nitrate concentrations commonly exceeded 10 mg/L (and, less frequently, 15 mg/L); the highest nitrate concentrations at MW 8A were also

most likely to be observed in November and December. Both the concentrations and temporal characteristics of nitrate in the MW 8A samples are comparable to those observed in water from MW 1A, where the origin of the nitrate was more decisively attributed to farming. These similarities suggest that recharge over parcel 1 is the predominant source of groundwater passing through MW 8A. Elevated nitrate levels were rarely detected in piezometers MW 8B or 8C. The lower nitrate levels are consistent with the projected recharge area for deeper groundwater, which includes mostly low-density development and mixed forest.

At other monitoring-well locations in the study area, nitrate concentrations in shallow groundwater (less than 30 ft) have rarely been observed to exceed 5 mg/L, but signs of nitrogen enrichment relative to background levels, assumed to be 0 to 2 mg/L, have been detected (Mueller and others, 1995). For example, at nested monitoring well MWs 4A–4C, located near the Crystal River and slightly west of the topographic

surface-water divide, nitrate concentrations in groundwater passing through MW 4A have intermittently exceeded 5 mg/L, but with no clear temporal pattern. Where the groundwater divide coincides with the surface-water divide, the land-cover maps indicate that the most likely source of nitrate to this well is parcel 1. However, pressure-transducer data indicate that the hydraulic head at MW 4A is higher than at MW 7A and MW 8A in the winter and most of the summer (fig. 16). During this time, groundwater flowing through MW 4A from west to east may originate over mixed forest and is less likely to contain high nitrate concentrations. Mixing between these sources may yield lower effective nitrate concentrations than might be encountered if the groundwater flow was consistently east to west toward the Crystal River.

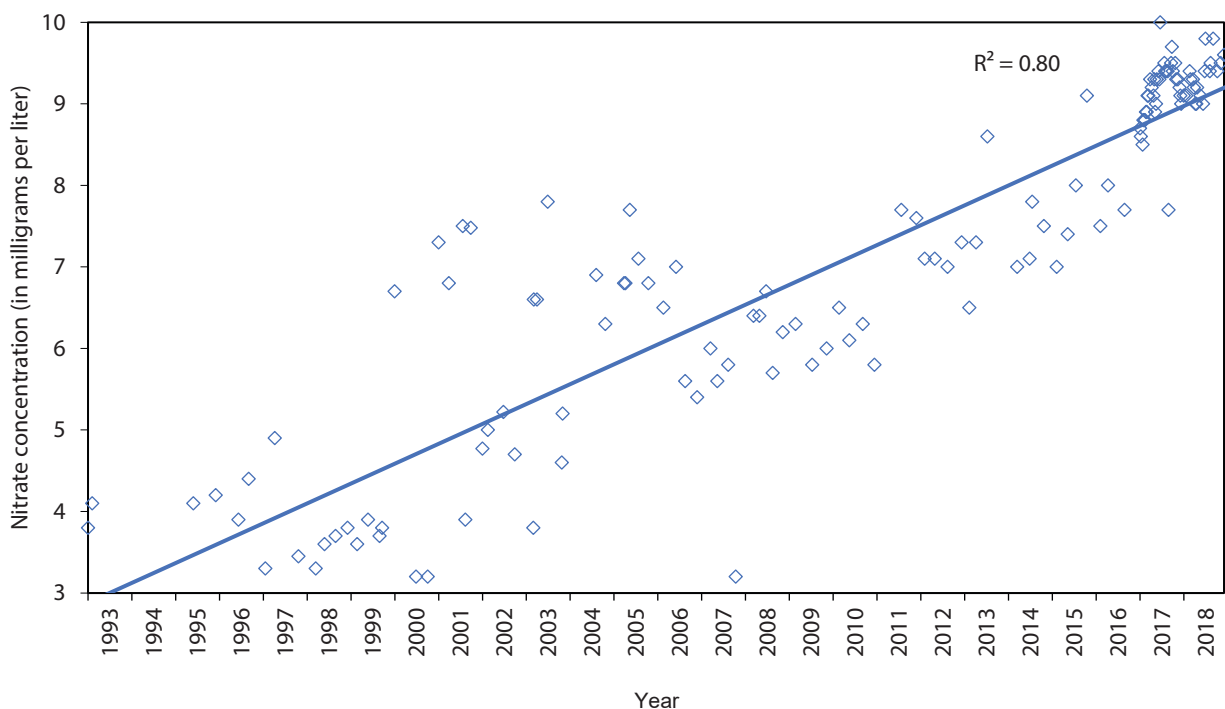
The pressure-transducer data also suggested that the direction of groundwater flow to MW 6A and MW 7A was seasonally variable. This variability may partially explain why, despite their proximity to parcel 1 and parcel 2, nitrate

concentrations in these two shallow wells were notably lower than those observed at nearby MW 1A and MW 8A. Pumping tests performed to estimate hydraulic conductivity showed that the municipal well BD773 induced drawdown in MW 6A and MW 7A, which may also have allowed mixing with groundwater originating over nearby grasslands. Given the difficulty in determining the origin of the water passing through these wells and the limited data available (no samples were taken at these locations between 2010 and 2018), however, it is difficult to hypothesize about the potential nitrate sources.

Study wells

Water-quality samples collected from study wells #5 and #6 from 1993 to 2018 show that the effective nitrate concentrations at each well have approached or even exceeded the Federal 10 mg/L limit several times during the period of record. Both wells are screened from 55 to 75 ft depth and are presumed to draw groundwater mainly from the east and southwest (fig. 15). A groundwater

Figure 28. Nitrate concentrations in study well #5 increased at a rate of about 0.2 mg/L from 1993 to 2019. Data courtesy of Justin Berrrens (Director of Public Works, City of Waupaca, Wisc., 2019, written communication). Abbreviation: R^2 = coefficient of determination.



model (see Section 3) may help delineate more detailed capture zones for each well. Data from the monitoring wells indicate that the nitrate reaching these wells has a local source. Because elevated nitrate concentrations have been rarely observed in the intermediate-depth (B) and deep (C) piezometers in the monitoring wells, the high nitrate concentrations in the study wells strongly suggest that the wells draw preferentially from shallower groundwater.

Since 1993, nitrate concentrations in study well #5 have been increasing at a rate of approximately 0.2 mg/L per year (fig. 28). The potential sources of nitrate include farming and other agricultural activity on parcels 1 through 4, residential septic systems, and lawn fertilizers. Within these parcels, there were no major land-cover changes between 2003 and 2018 that could easily explain either the long-term increase or the shorter episodic increases observed in the early 2000s and the late 2010s. A groundwater-flow model, developed in the next section, may provide additional insight.

Despite their proximity to one another, there were three notable differences in the histories of the nitrate concentrations in study wells #5 and #6. First, groundwater samples collected from study well #6 were consistently lower in nitrates than samples from study well #5. As of 2018, the mean nitrate concentration reported in study wells #5 and #6 was 9.3 mg/L and 8.2 mg/L, respectively. Second, the nitrate concentration in study well #6 has remained relatively stable since 1993. This well seemed to experience episodic increases in the nitrate concentration but, unlike study well #5, no long-term trend is apparent (fig. 29). Third, each well responded differently to the seasons. A best-fit line was added to the seasonal data for study well #5 (fig. 30), and what little seasonality was apparent in study well #6 in 1993 was essentially absent from 2010 to the present. The gap between the high nitrate concentrations in the fall and lower nitrate concentrations in the winter, spring, and summer was closed because nitrate levels increased at a slower rate in the fall than during

the other three seasons. A similar trend was observed in study well #6, except that both the winter and fall nitrate concentrations were historically more likely to have been elevated at this location (fig. 31). The highest concentrations were observed in the spring and winter months. Summer and fall concentrations were historically lower than in spring and winter, but the upward slope of these trend lines changed this order, and monthly measurements collected in 2017 and 2018 indicated that the highest nitrate concentrations in study well #6 occurred between June and November. Without a better understanding of the capture zone for study well #6 and how it might be affected by well pumping, it is difficult to hypothesize about the cause of this change or whether it is projected to continue.

Figure 29. Nitrate concentrations in study well #6 from 1993 to 2019. Data courtesy of Justin Berrens (Director of Public Works, City of Waupaca, Wisc., 2019, written communication). Abbreviation: R^2 = coefficient of determination.

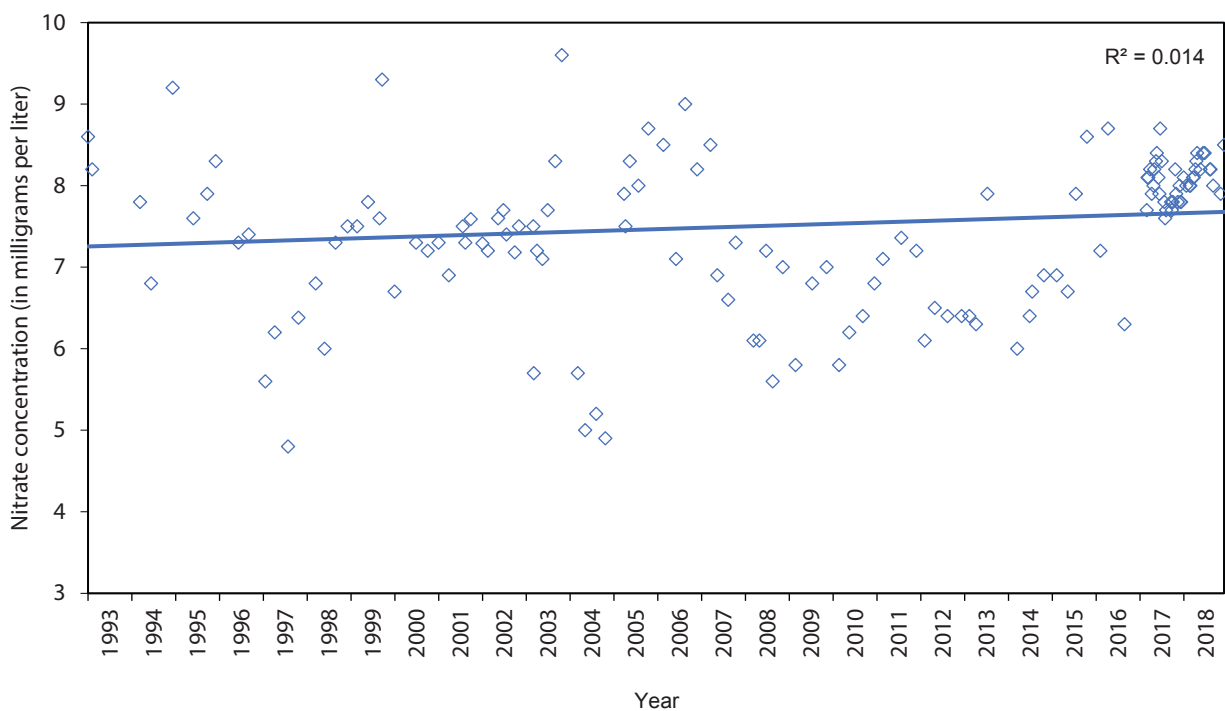


Figure 30. Seasonal trends in nitrate concentrations sampled in study well #5 from 1993 to 2018. A line of best fit has been added for each season. Solid blue line = winter; green dashed line = spring; orange dotted line = summer; burgundy dot-dash line = fall.

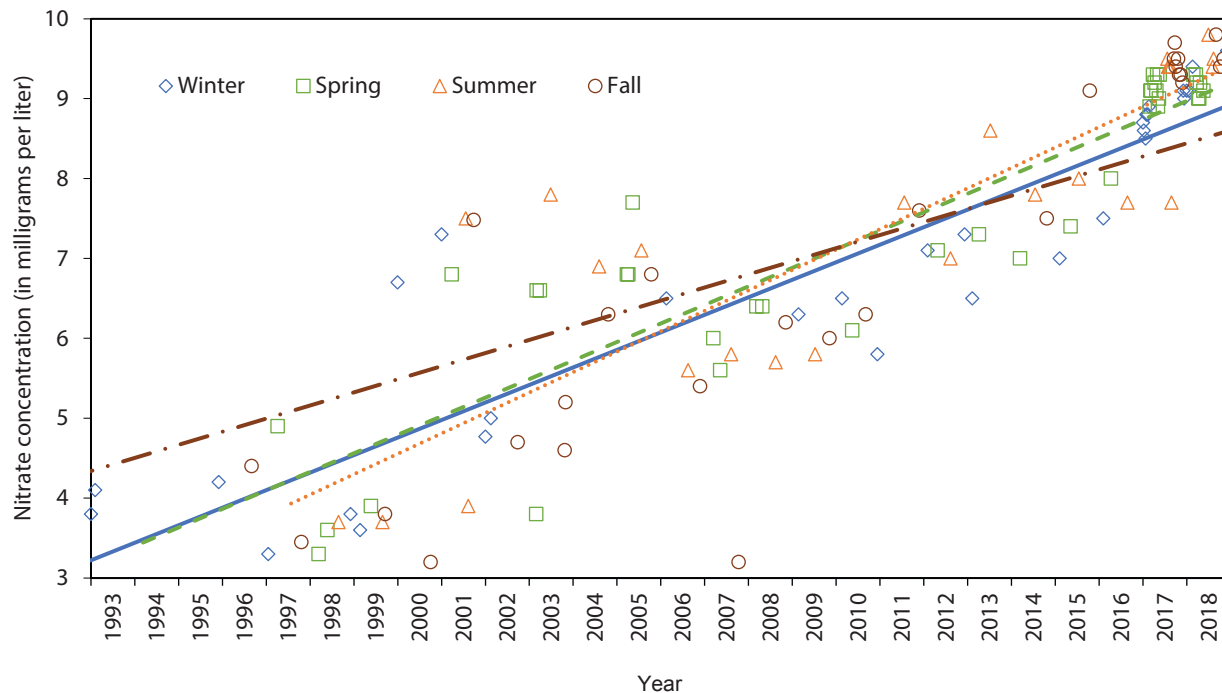
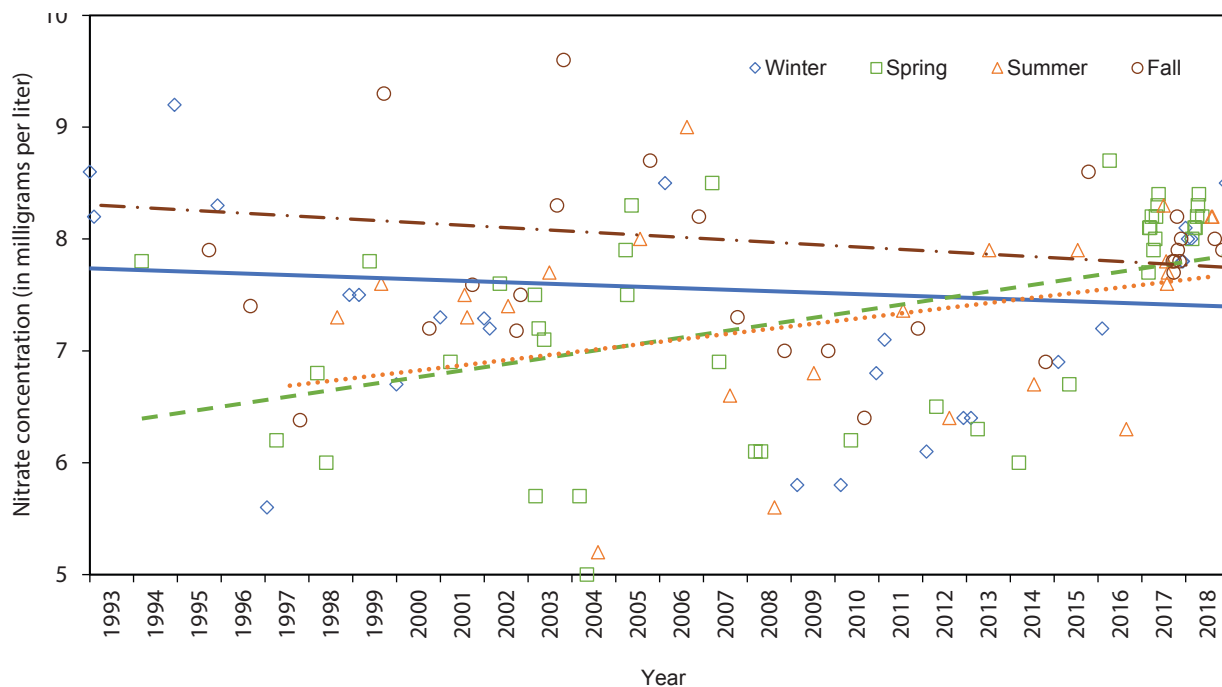


Figure 31. Seasonal trends in nitrate concentrations sampled in study well #6 from 1993 to 2018. A line of best fit has been added for each season. Solid blue line = winter; green dashed line = spring; orange dotted line = summer; burgundy dot-dash line = fall.



Section 3: Groundwater-flow model

Objectives

The primary objective of this project was to investigate how changes to land cover and (or) well-pumping rates impact nitrate concentrations in study wells #5 and #6 of the City of Waupaca, Wisc. To achieve this objective, steady-state groundwater-flow models were used to simulate groundwater flow and contaminant transport paths for the years 2013 through 2018. Each model consists of a three-dimensional groundwater-flow model constructed using MODFLOW by preparing gridded input data to represent recharge to the aquifer, hydraulic conductivity of the aquifer, and the top and bottom elevation of each model layer. Additionally, point, polyline, and polygon datasets were prepared to represent analytic elements (discharge wells) and hydraulic boundaries (rivers, lakes, drains). All of the files necessary to run the final models are available in the Supplementary Materials (dataset 2) that accompany this report.

A three-dimensional groundwater model was developed and calibrated to data for recharge, streamflow, and water-table elevation for 2018 because of the good availability of data for that year. The resulting MODFLOW model was modified to make a steady-state model for each year from 2013 to 2017 by adjusting the rates of recharge and mean pumping rates to reflect the values reported for all high-capacity wells in the modeled area during those years. These models contributed to the goals of this project by simulating water-table elevations, flow paths, flow rates, and particle movement for each year, which allowed for the delineation of capture zones that were analyzed and compared to historical nitrate concentrations. These comparisons were used to examine how annual variabilities in land cover, recharge, and well-pumping rates

impacted the nitrate concentrations observed at the study wells. In future studies, the steady-state models could also be refined to simulate transient flow to better evaluate seasonal variability and water-management impacts on groundwater flow and particle transport to the study wells.

Simulation approaches

Two methods were used to simulate groundwater flow in the study area: (1) a two-dimensional analytic element model and (2) a three-dimensional, finite-difference groundwater-flow model. The two-dimensional analytic element model uses the GFLOW code (Haitjema, 1995) and was developed to produce hydraulic boundaries for the perimeter of the three-dimensional, high-resolution MODFLOW model. The MODFLOW model was used in conjunction with the MODPATH code (described later in the section “Particle tracking”) to perform particle tracking and delineate capture zones for each of the study wells. A complete description of the analytic element method is provided by Strack (1989) and Haitjema (1995). Hydraulic boundaries for the MODFLOW model perimeter were extracted from the GFLOW model using code (provided by Paul Juckem, USGS, 2019, written communication) that was based on methods described by Hunt and others (1998).

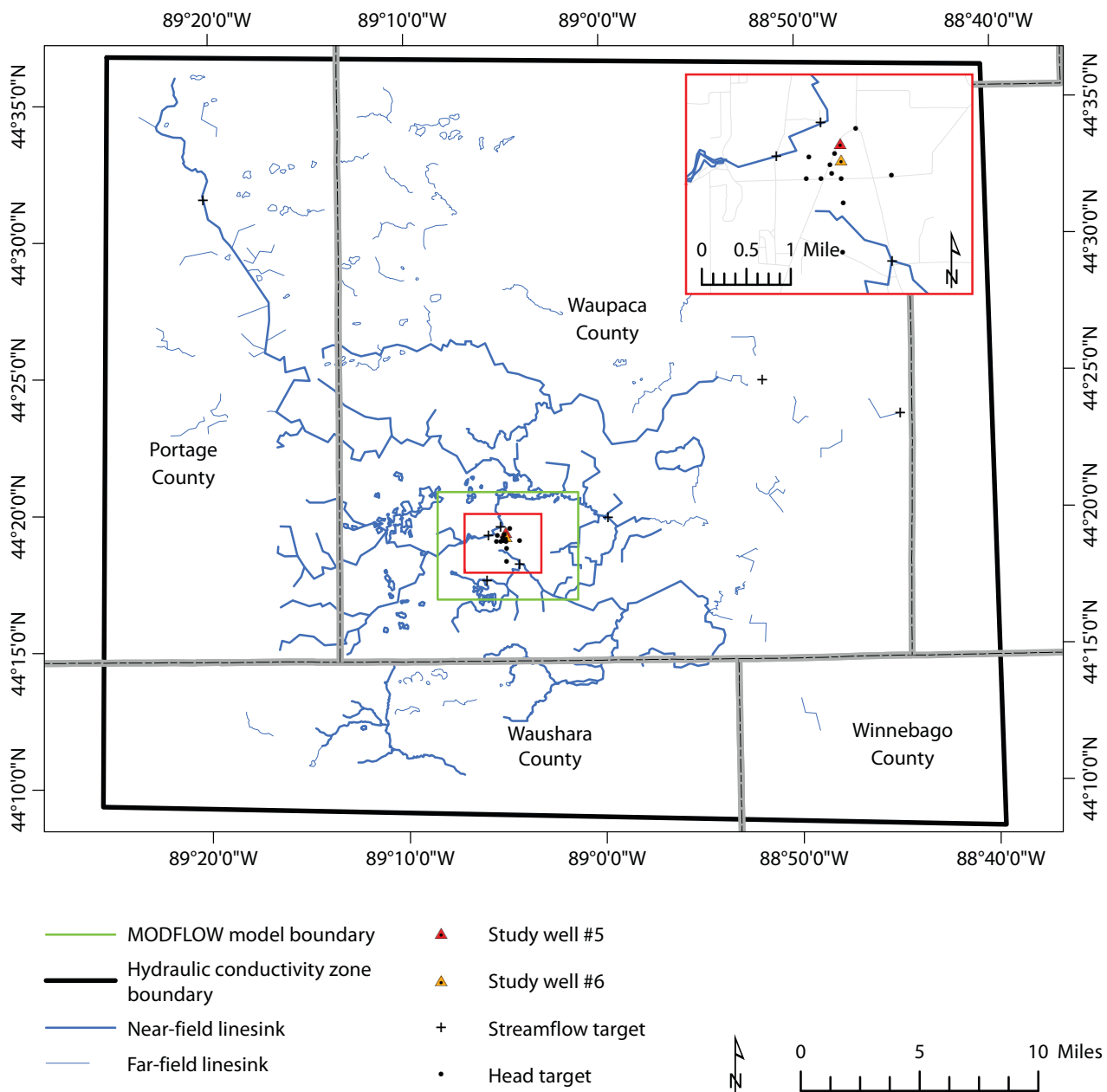
GFLOW model

The GFLOW model (figs. 32, 33) was constructed by setting properties (recharge, hydraulic conductivity) and adding hydrologic features (streams, lakes) that affect groundwater flow. The geometry of the single-layer GFLOW model included a uniform bottom elevation of 750 ft above National Geodetic Vertical Datum of 1988 and a thickness of 200 ft. Streams were simulated using graphical features called linesinks. Each linesink

contains the surface-water elevation at the start and end of the stream segment it represents. All linesinks with headwaters that originated in Portage, Waupaca, and Waushara Counties and converged downstream in the north-eastern corner of Winnebago County were represented, along with the Wolf River in the southern half of Waupaca County. Interior streams were simulated using the streamflow-routing option, which quantifies groundwater discharge to surface water and prevents the loss of streamflow to the aquifer from exceeding the upstream simulated baseflow. The routed streams (line sinks) were simulated with a streambed resistance of 0.01 days (1-ft-thick sediment with a hydraulic conductivity of 100 ft/day) and widths ranging from 5 to 100 ft. Study wells #5 and #6 were represented as analytic elements extracting 65,000 ft³/d and 35,000 ft³/d, respectively. High-capacity wells located outside the boundaries of the model domain were excluded from the GFLOW model because (1) the volume of water extracted by these wells was extremely small compared to the volume of water moving through the aquifer and (2) they did not affect the GFLOW model results in a way that was meaningful for its intended use, which was to provide an estimate of groundwater flow across the MODFLOW boundaries.

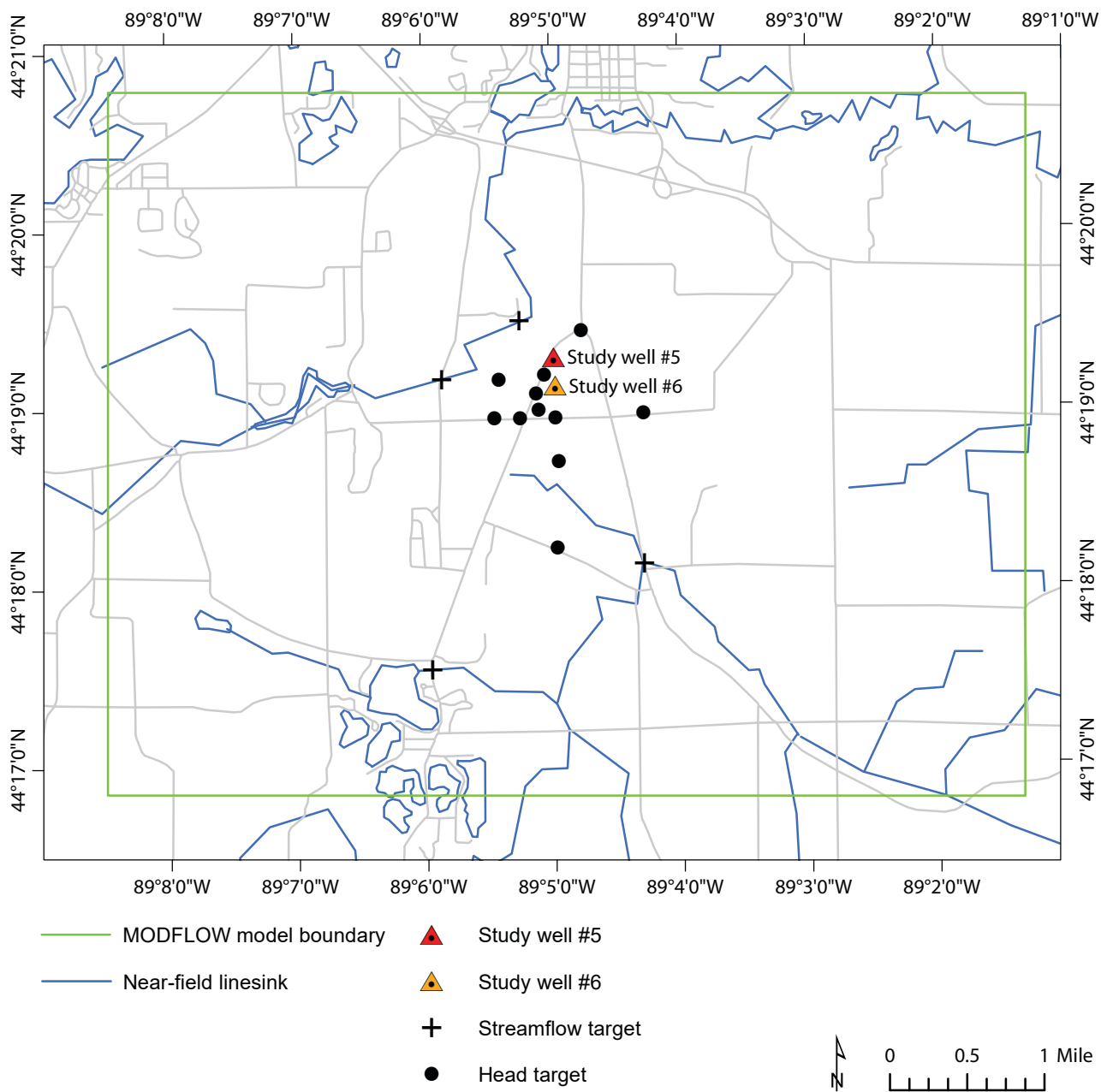
The calibrated GFLOW model had a uniform recharge rate of 13.1 in./yr and a hydraulic conductivity of 60 ft/d across the entire model domain. Calibration targets included water levels measured in 11 monitoring wells and streamflow measurements obtained through direct measurement (the Crystal River and Walla Walla Creek) and USGS streamflow data (see appendix C). Although the GFLOW model was developed only to provide hydraulic boundary conditions for the MODFLOW model, the model simulated heads with acceptable

Figure 32. Analytic elements included in the GFLOW model, including one heterogeneous element (hydraulic conductivity zone, bounded by black box), near- and far-field line sinks representing streams, and two high-capacity pumping wells. The extent of the MODFLOW model is shown by the green bounding box. Inset map (shown by the red bounding box) shows locations of study wells and targets.



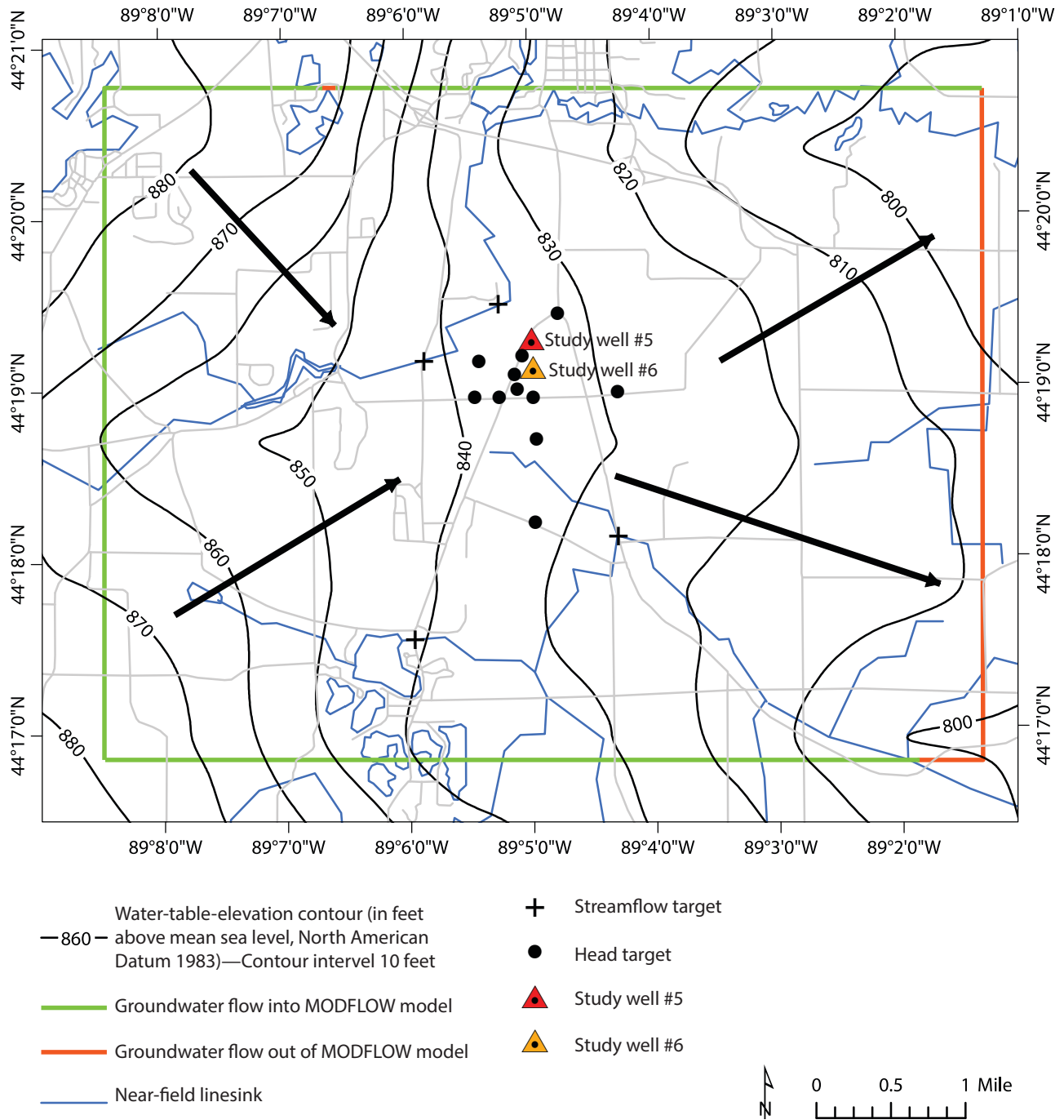
Political boundaries from Wisconsin Department of Natural Resources, 2011. Wisconsin Transverse Mercator projection, 1991 Adjustment to the North American Datum of 1983 (NAD 83/91); EPSG 3071.

Figure 33. Map of the model domain that displays polyline data representing the MODFLOW model boundary and near-field linesinks. Point data representing study well #5, study well #6, streamflow targets, and head targets—all of which were used to calibrate the GFLOW model—are displayed.



Roads from U.S. Census Bureau, 2015. Wisconsin Transverse Mercator projection, 1991 Adjustment to the North American Datum of 1983 (NAD 83/91); EPSG 3071.

Figure 34. GFLOW model results showing the direction of groundwater flow across the MODFLOW model boundaries. Black arrows indicate the direction of flow.



Roads from U.S. Census Bureau, 2015. Wisconsin Transverse Mercator projection, 1991 Adjustment to the North American Datum of 1983 (NAD 83/91); EPSG 3071.

accuracy. For the 11 monitoring wells, the average mean difference

$$\left(\frac{\sum \text{observed head}}{11} - \frac{\sum \text{simulated head}}{11} \right)$$

and mean absolute difference

$$\frac{(\sum \text{observed head}_n - \sum \text{simulated head}_n)}{11}$$

between the simulated and measured groundwater levels were 1.3 and 1.9 ft, respectively.

MODFLOW

The primary tool used to simulate groundwater flow through the study area was MODFLOW-NWT (Niswonger and others, 2011), a MODFLOW solver that uses an upstream-weighted, block-centered, finite-difference method to solve the groundwater-flow equations. This solution helps to prevent dry cells from developing when the simulated water level falls below the bottom of a layer. The model was developed assuming steady-state conditions using recharge, near-field head-observation targets, and streamflow data corresponding to calendar year 2018.

Model grid

The MODFLOW model was designed as a rectangular grid with 239 rows and 312 columns of square cells ($\Delta x/\Delta y = 100$ ft), resulting in 74,568 cells in each of the three model layers (defined in the “Hydrostratigraphy” subsection of Section 1). The model perimeter was selected to include nearby hydrogeological boundaries, including those of the Crystal and Waupaca Rivers and Walla Walla Creek.

Boundary conditions

The hydraulic properties of the perimeter of the MODFLOW model were extracted from the two-dimensional GFLOW model. Parsen and others (2019) described the theoretical approach to this extraction method, which simulated flow into and out of the MODFLOW model using the well (.wel) package

(Harbaugh and others, 2000). According to the GFLOW model results, regional groundwater flows into the MODFLOW model domain at a rate of 4,300,000 ft³/day through the northern, western, and southern boundaries (fig. 34). Regional flow out of the MODFLOW model domain is constrained to the eastern and southeastern corner boundaries at a combined rate of 582,871 ft³/d. Most of the balance discharges through surface water.

Stratigraphic layer elevation data

The upper and lower elevation boundaries for the stratigraphic layers in MODFLOW consist of a set of gridded raster datasets that use a combination of lidar surface-elevation data and depth-to-bedrock measurements. The bottom elevations of layers 2 and 1 were calculated by adding 50 ft and 25 ft, respectively, to the bedrock-elevation dataset.

Surface-water network

The streams and rivers simulated in this model included the Crystal River system and the Walla Walla Creek system (fig. 35). In the eastern half of the model, a series of drainage ditches contributes surface water to the Walla Walla Creek system. In the MODFLOW model, gaining streams were simulated using the river (.riv) package, and losing streams were simulated using the drain (.drn) package. Both packages simulated head-dependent boundaries that calculated the flow between the stream and the aquifer as a function of streambed conductance and aquifer head (Harbaugh and others, 2000). They differ only in that the drain package was active only when the head of the aquifer was greater than the elevation of the drain and the flow through the drain was removed from the model.

The hydraulic conductivity of all the rivers and drains was set to be equal to the geometric mean of the glacial aquifer—or 36 ft/day—with a bed thickness of 1 ft. The river depth was set to 2 ft for

all tributaries and Walla Walla Creek and 2.5 ft for the Crystal and Waupaca Rivers. The streambed elevation was calculated by subtracting the feature’s depth from the head at the start and end of each segment. Lakes were also simulated in the MODFLOW model using the river (.riv) package to simplify the solution. Other packages allow a more direct simulation of the changes in lake levels in response to a variety of additions and subtractions; however, an analysis of these changes was not an objective of the current model.

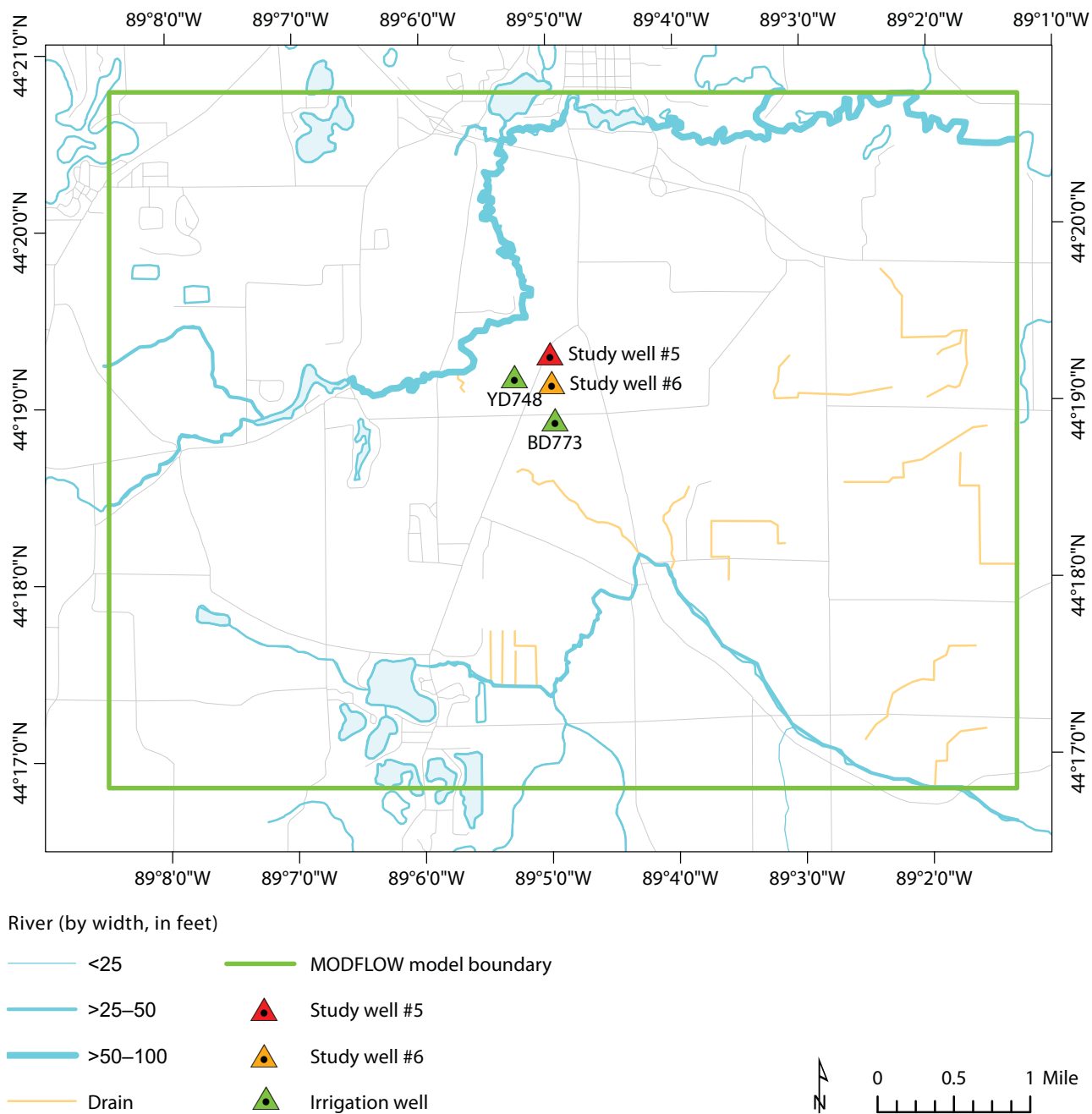
Recharge

Deep infiltration estimated by the SWB model for 2018 was manually edited using ArcMap software to account for the estimated irrigation recharge. The irrigation-modified raster data was used as the input for groundwater recharge in the MODFLOW model (.rch package; Harbaugh, 2005). Recharge for 2018 was chosen for the steady-state model because the observed head values used for calibration were collected in the same year. Climate data indicate that 2018 was an exceptionally wet year, with rainfall nearly 1 ft above the annual average (44 in. versus 33.5 in.), which led to above-average groundwater levels that were presumably reflected in the 2018 field observations. Using a long-term average with lower recharge values may inadvertently have led to high parameter estimates during model optimization. The average recharge rate applied to the model domain was 13.7 in./yr, which included irrigation modifications.

Groundwater withdrawals

The annual groundwater-use rates for four high-capacity wells simulated in the model domain were obtained from Wisconsin Department of Natural Resources (2020b). These included rates for study wells #5 and #6 and nearby irrigation wells BD773 and YD748. In the models, the sum of withdrawals (in gallons) reported in 2018 for these wells was converted to cubic feet and

Figure 35. Streams, lakes, drains, and wells included in the MODFLOW simulation.



Roads from U.S. Census Bureau, 2015. Hydrography from U.S. Geological Survey National Hydrography Dataset, 2016. Wisconsin Transverse Mercator projection, 1991 Adjustment to the North American Datum of 1983 (NAD 83/91); EPSG 3071.

divided by 365 days to obtain an average pumping rate for each well in cubic feet per day. These wells were simulated in the MODFLOW model as analytic elements.

Head calibration targets

A total of 18 near-field head-observation targets from the monitoring-well-network data were placed in layers 1 and 2 (11 and 7 targets in each layer, respectively). An additional 91 far-field head-observation targets were placed throughout the model; their placements were informed by static water-table elevations reported in well construction reports corresponding to wells constructed between 1971 and 2009. These targets were distributed throughout all three layers with 22, 48, and 21 targets located in layers 1, 2, and 3, respectively. For calibration purposes, all near-field targets were assigned a weight of 1 and all far-field targets were assigned a weight of 0.05. The inclusion of low-weight far-field targets was intended to constrain parameters in the far field while focusing calibration on the area closest to the study wells, where the head targets were based on field measurements collected in the relatively wet year of 2018.

Streamflow calibration targets

Four streamflow targets were chosen for the MODFLOW model calibration. The targets were located along the Crystal River or Walla Walla Creek (fig. 33). The

target values were based on streamflow measurements collected on October 18, 2018, and they represent moderate to high flow conditions.

Hydraulic conductivity

The glacial aquifer that was modeled for this study is composed of discontinuous deposits of clay, silt, sand, gravel, and till. To best represent hydraulic conductivity across the domain, lithologic descriptions provided in the WCRs corresponding to wells located inside the model domain were used to prepare geologic maps of the layers defined in the MODFLOW model (see Section 1). The initial values of hydraulic conductivity for each geologic zone (table 10) were based on estimates calculated using TGUSS and optimized using parameter estimation software (described below).

Parameter estimation using PEST with pilot points

Parameter estimation is a process used to modify model parameters in a way that increases the level of agreement between simulated and observed water levels while also considering professional judgment when choosing reasonable model parameters. In this model, horizontal hydraulic conductivity (K_x/K_y) and vertical hydraulic conductivity (K_z) were parameterized using the model-independent software Parameter ESTimation (PEST; Doherty and Hunt, 2010) with zones of uniform hydraulic conductivity and pilot points.

Geologic maps corresponding to each layer of the MODFLOW grid were imported into MODFLOW to define the hydraulic conductivity zones. The initial values of horizontal hydraulic conductivity (K_x/K_y) in zones 1 to 3 were based on the geometric mean of the hydraulic conductivity estimates derived from the WCRs for the points corresponding to each zone. For each zone, a vertical anisotropy ratio of 1:5 (Kenoyer, 1988) was applied and vertical hydraulic conductivity (K_z) was fixed at 20 percent of K_x for each zone. The initial values and bounds of the PEST run are summarized in table 10.

Pilot points

Pilot points represent model properties at fixed locations in the model grid. PEST optimizes the parameter value at each point within a user-defined set of bounds and interpolates property values at remaining nodes between points. The advantage of using pilot points is that the heterogeneous composition of the aquifer can be represented with more detail than possible by using a purely zonal approach but without the complexity of a cell-by-cell approach (Doherty and Hunt, 2010). In this model, pilot points were placed using target triangulation, which places points at the midpoints of each side of a triangle formed by three calibration targets. A few additional points were manually placed into small hydraulic conductivity zones where, with only one pilot point

Table 10. Initial values and bounds for pilot points used for PEST optimization of hydraulic conductivity.

Type	Zone	Initial value (ft/d)	Bound (minimum)	Bound (maximum)
K_x	1	68.0	6.8	680
K_x	2	124	12.4	1240
K_x	3	16.7	1.7	170
K_z	1	13.6	Tied to K_x/K_y (20%)	Tied to K_x/K_y (20%)
K_z	2	24.9	Tied to K_x/K_y (20%)	Tied to K_x/K_y (20%)
K_z	3	3.33	Tied to K_x/K_y (20%)	Tied to K_x/K_y (20%)

Abbreviations: ft/d = feet per day; K_x/K_y = horizontal conductivity; K_z = vertical conductivity.

present, the PEST solution would have been a uniform property value inside that zone. This method resulted in the creation of 67, 43, and 42 pilot points in layers 1, 2, and 3, respectively. The initial values for the pilot points were set to the zonal database values (table 10) with the bounds set as multipliers ranging from 0.1 to 10 times the initial point values.

Results

PEST optimization yielded K_x values ranging from 1.67 to 1,020 ft/d, with a geometric mean of 46 ft/d (fig. 36). These results are consistent with the geometric mean hydraulic con-

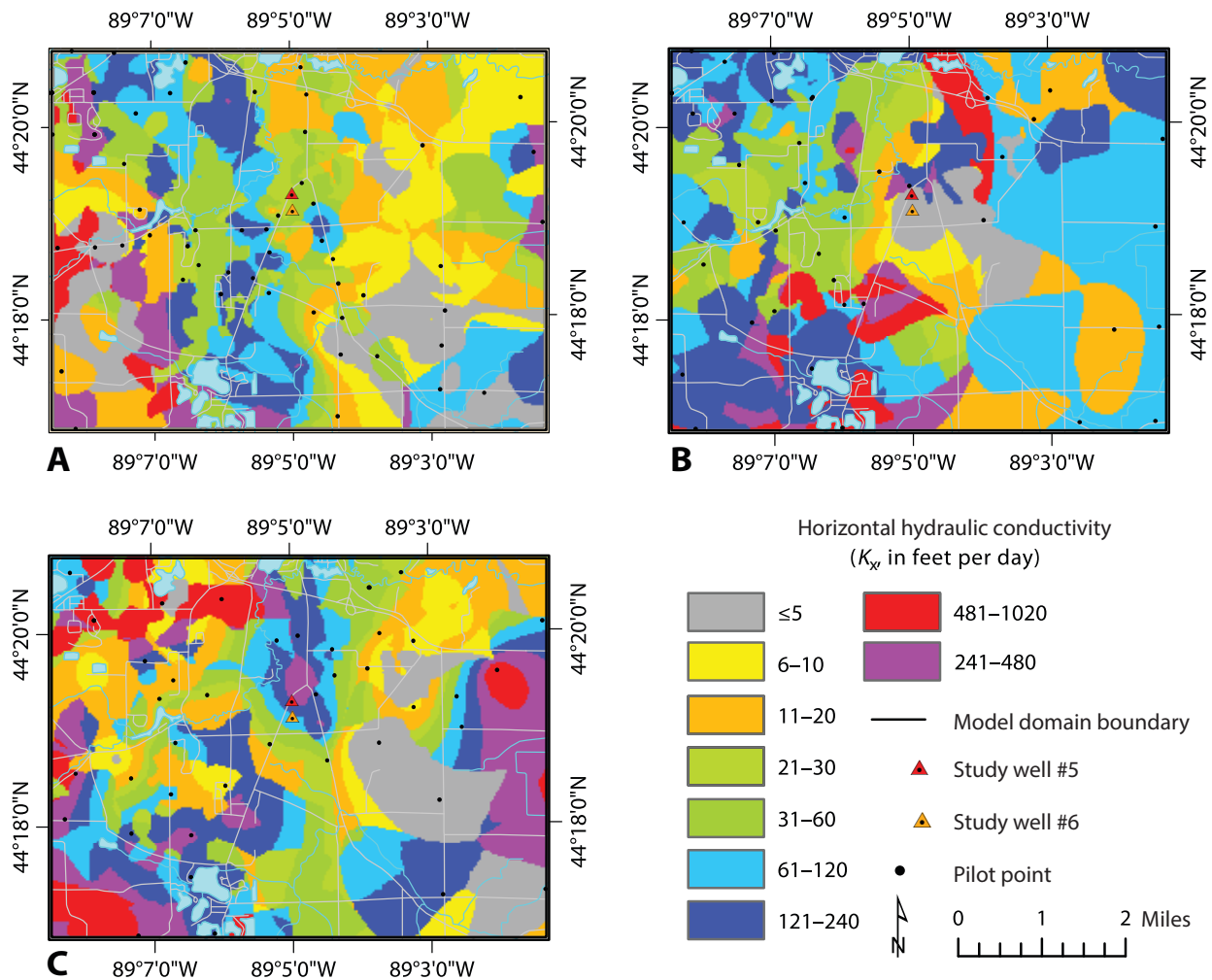
ductivity (36 ft/d) estimated by field tests and TGUESS. The plots of simulated head versus measured head for the full model domain (fig. 37, left) and for near-field observation wells (fig. 37, right) show that the simulated head values fit well to the observed water table in most parts of the model domain. An exception occurs in the northeastern corner of the model domain, where the number of pilot points was limited by a low density of well data. The result is that the simulated head in this region is much less (<20 ft) than the head recorded at seven far-field locations in the historical WCRs, and these points fall in a cluster

below the calibration line (fig. 37, left). A plot of simulated streamflow versus observed streamflow is shown in figure 38. The field-to-model agreement is quite good for streamflow at the two points located on Walla Walla Creek, but streamflow across the Crystal River is strongly underestimated by the model.

Particle tracking

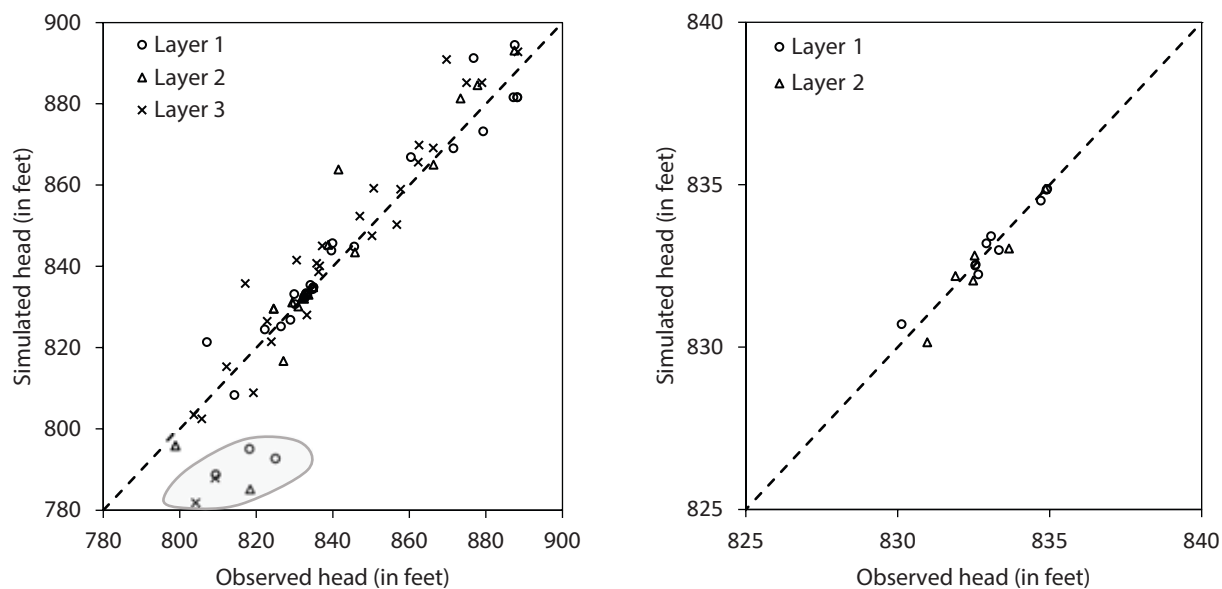
The particle-tracking model, MODPATH (Pollock, 2012), was first run in reverse-tracking mode; that is, the model followed particles as they traveled backward from a designated discharge location to a starting loca-

Figure 36. Gridded horizontal hydraulic conductivity (K_x) values resulting from PEST parameterization and pilot points. A, layer 1; B, layer 2; C, layer 3.



Roads from U.S. Census Bureau, 2015. Hydrography from U.S. Geological Survey National Hydrography Dataset, 2016. Wisconsin Transverse Mercator projection, 1991 Adjustment to the North American Datum of 1983 (NAD 83/91); EPSG 3071.

Figure 37. Calibration data for the MODFLOW model. Left panel shows calibration of all head targets; right panel shows only near-field head targets. The dashed line corresponds to a 1:1 fit between observed and simulated head measurements. A cluster of six far-field calibration points that deviate from the line is highlighted in gray in the left panel.



tion at the surface of the water table. The maximum particle travel time to study wells #5 and #6 estimated by this method was 26 yr. Next, MODPATH was used in forward-tracking mode to delineate steady-state capture zones for each high-capacity well in the model area corresponding to travel times of 1, 2, 3, 4, 5, 6 to 10, 11 to 15, and 16 to 25 yr. In this mode, a single particle was placed into each grid cell in layer 1 and tracked as it traveled away from its point of origin. Particle traces that terminated in the study wells and nearby irrigation wells were exported to ArcMap software and used to identify their starting points (fig. 39). Capture zones based on the travel times referenced above were manually drawn around the starting point locations associated with each well using ArcMap's editing tools. The resulting map (fig. 40) shows that the capture zones overlap and interfere with each other. Study well #5 has a higher pumping rate than study well #6 and its capture zone envelops the capture zone for study well #6. Likewise, the capture zones for both study wells envelop the capture zone for the smaller irrigation well (BD773).

Figure 38. Calibration data corresponding to streamflow targets. The dashed line corresponds to a 1:1 fit between observed and simulated streamflow measurements. Negative flow indicates that the stream is losing water to the aquifer.

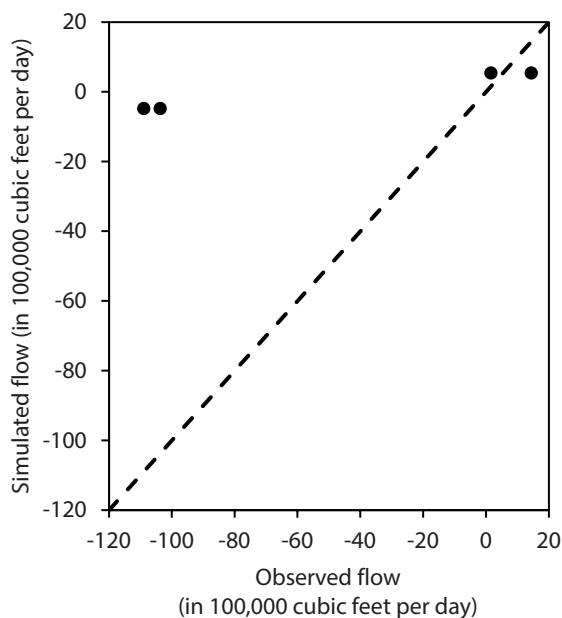
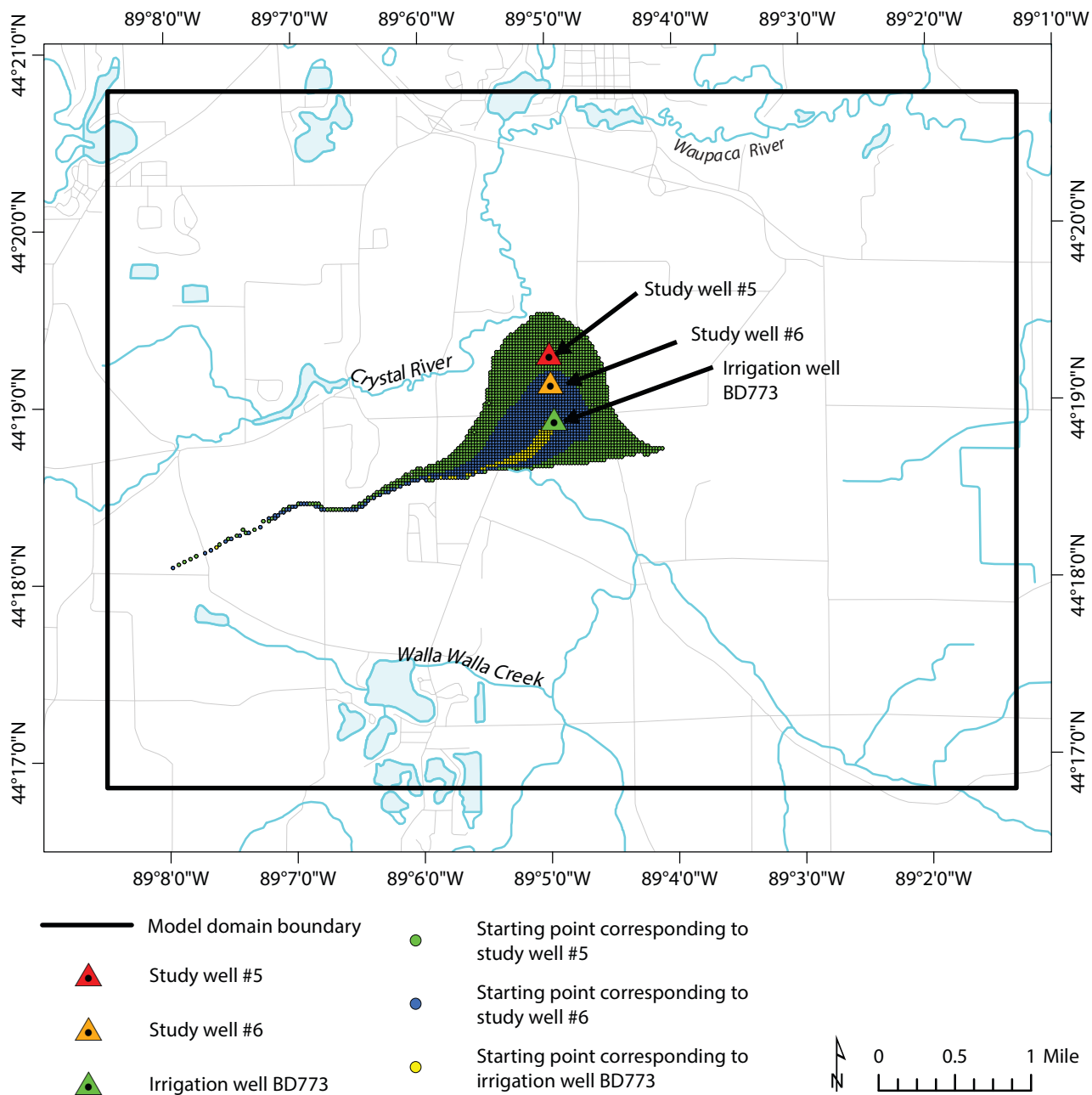
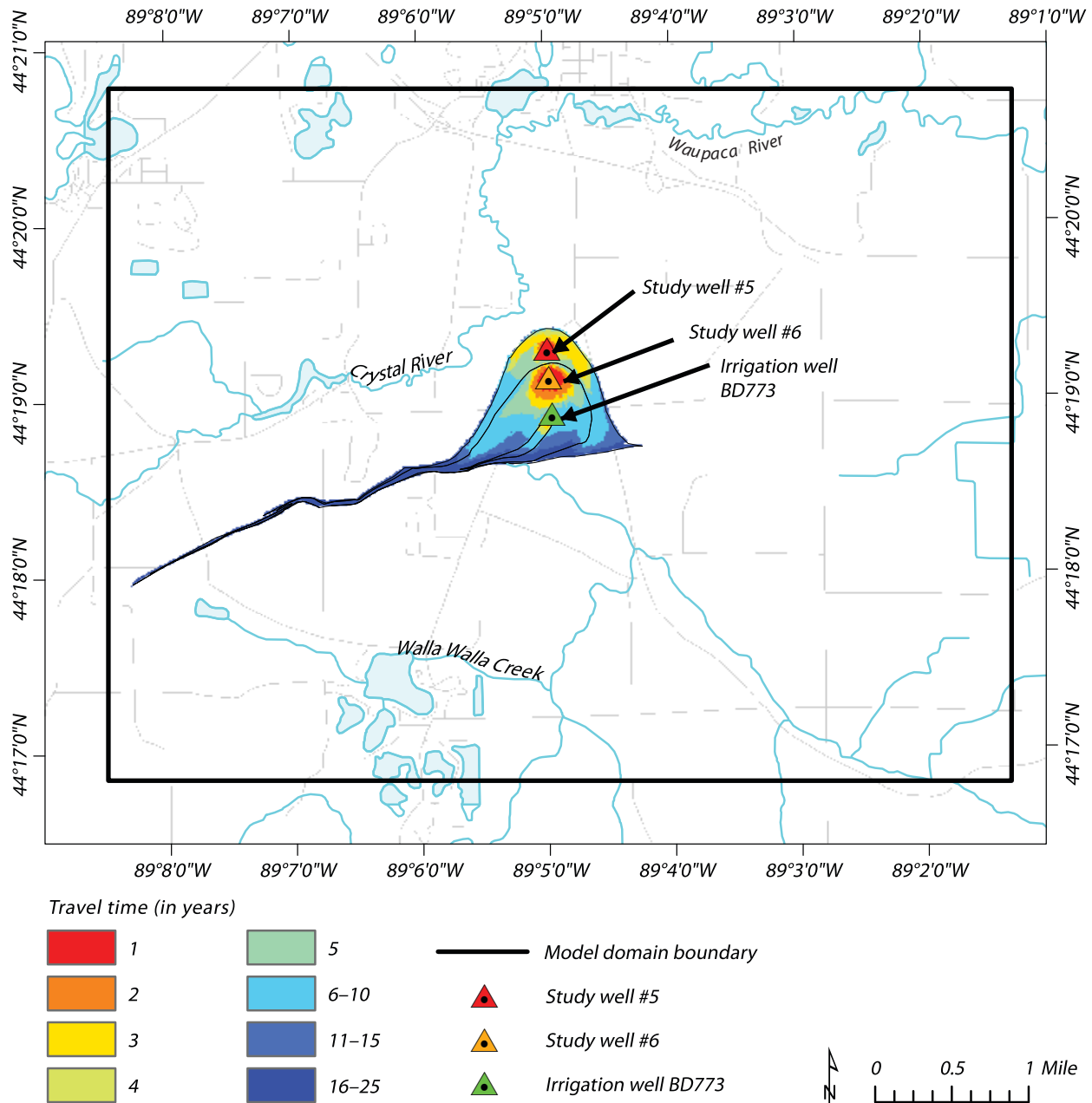


Figure 39. Example of starting points corresponding to the 25-year capture zones for study wells #5 and #6 and irrigation well BD773. Points corresponding to each well represent locations on the land surface from which MODPATH simulations predict groundwater will flow to the indicated well; that is, the green points (well #5) represent the starting point for water that is captured by well #5.



Roads from U.S. Census Bureau, 2015. Hydrography from U.S. Geological Survey National Hydrography Dataset, 2016. Wisconsin Transverse Mercator projection, 1991 Adjustment to the North American Datum of 1983 (NAD 83/91); EPSG 3071.

Figure 40. Example of time-of-travel capture zones delineated from MODPATH particle traces for study wells #5 and #6 and irrigation well BD773.



Roads from U.S. Census Bureau, 2015. Hydrography from U.S. Geological Survey National Hydrography Dataset, 2016. Wisconsin Transverse Mercator projection, 1991 Adjustment to the North American Datum of 1983 (NAD 83/91); EPSG 3071.

Section 4: Effective nitrate calculator

Overview

The calibrated groundwater-flow model described in Section 3 was modified using appropriate recharge arrays and well-pumping rates to simulate steady-state conditions in each of the six years between 2014 and 2019. These models were used, in conjunction with MODPATH, to delineate capture zones corresponding to each of these years (fig. 41). The capture zones were then used to develop a spreadsheet-based model (dataset 3) that estimated the nitrate concentration in study wells #5 and #6 as a function of land cover and time of travel. This section presents the theoretical approach and results of the nitrate model.

General approach

The effective nitrate calculator is based on a conceptual model in which the water entering the well screen contains groundwater that ranges in age from less than 1 yr (recent recharge) to the maximum travel time for water recharged within the capture zone (about 25 yr; see Section 3). According to this model, when the nitrate concentration of each water year is known, the nitrate that results from mixing of groundwater of different ages as it is pumped through the municipal well screen is known as the effective nitrate concentration, which can be estimated as a simple volume-weighted average. This conceptual model is based on the following assumptions:

- The concentration of nitrates in recharge directly relates to land cover and is uniform for all recharge that originates under a given land-cover designation.
- Nitrates behave conservatively in groundwater.
- Recharge enters the aquifer along discrete flow paths that mix only slightly within the aquifer; therefore, the nitrate concentration at each point along a flow path is representative of the concentration at its point of origin at the water table.
- Recharge is uniform across the capture zone and the volume of recharge originating from a specified region of the capture zone is equal to the well-pumping rate multiplied by the fraction of the capture zone represented by that region.
- Recharge is displaced downward as it travels through the aquifer, and a vertical column of groundwater adjacent to a high-capacity study well can be represented as a “stack” of water in which the oldest water (about 25 yr) is at the bottom and the youngest (0 to 1 yr) is at the top (fig. 42).
- When groundwater is withdrawn at the study wells, complete mixing occurs in and around the well screen and the resulting nitrate concentration is the volume-weighted average from each contributing water year.

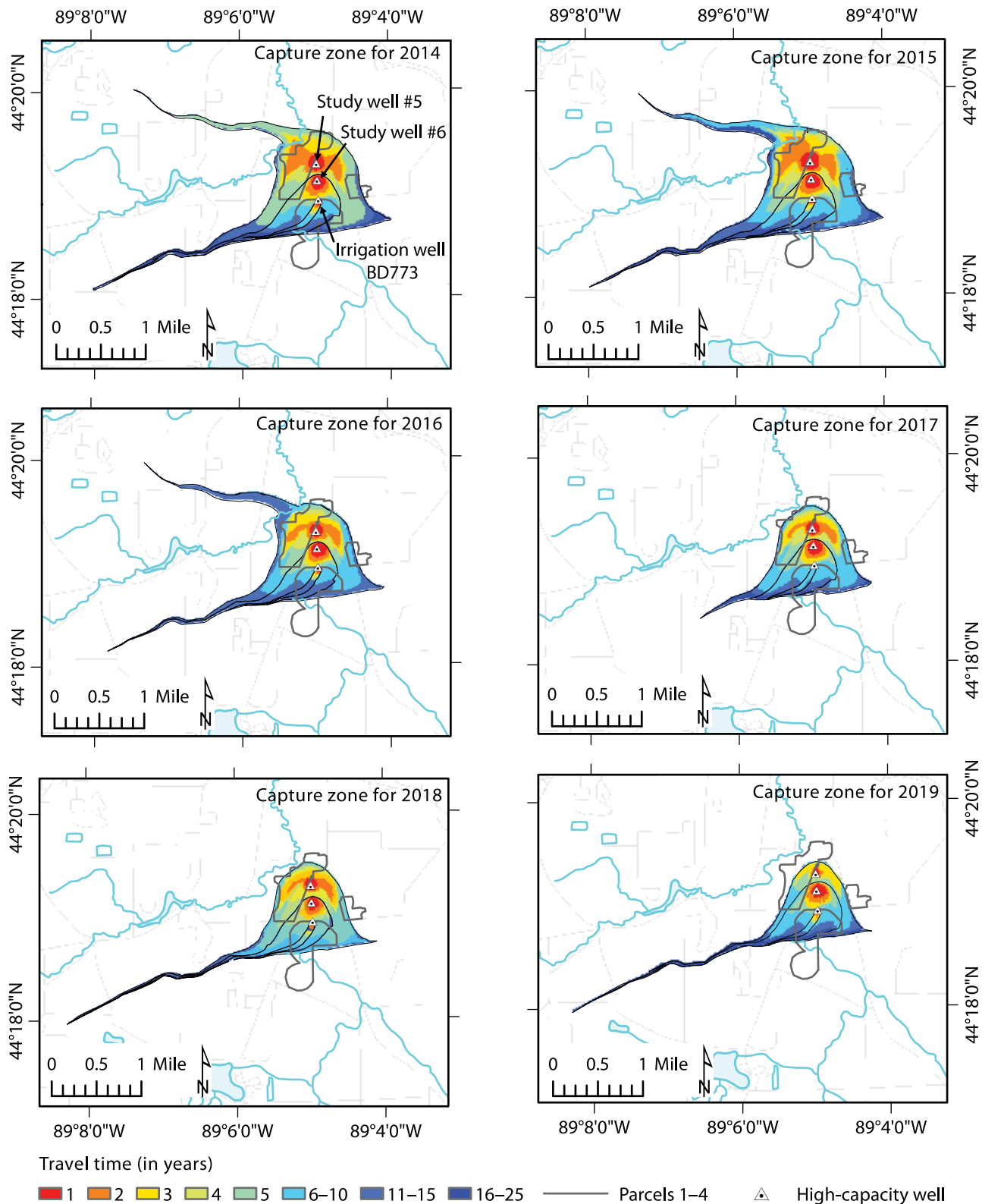
We note that the assumption of limited mixing along flow paths would be unlikely to hold in the most stratified or heterogeneous aquifers, but we argue that the assumption is reasonable in the shallow sandy aquifer of the study area.

Estimating nitrate concentrations in recharge (1994–2018)

The approach to estimating nitrate concentrations in recharge focused on parcels 1 through 4, which were previously identified as areas of interest with respect to elevated nitrate concentrations in groundwater near the study wells (fig. 23). The portion of the model domain outside the boundaries of parcels 1 through 4 was treated as a single unit of uncultivated land where the annual contribution to nitrates in the groundwater was based on monitoring-well data. Two monitoring wells (MW 2A and MW 3A) were determined to capture water recharging over uncultivated, mixed-use land south of parcel 1 (see Section 2). MW 2A was selected to represent recharge over uncultivated land in the effective nitrate calculator because it had been more frequently sampled over the study period (1994–2018). The assigned value, 4.6 mg/L, was based on the mean nitrate concentration observed in MW 2A during the period of record.

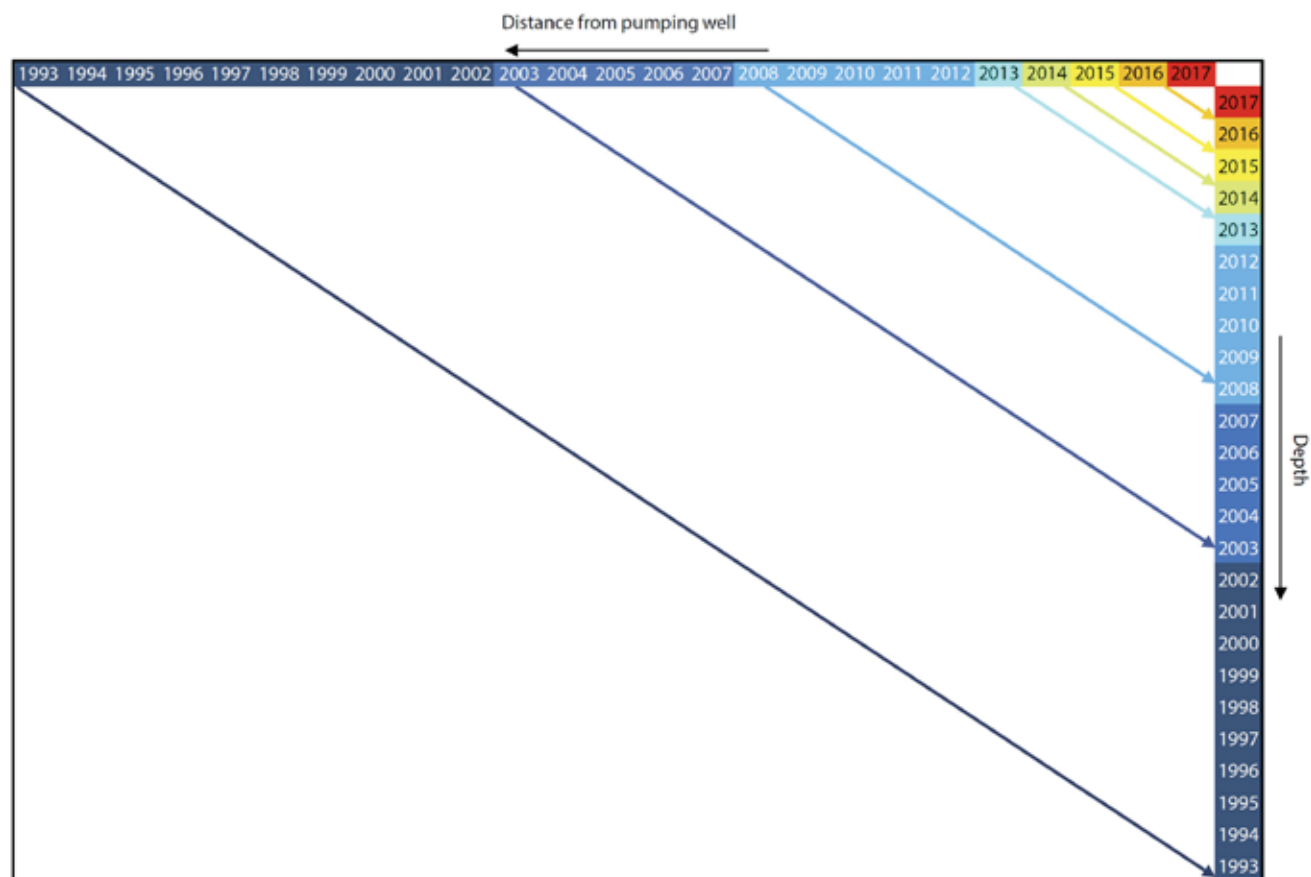
The nitrate concentration in recharge originating from parcel 4 was also assigned a fixed value. Parcel 4 is an unlined manure lagoon located a few hundred meters northwest of study well #5 (fig. 23). Because this lagoon does not have a concrete liner, it serves as a continuous point source of nitrates to groundwater and was treated separately from parcels 1 through 3. Seepage losses of up to 2.5 millimeters per day have been reported for unlined lagoons constructed with coarse soil, and the corresponding leached nitrate concentrations may be as high as 480 mg/L (Ham and DeSutter, 2000), which is equivalent to nearly 4,500 pounds of nitrogen per acre. The input concentrations of 200 to 480 mg/L were tested in the effective nitrate calculator for the

Figure 41. Time-of-travel capture zones delineated from steady-state MODFLOW models for the years 2014 to 2019. Models were varied by adjusting the recharge array and the known pumping rates of study wells #5 and #6 and irrigation well BD773. Study parcels 1 through 4 from figure 23 are outlined in each panel.



Roads from U.S. Census Bureau, 2015. Hydrography from U.S. Geological Survey National Hydrography Dataset, 2016. Wisconsin Transverse Mercator projection, 1991 Adjustment to the North American Datum of 1983 (NAD 83/91); EPSG 3071.

Figure 42. Schematic diagram demonstrating the conceptual flow of recharge and the associated age distribution of groundwater at a pumping well for the year 2018. The horizontal axis (top) represents an increasing distance from a pumping well. The vertical axis represents the depth of the well screen from the ground surface. As water flows toward the well, it is displaced vertically downward by newer recharge, resulting in a “stack” of water in the well screen that is youngest at the top and oldest at the bottom.



calendar year 2018. A better match to the observed nitrate concentrations was achieved with more conservative values, and the quantity used in the effective nitrate calculator for all model years was set to 309 mg/L.

The total annual nitrate loading to groundwater (in kilograms N) from parcels 1 through 3 was estimated for the years 1994 through 2018 using one of two different approaches. The first approach used USGS monitoring-well data to assign a nitrate load to recharge. The second approach assigned the nitrate load to recharge on the basis of specific land-cover categories or crops. The latter method was particularly useful because it allowed users to evaluate how specific land-management deci-

sions in the model domain influenced the quality of groundwater withdrawn from the study wells.

Monitoring-well approach

The monitoring-well approach assumed that the nitrate concentration in recharge originating over parcels 1 through 3 varied over time. These variations were represented in the effective nitrate calculator by assigning a unique nitrate concentration (in milligrams per liter) to each year of recharge. For the years 1994 through 2018, the assigned value for each parcel was set to be equal to the maximum nitrate concentration observed in an appropriate monitoring well during the same calendar year. Using the maxi-

mum value had the benefit of providing the most conservative or “worst-case” estimate while also acknowledging that incomplete sampling records may have led to an underestimation of the annual mean nitrate concentration (see Section 2). Using the maximum annual nitrate concentration avoids carrying this underestimated annual mean through to the final calculation of nitrate concentrations in well water.

As discussed in Section 2, the nitrate concentration in recharge originating under parcel 1 appeared to be best captured by MW 8A, and recharge originating under parcel 2 appeared to be best captured by MW 1A. Because parcels 2 and 3 are managed by the same operator, the monitoring-well approach

assumed that the nitrate concentrations in MW 1A were also representative of recharge under parcel 3. Appendix D, table D.1, summarizes the parcel-specific nitrate concentrations determined by the monitoring-well approach for the years 1994 to 2018.

Land-use approach

The land-use approach assigned static nitrate concentrations to recharge originating over parcels 1 through 3 on the basis of specific land-cover categories. Nitrate-loading rates associated with specific crops or land covers were estimated using a combination of values found in the literature and observed nitrate values in representative monitoring wells (table 11). The nitrate concentrations in recharge from grazed pasture and alfalfa in parcel 1 were adjusted from the values found in the literature to reflect planned nitrogen-application rates reported in the nutrient management plans (NMPs) prepared for parcel 1 in 2016 and 2018. The adjusted values are shown below the values derived from the literature, and they are marked

with an asterisk in table 11. Because MW 1A lies immediately upgradient of parcel 2 (fig. 23), which was planted with 75 to 100 percent soybeans in 2016 and 2017, the nitrate concentrations in groundwater observed at this location during those years were taken to represent typical nitrate concentrations of recharge originating under the soybean crop. Similarly, the estimated nitrate concentration in groundwater originating under the dry beans crop was taken from the MW 1A samples collected in 2012. The nitrates originating from residential land cover (mainly lawn) within parcel 1 were estimated by assuming that septic-tank effluent from a single household was the primary nitrogen source. The total nitrogen concentration was taken as 81 mg/L in septic-tank leachate, discharged at a rate of 120 gallons per day, which corresponded to the estimated wastewater production for a household of two (Lusk and others, 2017). Although septic-tank effluent contains a mixture of organic and inorganic nitrogen, this model assumed that organic nitrogen as

ammonia ($R-NH_3$) and ammonium (NH_4^+) in septic-tank effluent is fully oxidized to nitrate in groundwater. Nitrate in septic-tank effluent was assumed to have been distributed uniformly across the residential land area (3 percent of parcel 1) and the final nitrate concentration in recharge from the residential portion of parcel 1 was estimated by dividing the total nitrogen concentration in the daily septic-tank effluent by the total volume of daily recharge originating in the residential portion of this parcel. The result was 1.8 mg/L of nitrate.

A visual inspection of the U.S. Department of Agriculture's CropScape data layers (appendix B; National Agricultural Statistics Service, 2020) indicates that parcels 1 and 2 were often subdivided into smaller subparcels that supported different crops. The boundaries separating the subparcels appear to have remained constant over time and are illustrated in figure 43. In this model, the nitrate concentration in recharge to the water table originating under parcels 1 through 3 in years 1994

Table 11. Average nitrate concentrations in soil leachate under different land covers.

Land-cover category	Nitrate concentration below root zone (in mg/L)	Source
Alfalfa	4–4.9 *10	(Robbins and Carter, 1980) (Toth and Fox, 1998)
Corn	15–24	(Kraft, 2000) (Toth and Fox, 1998)
Grazed pasture	9–11 *35	(Pakrou and Dillon, 2004)
Residential in parcel 1**	1.8	(Lusk and others, 2017)
Soybeans**	20.4	MW 1A (2016–2017)
Dry beans	9.1	MW 1A (2012)
Uncultivated***	4.6	Kevin Masarik (University of Wisconsin–Stevens Point, written communication, 2019)

Abbreviation: mg/L = milligrams per liter.

*Value was adjusted to account for planned nitrogen application rates reported in the nutrient management plan prepared for parcel 1 in 2016 and 2018.

**Soybeans and residential values were estimated from monitoring-well data.

***Uncultivated/mixed-use data are specific to the study area using average nitrate concentrations from residential drinking-water wells within the study area that are least likely to include recharge that originated over cultivated land.

through 2018 was estimated using an area-weighted average of field-level nitrate loading, as follows:

1. For each year that a CropScape Data Layer was available (2008–2018), the data were visually inspected and used to determine specific land-cover categories for each parcel.
2. The percent of each parcel allocated to a specific land-cover category was tallied using the zonal statistics tool in ArcMap (fig. 43).
3. A nitrate-loading rate (in milligrams per liter) was assigned to each specific land-use category (table 11).
4. The area-weighted nitrate-loading rate for each parcel was calculated by multiplying the percentage of the parcel allocated to a specific land-cover category by the nitrate-loading rate assigned to that same land-use category.

As an example, see figure 43, which illustrates the specific land-cover categories in parcels 1 through 3 for the year 2017. Parcels 1 and 2 were subdivided into smaller sections on the basis of historical crop patterns, and the size of each section was shown as a percentage of the total parcel. The area-weighted nitrate concentration for parcel 1 was calculated as shown in table 12.

The annual land-cover designations and area-weighted nitrate concentrations for parcels 1 through 3 are shown in appendix E, tables E.1–E.3. Appendix E, table E.4, summarizes the parcel-specific nitrate concentrations determined by this method for the years 1994 through 2018.

Estimating nitrate concentrations in high-capacity wells

The nitrate concentrations in the high-capacity well discharges during 2019 were estimated as follows:

1. The steady-state MODFLOW model (see Section 3) was modified using 2019 values of potential recharge and high-capacity-well pumping.
2. Capture zones were delineated for the following travel times: 1, 2, 3, 4, 5, 6 to 10, 11 to 15, and 16 to 25 yr.
3. Each time-of-travel (TOT) capture zone was split along boundaries of parcels 1 through 4 using the ArcGIS “Split Polygons” tool.
4. The depth of recharge (in feet per day) originating from parcels 1 through 4 and the surrounding uncultivated land area was estimated for each TOT zone using the zonal statistics tool in ArcMAP software (table 13). This tool determines the mean value of the raster data within a defined boundary. In this example,

the raster file was the 2019 recharge dataset from the SWB model (see previous section), and the boundaries were polygons corresponding to each TOT zone in the 2019 well-capture zone.

5. The contributing area (in square feet) from parcels 1 through 4 and the surrounding uncultivated land corresponding to each TOT zone was calculated using the “calculate geometry” tool in ArcGIS.
6. The nitrate concentration (in milligrams per liter, mg/L) in recharge (in liters, L) originating under parcels 1 through 3 was determined for each TOT zone using either the monitoring-well approach or the land-cover approach.
7. The mass of nitrogen (N, in milligrams, mg) conveyed to groundwater through parcels 1 through 3 was calculated for each TOT zone and parcel combination as follows (equation 1):
8. The mass of nitrogen (in milligrams) conveyed to groundwater through parcel 4 was calculated as follows (equation 2):
9. The mass of nitrogen (in milligrams) conveyed to groundwater through uncultivated land within the TOT capture zones but outside the boundaries of parcels 1 through 4 was calculated as follows (equation 3):

$$\text{mg N}_{(\text{TOT, parcel})} = \text{nitrate (mg/L)} \times \text{recharge}_{(\text{TOT, parcel})} (\text{L})$$

$$\text{mg N}_{(\text{Parcel 4})} = 309.2 (\text{mg/L}) \times \text{recharge}_{(\text{Parcel 4})} (\text{L})$$

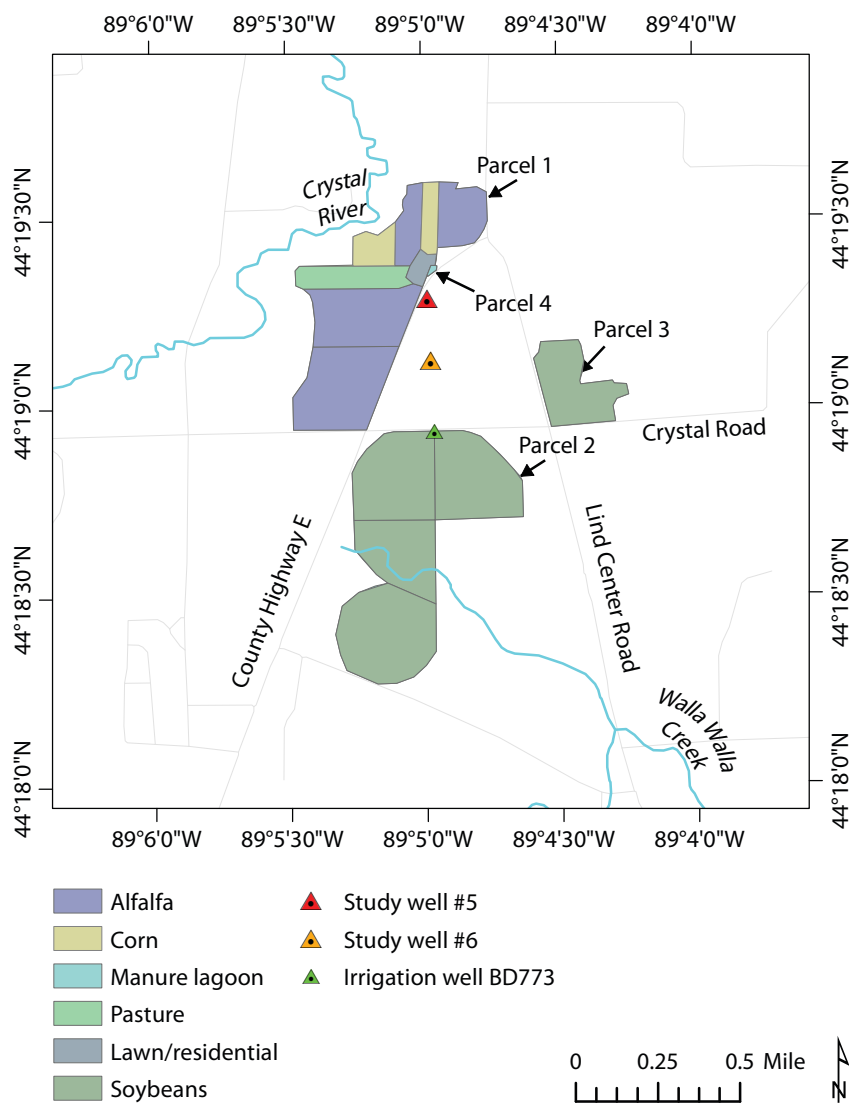
$$\text{mg N}_{(\text{uncultivated})} = 4.6 (\text{mg/L}) \times \text{recharge}_{(\text{uncultivated})} (\text{L})$$

Table 12. Sample calculation of area-weighted nitrate concentrations in recharge for a single year (2018) in a single parcel (parcel 1).

Land-cover category	Percentage (%) of parcel 1	Weighted nitrate concentration in recharge
Alfalfa	30% + 25% + 8% + 12% = 75%	75% × 10 mg/L = 7.5 mg/L
Corn	6% + 5% = 11%	11% × 24 mg/L = 2.6 mg/L
Residential	3%	3% × 1.8 mg/L = 0.05 mg/L
Pasture	11%	11% × 35 mg/L = 3.9 mg/L
Total		7.5 + 2.6 + 0.05 + 3.9 = 14.2 mg/L

Abbreviation: mg/L = milligrams per liter.

Figure 43. Example of 2017 land-cover data used to calculate the area-weighted nitrate-loading rate for parcels 1 through 4. No specific land-cover category is assigned to areas outside the boundaries of parcels 1 through 4.



The effective nitrate concentration at the pumping well was calculated by summing the total mass of nitrogen originating from each parcel, subparcel, or uncultivated land area and dividing by the total recharge. Table 13 provides a sample of these calculations for the capture zones delineated from a MODFLOW simulation that was based on pumping rates and recharge in 2019. Note that if the TOT zone represents more than 1 yr of recharge, the mass of nitrogen used in the effective nitrate calculator for parcels 1 through 3 is an average of the mass calculated for each contributing year. Copies of these calculations are also available online in the Supplemental Material (dataset 3) for this report.

Results

The results of the monitoring-well approach and land-use approach to construct effective nitrate calculators for study well #5 and study well #6 are presented in figure 44 and figure 45, respectively.

Roads from U.S. Census Bureau, 2015. Hydrography from U.S. Geological Survey National Hydrography Dataset, 2016. Wisconsin Transverse Mercator projection, 1991 Adjustment to the North American Datum of 1983 (NAD 83/91); EPSG 3071.

Table 13. Sample calculations of the effective nitrate concentration in study well #5 in 2019. Note: cells highlighted in yellow require user input.

	Estimated nitrate ¹ in recharge (mg/L)								
	2018	2017	2016	2015	2014	2009–2013	2004–2008	1994–2003	Average
Parcel 1	11.2	20.8	15.5	9.8	4.0	20.0	24.0	24.7	16.24
Parcel 2	14.2	23.4	22.9	17.0	11.0	19.0	14.9	16.1	17.30
Parcel 3	14.2	23.4	22.9	17.0	11.0	19.0	14.9	16.1	17.30
Parcel 4	309.2	309.2	309.2	309.2	309.2	309.2	309.2	309.2	309.20
Uncultivated land	4.60	4.60	4.60	4.60	4.60	4.60	4.60	4.60	4.60
	Depth of recharge ² by TOT zone and parcel (ft/d)								
	2018	2017	2016	2015	2014	2009–2013	2004–2008	1994–2003	Average
Parcel 1	0.001	0.002	0.002	0.002	0.003	0.002	0.002	0.002	0.002
Parcel 2	0.005	0.002	0.002	0.002	0.003	0.002	0.002	0.002	0.003
Parcel 3	0.003	0.002	0.002	0.002	0.003	0.003	0.003	0.003	0.003
Parcel 4	0.004	0.002	0.002	0.002	0.002	0.002	0.002	0.002	0.002
Uncultivated land	0.004	0.002	0.002	0.002	0.003	0.002	0.002	0.002	0.002
	Contributing area by TOT zone and parcel (ft ²)								
	2018	2017	2016	2015	2014	2009–2013	2004–2008	1994–2003	Total
Parcel 1	24,055	41,312	398,231	253,711	619,282	745,805	48,715	37,287	2,168,398
Parcel 2	0	0	0	0	0	88,232	116,123	180,899	385,254
Parcel 3	0	0	0	0	0	0	69,786	9,331	79,117
Parcel 4	0	0	2,311	11,921	0	0	0	0	14,232
Uncultivated land	132,513	131,519	815,403	429,023	320,091	1,721,167	802,669	1,513,423	5,865,808
	Volume of recharge by TOT zone and parcel (L/d)								
	1 year	2 years	3 years	4 years	5 years	6–10 years	11–15 years	16–25 years	Total
Parcel 1	952	2,417	25,560	15,565	52,830	49,943	3,262	2,497	153,028
Parcel 2	0	0	0	0	0	6,112	8,044	12,531	26,687
Parcel 3	0	0	0	0	0	0	4,947	661	5,608
Parcel 4	0	0	109	510	0	0	0	0	619
Uncultivated land	15,009	7,076	50,278	25,679	25,175	106,951	49,877	94,042	374,086
	Mass loading of nitrogen by parcel and travel time (mg)								
	1 year	2 years	3 years	4 years	5 years	6–10 years	11–15 years	16–25 years	Total
Parcel 1	10,665	50,270	396,186	151,762	211,321	998,865	78,294	61,674	1,959,038
Parcel 2	0	0	0	0	0	116,127	119,453	202,126	437,705
Parcel 3	0	0	0	0	0	0	73,459	10,669	84,128
Parcel 4	0	0	33,604	157,719	0	0	0	0	191,323
Uncultivated land	69,043	32,549	231,277	118,123	115,806	491,974	229,433	432,593	1,720,798
mg N (Total)	79,709	82,820	661,066	427,605	327,127	1,606,966	500,639	707,062	4,392,992
Effective nitrate concentration in well (mg/L)	4.99	8.72	8.70	10.24	4.19	9.86	7.57	6.44	7.84

Abbreviations: ft² = square feet; ft/d = feet per day; L/d = liters per day; mg N = milligrams of nitrogen; mg/L = milligrams per liter; TOT = time of travel.

¹In this example, estimated nitrate concentrations in recharge for parcels 1 through 3 are based on the weighted volume method described in step 4 of the land-cover approach to estimating nitrates in recharge.

²Depth of recharge (ft/day) is specific to each TOT zone delineated from a MODFLOW model using well-pumping rates and recharge for 2019. Where the TOT zone includes multiple years, a 10-year average (2010–2019) recharge rate is applied.

Figure 44. Results of the effective nitrate calculator for study well #5 from 2014 to 2019, comparing the monitoring-well and land-use approaches. Gray bars represent the range of nitrate concentrations measured in municipal water samples for each model year.

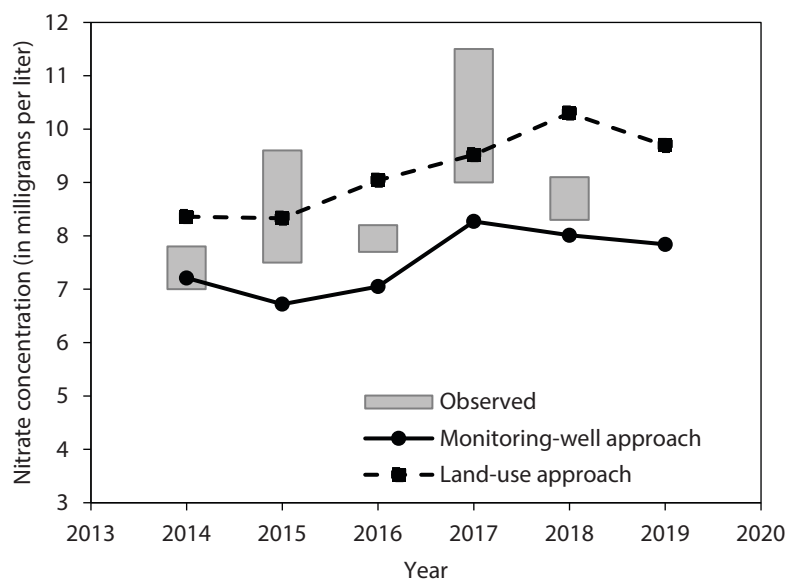
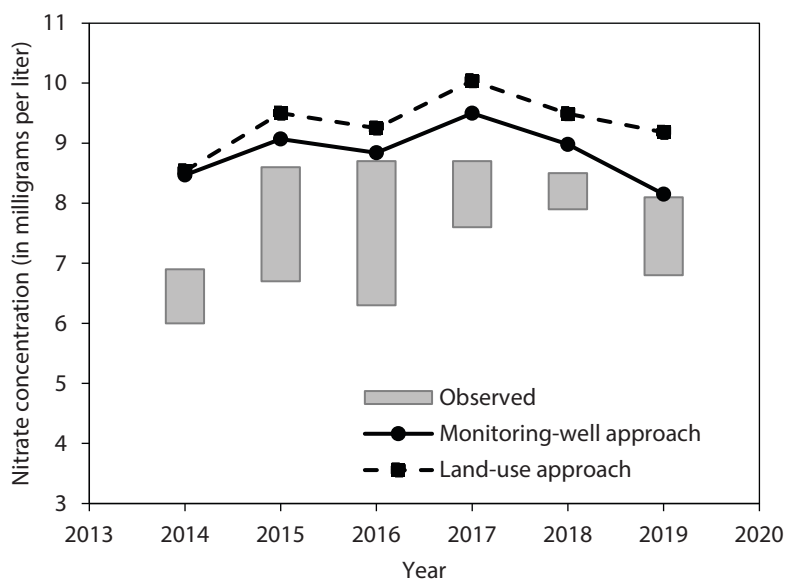


Figure 45. Results of the effective nitrate calculator for study well #6 from 2014 to 2019, comparing the monitoring-well and land-use approaches. Gray bars represent the range of nitrate concentrations measured in municipal water samples for each model year.



Monitoring-well approach

The monitoring-well approach to estimate the nitrate concentration in recharge provides good estimates of the nitrate concentrations for study well #5 (fig. 44) and study well #6 (fig. 45). In general, however, the method underestimates the nitrate concentration in study well #5 and overestimates the nitrate concentration in study well #6. These differences probably reflect the quality of the assumption that groundwater sampled at MW 8A and MW 1A is representative of recharge from parcels 1 and 2, respectively. Groundwater recharge originating in the northwestern portions of parcel 1 is unlikely to be well-represented by groundwater capture at MW 8A, where the flow is generally from southwest to northeast. Historically, the southwestern corner of parcel 1 has most frequently been planted with alfalfa and the northeastern corner has more commonly included a corn rotation. Higher nitrate loads from corn in this portion of parcel 1 would not be captured by MW 8A, leading to an underestimation of nitrate concentrations in recharge under parcel 1 that reached study well #5. However, MW 1A is better situated to capture a mix of groundwater recharge from parcel 2, which is centered in the capture zone for well #6. The effective nitrate calculator generally agrees with the observed nitrate concentrations in study well #6, except in 2014, when the concentration was overestimated by more than 1 mg/L.

Land-cover approach

The land-cover approach to estimate the nitrate concentration in recharge over parcels 1 through 3 also provides good estimates of nitrate concentrations for study well #5 (fig. 44) and study well #6 (fig. 45) and appears to capture the temporal trend. When comparing the monitoring-well approach and the land-cover approach at study wells #5 and #6, the land-cover approach yields higher estimates of nitrate concentrations for each year and agrees slightly

better with field observations. The fit is improved probably because the land-cover method better accounts for a mix of crops with higher nitrate loads that are not well-captured by MW 8A. The effective nitrate concentrations predicted for study well #6 are also higher than those predicted using the monitoring-well approach. At this location, the monitoring-well approach yields a better overall fit to the observed nitrate concentration. The difference between the two results is comparable for each of the years simulated, which suggests that the nitrate-loading estimates used in the land-use approach are too high. The tendency for both approaches to overestimate nitrate concentrations also indicates a bias that is common to both of these approaches. The irrigation well located in parcel 2 may contribute to this bias. During the summer months, when nitrogen is applied to cultivated crops, the irrigation well extracts shallow groundwater recharging over parcel 2 and redistributes it over the entire parcel. Not all of the parcel is in the capture zone for study well #6, which may result in the “loss” of some nitrate through physical displacement. Additional nitrate losses may occur as a result of crop uptake as the irrigation water percolates through the rooting zone.

Application of the model

The MODFLOW groundwater-flow model and the effective nitrate calculator are useful decision-support tools for the management of Waupaca’s southern study-well field. MODPATH-generated capture zones can be used in conjunction with the effective nitrate calculator to evaluate how changes in mean well-pumping rates, irrigation, and crop rotations may impact the quality of municipal water supplies and provide a scientific basis for recommending changes that reduce nitrate loading to the study-well system.

Evaluating the effects of a concentrated source of nitrates

The effective nitrate calculator can be a useful tool for evaluating the overall impact of a concentrated source of nitrates. In this study, an unlined manure lagoon (parcel 4) was estimated to add 0.33 kg of nitrate to the groundwater each day, which adds approximately 0.09 mg/L to the effective nitrate concentration in study well #5. The results of this study indicate that lining the pond would yield only modest improvements to the nitrate concentrations at this well. In future studies, the effective nitrate calculator could be used to evaluate the potential impact of a new manure pond on well-water quality or help to optimize the size and (or) placement of a lagoon with respect to a municipal water source.

Evaluating the effects of residential septic systems

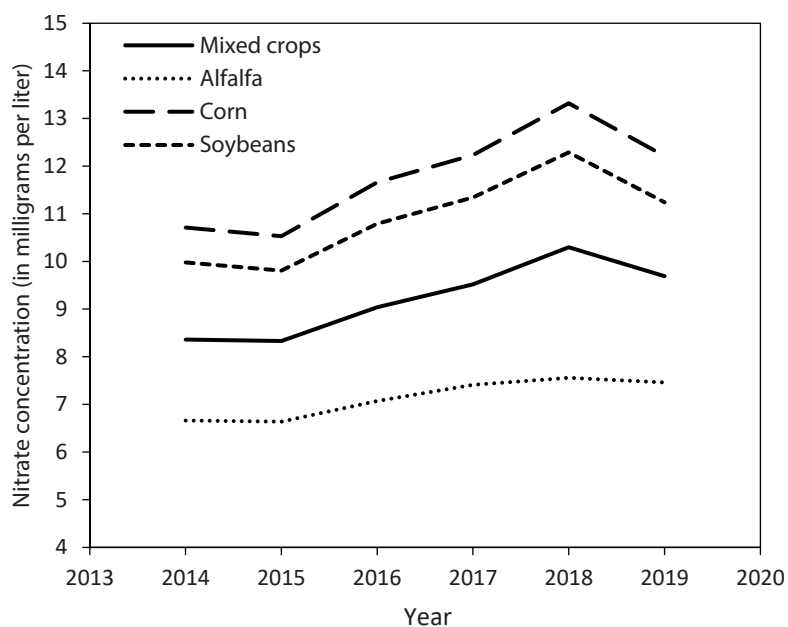
In this study, residential septic systems were not considered to be a major source of nitrates because the modeled capture zones are predominantly used for agriculture. However, the effective

nitrate calculator could be used in future studies to estimate the impacts of a new or expanded rural housing development on nitrates in groundwater.

Evaluating the effects of crops

The land-cover-based effective nitrate calculator may also be used to determine how the crops grown on an individual parcel may influence the effective nitrate concentration at the study wells. For example, the land-cover-based calculator estimates that the effective nitrate concentration at well #5 was reduced by up to 21 percent under pumping rates for 2016 through 2019, when alfalfa was the only crop grown on parcel 1; however, the calculator estimates that converting all the cultivated fields on parcel 1 to soybeans or corn may increase their nitrate concentrations by 19 or 28 percent, respectively (fig. 46). For future uses, the calculator could be refined by treating each of the subparcels in parcels 1 and 2 (fig. 43) as unique parcels to explore the relative importance of crop type as a function of location on the effective nitrate concentration at the study wells.

Figure 46. Results of land-cover-based effective nitrate calculator for study well #5 if the crops grown on parcel 1 were mixed (based on parcel 1’s actual land-cover history) or if they consisted solely of alfalfa, corn, or soybeans.



Evaluating the effect of pumping rates

When well-pumping rates are less than 80,000 ft³/d, the effective nitrate concentration generally increases as the fraction of the well's capture zone under cultivation increases (fig. 47). This trend is consistent with the conclusion that cultivated crops are the dominant contributor to nitrates in groundwater captured by study wells #5 and #6. The relation between the fraction of cultivated land and the effective nitrate concentration is poorly defined for study well #5 before the simulations from 2014 to 2016, when pumping rates exceeded 80,000 ft³/d. The lack of a clear relation may be the result of changes in local groundwater-flow boundaries caused by high pumping rates recorded during these years. For instance, there are two distinct pumping regimes at study well #5: pumping below 80,000 ft³/d (2017 to present) and above 80,000 ft³/d (before 2016) (fig. 48). These two regimes appear to be linked to the pumping-rate threshold at which the MODFLOW model begins to simulate flow across (and possibly from) the Crystal River. Under this scenario, a mass balance in the MODFLOW model indicates that some portion of water captured by the well originates as surface water flowing through the Crystal River. Nitrates in water flowing through the Crystal River are not represented in the effective nitrate calculator; they would most likely have the effect of diluting the effective nitrate concentration while also masking the relation between the percentage of cultivated land in the capture zone and the effective nitrate concentration in a pumping well.

At study well #6, the relation between the pumping rate and the percentage of cultivated land in the capture zone is not well defined when both parcels 1 and 2 are considered, even if the pumping rate from the high-capacity irrigation well BD773 is added (fig. 49). A stronger correlation exists

Figure 47. Results of the land-cover-based effective nitrate calculator plotted as a function of the percentage of a well's capture zone that is actively cultivated. Data for study well #5 were separated into two groups that were based on pumping rates. Dotted lines are lines of best fit. Abbreviations: ft³/d = cubic feet per day; R² = coefficient of determination.

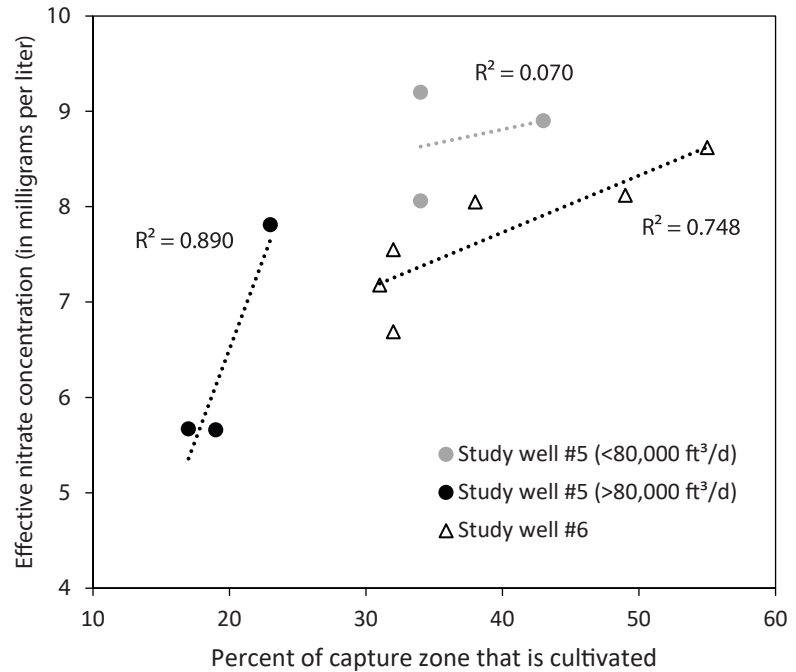
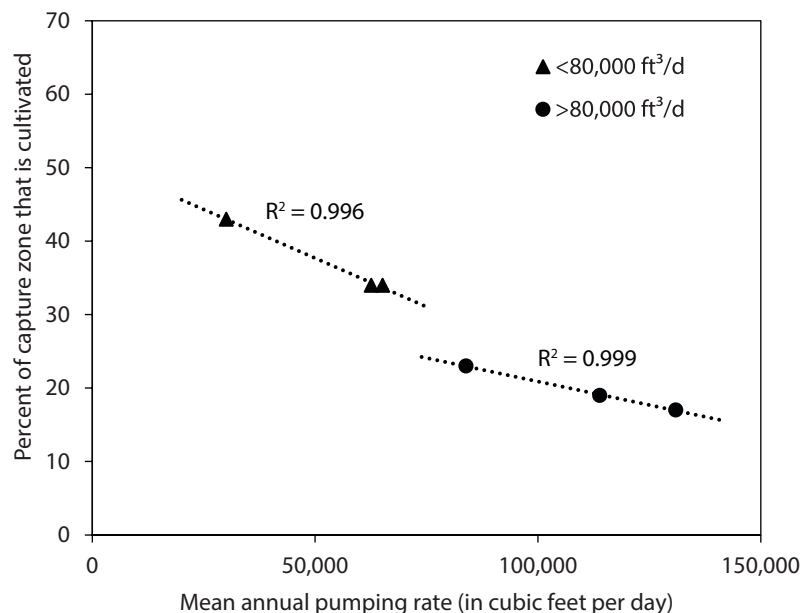


Figure 48. The percentage of the study well #5's capture zone that is under cultivation as a function of the mean annual pumping rate. A direct relation exists between the percentage of the well's capture zone that is cultivated and the specific pumping regime. Dotted lines are lines of best fit. Abbreviations: ft³/day = cubic feet per day; R² = coefficient of determination.



between study well #6's pumping rate and parcel 2 as a percent of the total capture zone (fig. 50).

These relations suggest that the mean annual pumping rates at study well's #5 and #6 can be optimized, depending on municipal needs, to reduce the overall influence of cultivation on their effective nitrate concentrations. The MODFLOW model and land-cover-based effective nitrate calculator can be used toward that goal by generating capture zones for a range of predefined pumping rates for each well.

Model limitations

The effective nitrate calculator aims to predict nitrate concentrations and annual trends in study wells #5 and #6 on the basis of (1) the land cover and (2) the time of travel between recharge at the land surface and groundwater pumping rates. Although the modeled estimates of nitrate loading in recharge were comparable to independent observations (figs. 44, 45), the model tended to overestimate nitrate concentrations in the municipal wells targeted by this study. This bias points to some limitations in the model, particularly with respect to nitrogen-loading estimates, recharge calculations, and irrigation impacts.

Nitrate-loading estimates

The nitrate-loading estimates were based on several assumptions that could affect the quality of those estimates. First, the default value of 4.6 mg/L for uncultivated land may be too high. This value is the historical mean nitrate concentration reported for MW 2A, which is believed to capture groundwater that recharges over mixed forest and low-density residential development. However, this monitoring well is also immediately adjacent to parcel 1 (fig. 26) and subtle variations in the water table may introduce some recharge from parcel 1 that has higher nitrate concentrations. Estimates of nitrate loading from uncultivated land could be improved by treating each

Figure 49. The percentage of study well #6's capture zone that is under cultivation as a function of the mean annual pumping rate with or without data from high-capacity irrigation well BD773. Dotted lines are lines of best fit. Abbreviation: R^2 = coefficient of determination.

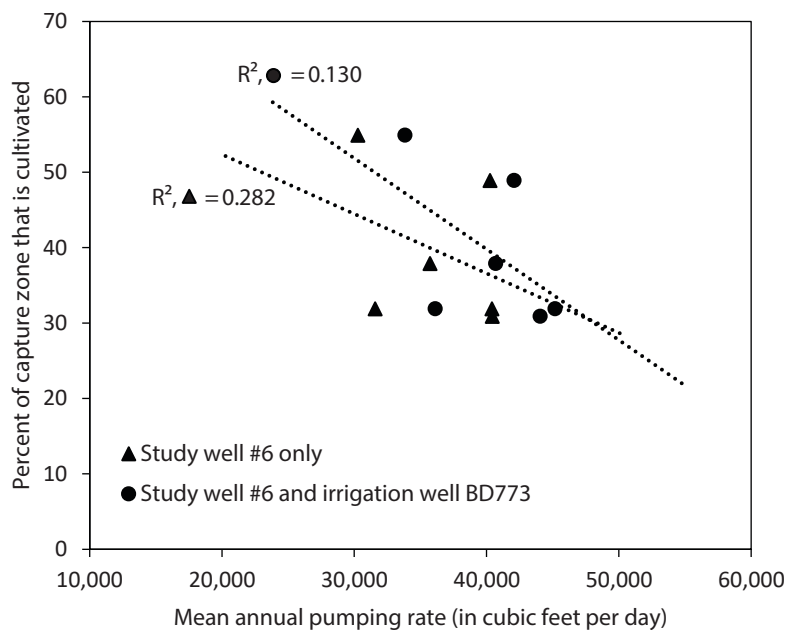
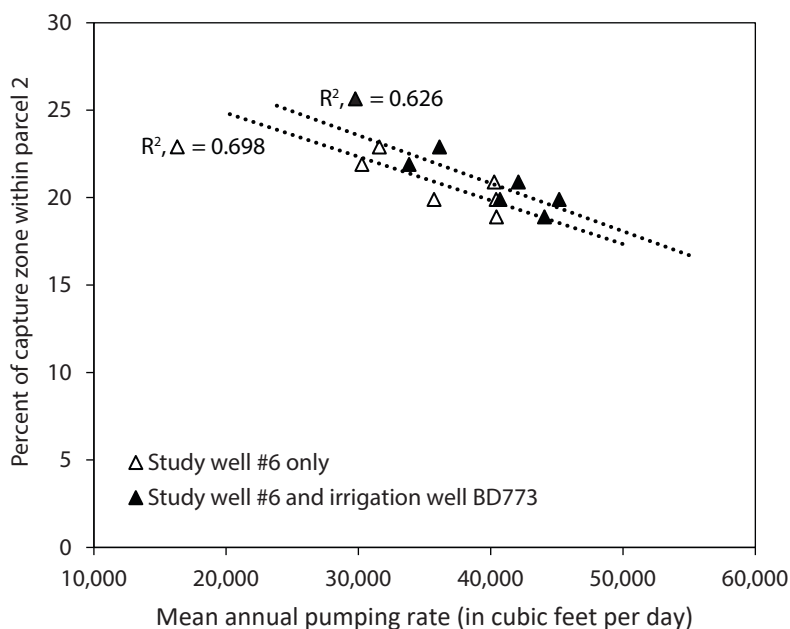


Figure 50. Relation between the mean annual pumping rate of study well #6, with or without data for high-capacity irrigation well BD773, to the percentage of the capture zone that lies within parcel 2. Dotted lines are lines of best fit. Abbreviation: R^2 = coefficient of determination.



type of uncultivated land coverage separately rather than by combining all uncultivated land coverages into one category. Additionally, not all of the values from the literature that were used to represent nitrate loading from different crop types were based on samples from well-drained sandy soils. Better estimates may be obtained if studies were performed locally and irrigation patterns were considered. For example, parcel 1 historically has not been irrigated, whereas parcel 2 has, a factor that could lead to important differences in how much nitrate is lost from the different crops grown on these parcels.

Recharge estimates in the effective nitrate calculator

A water balance was calculated in MODFLOW by drawing a polygon corresponding to the well-capture zone over the model grid and examining the sources of flow into and out of the capture zone. The water balance shows that recharge estimates (using the SWB model) within these capture zones account for nearly 100 percent of the water being extracted by each pumping well, except in 2014, 2015, and 2016. In those years, parts of study well #5's capture zone extend across the Crystal River, and in these instances the water balance consists of water that exits the stream channel and is cap-

tured by the pumping well. However, the recharge volumes calculated for the effective nitrate calculator using the areal mean within each capture zone (see "Estimating nitrate in high-capacity wells," above) account for only 47 to 66 percent of the volume of water extracted by the study wells from 2014 to 2019 (table 14). The discrepancy between these two methods for estimating recharge volume suggests that the effective nitrate calculator could be improved by calculating recharge inside each TOT zone using zonal math; that is, calculate the volume of recharge for each 30-meter × 30-meter raster grid cell in the SWB and sum the results inside the boundaries of each TOT zone. We note, however, that underestimating recharge volume does not greatly affect the results of the effective nitrate calculator because volume recharge appears in both the numerator and the denominator of the following equation (equation 4).

The subscript "n" in equation 4 indicates a subportion of the capture zone whose boundaries are defined by the TOT zone and land-use designation.

$$\frac{\sum (\text{nitrate, mg/L})_n (\text{volume recharge})_n (\text{recharge area})_n}{\text{total volume recharge}}$$

To verify this assertion, the effective nitrate concentration in 2019 was recalculated using twice the recharge. The result, 9.69 mg/L, is equal to the result obtained using recharge values calculated using the areal mean inside each TOT zone.

Irrigation impacts

An irrigation well (BD733) located on the northern edge of parcel 2 withdraws water that recharges over a portion of the parcel itself, potentially reducing the mass of nitrate leached from parcel 2 that reaches study well #6. This presumed benefit is based on the assumption that the irrigation well captures a portion of water with a high nitrate load that would, in its absence, be captured by study well #6. Instead, the capture zone for study well #6 broadens slightly, increasing the contributions from non-agricultural recharge areas and consequently reducing the estimated nitrate concentration at this well. A second irrigation well (YD748) was installed in the southeastern corner of parcel 2 in 2017 and may yield a similar benefit to study well #5 in the future.

Table 14. Recharge for the full capture zones of study wells #5 and #6 compared to the well discharge.

Year	Study well #5			Study well #6		
	Recharge (MODFLOW, ft ³ /d) ¹	Recharge (calculated, ft ³ /d) ²	Well discharge (ft ³ /d)	Recharge (MODFLOW, ft ³ /d) ¹	Recharge (calculated, ft ³ /d) ²	Well discharge (ft ³ /d)
2014	109,999*	58,258	119,878	44,710	22,403	40,406
2015	107,592*	63,682	130,933	48,242	21,646	40,430
2016	85,497	51,424	83,886	39,788	19,669	31,578
2017	63,778	29,394	62,571	47,457	17,288	35,717
2018	72,353	37,658	65,120	38,792	16,918	30,265
2019	71,455	19,777	30,030	37,147	25,473	40,257

Abbreviation: ft³/d = cubic feet per day.

*Additional recharge originating from the Crystal River indicated by MODFLOW mass balance.

¹Using a mass balance.

²Using a depth-x calculation in the effective nitrate calculator.

Summary

- The aquifer supplying the City of Waupaca's municipal well #5 and municipal well #6 consists of glacial sand and gravel deposits. The aquifer is relatively thin (less than 200 ft) but highly productive. The mean estimated hydraulic conductivity of the aquifer is 36 ft/d, with a range of 0.09 to 1,432 ft/d, and it can supply both wells at a combined rate of more than 3,000 gallons per minute.
- The SWB-modeled mean potential groundwater recharge is relatively high (13.7 in./yr), with higher potential in areas of low topographic relief. Where irrigation recharge was added (0.67 in./yr), it accounts for less than 5 percent of total annual recharge and does not lead to a major change in the daily recharge rate.
- Water quality in the groundwater-shed is impacted by human activity. Nitrate concentrations above background concentrations (greater than 2 mg/L) were observed in seven shallow (17–22 ft) monitoring wells on one or more occasions from 1993 to 2018. At some locations at or near the edge of cultivated fields, nitrate concentrations have periodically exceeded enforcement standards (10 mg/L) by as much as 100 percent. Agricultural elements including crop cultivation and cattle manure (grazing pasture and lagoon) are the most probable sources of the nitrate in the municipal wells.
- The GFLOW and MODFLOW models are a useful set of decision-support tools that can be used to evaluate many aspects of the local groundwater-flow system—such as the direction of groundwater flow or contaminant transport—and to delineate capture zones contributing recharge to the study wells.
- The effective nitrate calculator is a useful decision-support tool that can be used to evaluate how changes to land management could impact the quality of water discharged to the municipal pumping wells. Recommended future activities include the following:
 - a. Perform an isotope study to estimate the age of groundwater extracted by the study wells as a means of evaluating the accuracy of the capture zones delineated using MODPATH; the current method indicates that the groundwater in this aquifer is no more than 30 years old.
 - b. Improve the simulations of the exchange between surface water and groundwater across the Crystal River.
 - c. Evaluate and improve recharge estimates to achieve better agreement between the calculated recharge and published well discharge.
 - d. Develop a transient MODFLOW model to investigate the possibility that changing the rate or times at which study wells #5 and #6 withdraw groundwater can be used to purposefully modify the capture zones for each well in a way that will reduce nitrate concentrations in the raw municipal water supply through dilution or blending.
 - e. Develop a geospatial-data tool to quickly convert MODPATH particle traces into capture zones that correspond to user-defined travel-time periods.
 - f. Develop a land-use-based effective nitrate calculator that can estimate nitrate concentrations in recharge directly from CropScape Data Layers. This tool would be more broadly applicable to other areas where different crop rotations may be in use.

Supplemental material

The results of the inventory, modeling, and analysis described in this report are publicly available via the online WGNHS Publication Catalog (<https://wgnhs.wisc.edu/catalog/>).

Supplemental materials include:

Dataset 1: Geodatabase of study data from Waupaca, Wisconsin

GIS data (.gdb format) of well, geology, hydraulic property, recharge, and groundwater data used in this study, as well as groundwater modeling output. Includes a ReadMe file (.txt).

Dataset 2: Groundwater flow modeling files from Waupaca, Wisconsin

GFLOW and MODFLOW flow models (.gfl and .nam format, respectively) and associated files. Includes a ReadMe file (.txt).

Dataset 3: Nitrate calculators for municipal wells in Waupaca, Wisconsin

Spreadsheet-based calculators (.xlsx format) of estimated nitrate loading and annual nitrate concentrations in study wells #5 and #6.

References

- Ahlfeld, D.P., Baker, K.M., and Barlow, P.M., 2009, GWM-2005—A ground-water-management process for MODFLOW-2005 with local grid refinement (LGR) capability: U.S. Geological Survey Techniques and Methods 6–A33, 65 p., <https://pubs.usgs.gov/tm/tm6a33/>.
- Börner, F., and Berthold, S., 2009, Vertical flows in groundwater monitoring wells, *in* Kirsh, R., ed., *Groundwater geophysics*: Berlin, Springer, p. 367–389.
- Bradbury, K.R., Fienen, M.N., Kniffin, M.L., Krause, J.J., Westenbroek, S.M., Leaf, A.T., and Barlow, P.M., 2017, A ground-water flow model for the Little Plover River Basin in Wisconsin's Central Sands: Wisconsin Geological and Natural History Survey Bulletin 111, 82 p., <https://wgnhs.wisc.edu/catalog/publication/000946/resource/b111>.
- Bradbury, K.R., and Rothschild, E.R., 1985, A computerized technique for estimating the hydraulic conductivity of aquifers from specific capacity data: *Groundwater*, v. 23, no. 2, p. 240–246.
- Chandler, V., 2011, Application of the H/V passive seismic method in Minnesota: some preliminary insights: *Geological Society of America Abstracts with Programs*, v. 43, no. 5, p. 147.
- Doherty, J.E., and Hunt, R.J., 2010, Approaches to highly parameterized inversion: a guide to using PEST for groundwater-model calibration: U.S. Geological Survey Scientific Investigations Report 2010–5109, 59 p., <https://pubs.usgs.gov/sir/2010/5169/>.
- Dyke, A.S., and Prest, V.K., 1987, Late Wisconsinan and Holocene history of the Laurentide Ice Sheet: *Géographie Physique et Quaternaire*, v. 41, no. 2, p. 237–263.
- Haitjema, H.M., 1995, *Analytic element modeling of groundwater flow*: Cambridge, Mass., Academic Press, 394 p.
- Ham, J., and DeSutter, T.M., 2000, Toward site-specific design standards for animal-waste lagoons: protecting ground water quality: *Journal of Environmental Quality*, v. 29, no. 6, p. 1721–1732.
- Harbaugh, A.W., 2005, MODFLOW-2005, the U.S. Geological Survey modular ground-water model—The ground-water flow process: U.S. Geological Survey Techniques and Methods 6–A16, 253 p., <https://pubs.er.usgs.gov/publication/tm6A16>.
- Harbaugh, A.W., Banta, E.R., Hill, M.C., and McDonald, M.G., 2000, MODFLOW-2000, The U.S. Geological Survey modular ground-water model—User guide to modularization concepts and the ground-water flow process: U.S. Geological Survey Open-File Report 2000–92, 121 p., <https://pubs.er.usgs.gov/publication/ofr200092>.
- Hunt, R.J., Anderson, M.P., and Kelson, V.A., 1998, Improving a complex finite-difference ground water flow model through the use of an analytic element screening model: *Groundwater*, v. 36, no. 6, p. 1011–1017.
- Hyder, Z., Butler, J.J., Jr., and McElwee, C., 1993, An approximate technique for analysis of slug tests in wells: Kansas Geological Survey Open-File Report 93–44, 26 p., http://www.kgs.ku.edu/Hydro/Publications/1993/OFR93_44/index.html.
- Kenoyer, G.J., 1988, Tracer test analysis of anisotropy in hydraulic conductivity of granular aquifers: *Groundwater Monitoring & Remediation*, v. 8, no. 3, p. 67–70.
- Kraft, G.J., 2000, Nitrate loading and impacts on Central Wisconsin ground-water basins, *in* Proceedings of the 2000 Wisconsin Fertilizer, Agrilime and Pest Management Conference: Madison, University of Wisconsin-Extension, p. 18–20.
- Kraft, G.J., Browne, B.A., DeVita, W.M., and Mechenich, D.J., 2008, Agricultural pollutant penetration and steady state in thick aquifers: *Groundwater*, v. 46, no. 1, p. 41–50.
- Kraft, G.J., Stites, W., and Mechenich, D.J., 1999, Impacts of irrigated vegetable agriculture on a humid north-central U.S. sand plain aquifer: *Groundwater*, v. 37, no. 4, p. 572–580.
- Lippelt, I.D., 1981, Water table map of Waupaca County, map 8 *in* Lippelt, I.D., and Hennings, R.G., *Irrigable lands inventory—Phase I ground-water and related information*: Wisconsin Geological and Natural History Survey MP81–1, scale 1:127,720. <https://wgnhs.wisc.edu/catalog/publication/000467/resource/mp811plate08>.
- Lusk, M.G., Toor, G.S., Yang, Y.-Y., Mechtensimer, S., De, M., and Obreza, T.A., 2017, A review of the fate and transport of nitrogen, phosphorus, pathogens, and trace organic chemicals in septic systems: *Critical Reviews in Environmental Science and Technology*, v. 47, no. 7, p. 455–541.
- Mode, W.N., Hooyer, T.S., Attig, J.W., and Clayton, Lee, 2015, Data accompanying WOFR2015-3: Preliminary Quaternary geology of Waupaca County, Wisconsin: Wisconsin Geological and Natural History Survey Open-File Report 2015-03-DI [digital information], accessed 2019 at <https://wgnhs.wisc.edu/catalog/publication/000937/resource/wofr201503di>.
- Mudrey, M.G., Jr., Brown, B.A., and Greenberg, J.K., 1982, Bedrock geologic map of Wisconsin: Wisconsin Geological and Natural History Survey Map M078, scale 1:1,000,000, <https://wgnhs.wisc.edu/catalog/publication/000390/resource/m078paper>.

- Mueller, D.K., Hamilton, P.A., Helsel, D.R., Hitt, K.J., and Ruddy, B.C., 1995, Nutrients in ground water and surface water of the United States—An analysis of data through 1992: U.S. Geological Survey Water Resources Investigations Report 95-4031, 75 p., <https://pubs.er.usgs.gov/publication/wri954031>.
- Multi-Resolution Land Characteristics Consortium, 2011, NLCD 2006 Land Cover (CONUS): Multi-Resolution Land Characteristics Consortium database accessed February 18, 2019, at <https://www.mrlc.gov/data/nlcd-2006-land-cover-conus>.
- National Centers for Environmental Information, 2019, Global Historical Climatology Network: National Centers for Environmental Information database accessed May 13, 2019, at <https://www.ncdc.noaa.gov/data-access/land-based-station-data/land-based-datasets/global-historical-climatology-network-ghcn>.
- National Agricultural Statistics Service, 2020, CropScape and Cropland Data Layer: National Agricultural Statistics Service database accessed February 18, 2019, at https://www.nass.usda.gov/Research_and_Science/Cropland/SARS1a.php.
- Natural Resources Conservation Service, 2018, Soil Survey Geographic Database: Natural Resources Conservation Service database accessed October 29, 2018, at <https://data.nal.usda.gov/dataset/soil-survey-geographic-database-ssurgo>.
- Niswonger, R.G., Panday, S., and Ibaraki, M., 2011, MODFLOW-NWT, a Newton formulation for MODFLOW-2005: U.S. Geological Survey Techniques and Methods 6–A37, 44 p., <https://pubs.usgs.gov/tm/tm6a37/>.
- Pakrou, N., and Dillon, P.J., 2004, Leaching losses of N under grazed irrigated and non-irrigated pastures: *The Journal of Agricultural Science*, v. 142, no. 5, p. 503–516.
- Parsen, M.J., Juckem, P.F., Gotkowitz, M.B., and Fienen, M.N., 2019, Groundwater flow model for western Chippewa County, Wisconsin—Including analysis of water resources related to industrial sand mining and irrigated agriculture: *Wisconsin Geological and Natural History Survey Bulletin B112*, 74 p., <https://wgnhs.wisc.edu/catalog/publication/000964>.
- Pollock, D.W., 2012, User guide for MODPATH version 6—A particle-tracking model for MODFLOW: U.S. Geological Survey Techniques and Methods 6–A41, 58 p., <https://pubs.usgs.gov/tm/6a41/>.
- Robbins, C.W., and Carter, D.L., 1980, Nitrate-nitrogen leached below the root zone during and following alfalfa: *Journal of Environmental Quality*, v. 9, no. 3, p. 447–450.
- Sauer, V.B., and Meyer, R.W., 1992, Determination of error in individual discharge measurements: U.S. Geological Survey Open-File Report 92–144, 21 p., <https://pubs.usgs.gov/of/1992/ofr92-144/>.
- Strack, O.D.L., 1989, *Groundwater mechanics*: Englewood Cliffs, N.J., Prentice Hall, 732 p.
- Theis, C.V., 1935, The relation between the lowering of the piezometric surface and the rate and duration of discharge of a well using ground-water storage: *Eos, Transactions, American Geophysical Union*, v. 16, no. 2, p. 519–524.
- Toth, J., 1963, A theoretical analysis of groundwater flow in small drainage basins: *Journal of Geophysical Research*, v. 68, no. 16, p. 4795–4812.
- Toth, J.D., and Fox, R.H., 1998, Nitrate losses from a corn-alfalfa rotation: Lysimeter measurement of nitrate leaching: *Journal of Environmental Quality*, v. 27, no. 5, p. 1027–1033.
- U.S. Geological Survey, 1999, The quality of our nation's waters—Nutrients and pesticides: U.S. Geological Survey Circular 1225, 82 p., <https://pubs.usgs.gov/circ/circ1225/>.
- U.S. Geological Survey, 2017, USGS NED 1/3 arc-second n45w090 1 x 1 degree IMG: U.S. Geological Survey database accessed 2018 at <https://www.sciencebase.gov/catalog/item/58877ae2e4b02e34393befc1>. [Database is no longer available and was replaced in 2019.]
- Ward, M.H., Jones, R.R., Brender, J.D., De Kok, T.M., Weyer, P.J., Nolan, B.T., Villanueva, C.M., and Van Breda, S.G., 2018, Drinking water nitrate and human health: an updated review: *International Journal of Environmental Research and Public Health*, v. 15, no. 7, p. 1557.
- Westenbroek, S.M., Kelson, V.A., Dripps, W.R., Hunt, R.J., and Bradbury, K.R., 2010, SWB—A modified Thornthwaite-Mather Soil-Water-Balance code for estimating groundwater recharge: U.S. Geological Survey Techniques and Methods 6–A31, 60 p., <https://pubs.usgs.gov/tm/tm6-a31/>.
- Winter, T.C., 2001, The concept of hydrologic landscapes: *Journal of the American Water Resources Association*, v. 37, no. 2, p. 335–349.
- Wisconsin Department of Natural Resources, 2018, Central Sands background and outreach resources: Wisconsin Department of Natural Resources web page accessed March 22, 2019, at <https://dnr.wisconsin.gov/topic/Wells/HighCap/CSLBackground.html>.
- Wisconsin Department of Natural Resources, 2019, Drinking and Groundwater Use Information System: Wisconsin Department of Natural Resources database accessed 2019 at https://dnr.wi.gov/wateruse/pub_v3_ext/source/.
- Wisconsin Department of Natural Resources, 2020a, Drinking and Groundwater Use Information System: Wisconsin Department of Natural Resources database accessed 2020 at https://dnr.wi.gov/wateruse/pub_v3_ext/source/.

Wisconsin Department of Natural Resources, 2020b, High capacity wells: Wisconsin Department of Natural Resources database accessed 2020 at <https://dnr.wi.gov/topic/Wells/HighCap/>.

Wisconsin Department of Natural Resources, 2020c, Well Construction Information System: Wisconsin Department of Natural Resources database accessed 2020 at <https://dnr.wi.gov/WellConstructionSearch/#!/PublicSearch/Index>.

Wisconsin Groundwater Coordinating Council, 2018, Wisconsin Groundwater Coordinating Council report to the legislature: Wisconsin Department of Natural Resources web page accessed 2019 at <https://dnr.wi.gov/topic/groundwater/documents/GCC/ReportArchives/GCCreport2018.pdf>.

Appendix A: Water-table measurements

Table A.1. Depth-to-water measurements collected on June 27, 2018, from the USGS monitoring-well network for the City of Waupaca, Wisc.

Well ID	Screen or piezometer ¹	Depth to water (ft)	TOC elevation (ft)	Total head (ft)	Screen elevation (ft, top)	Screen elevation (ft, bottom)	Vertical gradient ²
MW 1	A	11.45	843.9	832.45	828.9	818.9	–
	B	NT	843.9	NT	802.9	797.9	–
	C	NT	843.9	NT	778.9	768.9	–
MW 2	A	13.15	847.1	833.95	833.1	822.1	–
	B	NT	847.1	NT	812.1	797.1	–
	C	NT	847.1	NT	789.1	772.1	–
MW 3	A	14.2	849.02	834.82	839.02	824.02	–
	B	NT	849.02	NT	816.02	801.02	–
	C	NT	849.02	NT	791.02	773.02	–
MW 4	A	13.23	846.08	832.85	836.08	821.08	–
	B	NT	846.08	NT	814.08	799.08	–
	C	NT	846.08	NT	789.08	771.08	–
MW 5	A	NT	846.09	NT	826.09	821.09	–
	B	NT	846.09	NT	806.09	801.09	–
	C	NT	846.09	NT	782.09	772.09	–
MW 6	A	14.4	846.91	832.51	836.91	821.91	–
	B	NT	846.91	NT	811.91	796.91	–
	C	NT	846.91	NT	788.91	771.91	–
MW 7	A	14.85	846.33	831.48	836.33	821.33	–
	B	NT	846.33	NT	811.33	796.33	–
	C	NT	846.33	NT	788.33	771.33	–
MW 8	A	15.8	845.32	829.52	835.32	820.32	–
	B	NT	845.32	NT	810.32	795.32	–
	C	NT	845.32	NT	787.32	770.32	–

Abbreviations: ft = feet; ID = identification; MW = monitoring well; NT = measurement not taken; TOC = top of casing; USGS = U.S. Geological Survey.

¹ A = shallow well; B = intermediate-depth piezometer; C = deep piezometer.

² Depth-to-water measurements were not collected from the intermediate-depth or deep piezometers, so vertical gradients could not be determined.

Table A.2. Depth-to-water measurements collected from July 10 to 11, 2018, from the USGS monitoring-well network for the City of Waupaca, Wisc.

Well ID	Screen or piezometer ¹	Depth to water (ft)	TOC elevation (ft)	Total head (ft)	Screen elevation (ft, top)	Screen elevation (ft, bottom)	Vertical gradient ²
MW 1	A	15.26	843.9	828.64	828.9	818.9	–
	B	NT	843.9	NT	802.9	797.9	–
	C	NT	843.9	NT	778.9	768.9	–
MW 2	A	13.3	847.1	833.8	833.1	822.1	–
	B	NT	847.1	NT	812.1	797.1	–
	C	NT	847.1	NT	789.1	772.1	–
MW 3	A	14.5	849.02	834.52	839.02	824.02	–
	B	NT	849.02	NT	816.02	801.02	–
	C	NT	849.02	NT	791.02	773.02	–
MW 4	A	13.6	846.08	832.48	836.08	821.08	–
	B	NT	846.08	NT	814.08	799.08	–
	C	NT	846.08	NT	789.08	771.08	–
MW 5	A	NT	846.09	NT	826.09	821.09	–
	B	NT	846.09	NT	806.09	801.09	–
	C	NT	846.09	NT	782.09	772.09	–
MW 6	A	15.94	846.91	830.97	836.91	821.91	–
	B	NT	846.91	NT	811.91	796.91	–
	C	NT	846.91	NT	788.91	771.91	–
MW 7	A	15.28	846.33	831.08	836.33	821.33	–
	B	NT	846.33	NT	811.33	796.33	–
	C	NT	846.33	NT	788.33	771.33	–
MW 8	A	115.85	845.32	829.47	835.32	820.32	–
	B	NT	845.32	NT	810.32	795.32	–
	C	NT	845.32	NT	787.32	770.32	–

Abbreviations: ft = feet; ID = identification; MW = monitoring well; NT = measurement not taken; TOC = top of casing; USGS = U.S. Geological Survey.

¹ A = shallow well; B = intermediate-depth piezometer; C = deep piezometer.

² Depth-to-water measurements were not collected from the intermediate-depth or deep piezometers, so vertical gradients could not be determined.

Table A.3. Depth-to-water measurements collected from August 27 to 31, 2018, from the USGS monitoring-well network for the City of Waupaca, Wisc.

Well ID	Screen or piezometer ¹	Depth to water (ft)	TOC elevation (ft)	Total head (ft)	Screen elevation (ft, top)	Screen elevation (ft, bottom)	Vertical gradient ²
MW 1	A	NT	843.9	NT	828.9	818.9	–
	B	NT	843.9	NT	802.9	797.9	–
	C	NT	843.9	NT	778.9	768.9	–
MW 2	A	NT	847.1	NT	833.1	822.1	–
	B	NT	847.1	NT	812.1	797.1	–
	C	NT	847.1	NT	789.1	772.1	–
MW 3	A	14.85	849.02	834.17	839.02	824.02	–
	B	14.76	849.02	834.26	816.02	801.02	0.011
	C	14.87	849.02	834.15	791.02	773.02	–0.011
MW 4	A	13.95	846.08	832.13	836.08	821.08	–
	B	13.95	846.08	832.13	814.08	799.08	0
	C	14.81	846.08	831.27	789.08	771.08	–0.086
MW 5	A	NT	846.09	NT	826.09	821.09	–
	B	NT	846.09	NT	806.09	801.09	–
	C	NT	846.09	NT	782.09	772.09	–
MW 6	A	16.93	846.91	829.98	836.91	821.91	–
	B	16.87	846.91	830.04	811.91	796.91	0.006
	C	15.35	846.91	831.56	788.91	771.91	0.19
MW 7	A	16.62	846.33	829.71	836.33	821.33	–
	B	16.35	846.33	829.98	811.33	796.33	0.027
	C	15.8	846.33	830.53	788.33	771.33	0.069
MW 8	A	17.9	845.32	827.42	835.32	820.32	–
	B	17.56	845.32	827.76	810.32	795.32	0.034
	C	16.44	845.32	828.88	787.32	770.32	0.14

Abbreviations: ft = feet; ID = identification; MW = monitoring well; NT = measurement not taken; TOC = top of casing; USGS = U.S. Geological Survey.

¹A = shallow well; B = intermediate-depth piezometer; C = deep piezometer.

²Where values are positive, vertical gradients are upward.

Table A.4. Depth-to-water measurements collected from November 13 to 14, 2018, from the USGS and WGNHS monitoring-well networks for the City of Waupaca, Wisc.

Well ID	Screen or piezometer ¹	Depth to water (ft)	TOC elevation (ft)	Total head (ft)	Screen elevation (ft, top)	Screen elevation (ft, bottom)	Vertical gradient ²
MW 1	A	13.73	843.9	830.17	828.9	818.9	–
	B	NT	843.9	NT	802.9	797.9	–
	C	NT	843.9	NT	778.9	768.9	–
MW 2	A	12.3	847.1	834.8	833.1	822.1	–
	B	12.3	847.1	834.8	812.1	797.1	0
	C	NT	847.1	NT	789.1	772.1	–
MW 3	A	14.1	849.02	834.92	839.02	824.02	–
	B	14	849.02	835.02	816.02	801.02	0.0125
	C	13.92	849.02	835.1	791.02	773.02	0.008
MW 4	A	13.08	846.08	833	836.08	821.08	–
	B	13.11	846.08	832.97	814.08	799.08	–0.0043
	C	13.77	846.08	832.31	789.08	771.08	–0.066
MW 5	A	NT	846.09	NT	826.09	821.09	–
	B	NT	846.09	NT	806.09	801.09	–
	C	NT	846.09	NT	782.09	772.09	–
MW 6	A	13.78	846.91	833.13	836.91	821.91	–
	B	13.77	846.91	833.14	811.91	796.91	0.001
	C	13.99	846.91	832.92	788.91	771.91	–0.0275
MW 7	A	13.8	846.33	832.53	836.33	821.33	–
	B	13.81	846.33	832.52	811.33	796.33	–0.001
	C	13.82	846.33	832.51	788.33	771.33	–0.00125
MW 8	A	15.15	845.32	830.17	835.32	820.32	–
	B	14.83	845.32	830.49	810.32	795.32	0.032
	C	14.33	845.32	830.99	787.32	770.32	0.0625
MW 9	A	15.23	845.29	830.06	845.29	825.29	–
MW 10	A	3.72	832.07	828.35	832.07	817.07	–
MW 11	A	8.62	843.49	834.87	843.49	828.49	–
MW 12	A	6.16	838.68	832.52	838.68	823.68	–

Abbreviations: ft = feet; ID = identification; MW = monitoring well; NT = measurement not taken; TOC = top of casing; USGS = U.S. Geological Survey; WGNHS = Wisconsin Geological and Natural History Survey.

¹A = shallow well; B = intermediate-depth piezometer; C = deep piezometer.

²Where values are positive, vertical gradients are upward.

Table A.5. Depth-to-water measurements collected July 23, 2019, from the USGS and WGNHS monitoring-well networks for the City of Waupaca, Wisc.

Well ID	Screen or piezometer	Depth to water (ft)	TOC elevation (ft)	Total head (ft)	Screen elevation (ft, top)	Screen elevation (ft, bottom)	Vertical gradient ²
MW 1	A	10.8	843.9	833.1	828.9	818.9	–
	B	NT	843.9	NT	802.9	797.9	–
	C	NT	843.9	NT	778.9	768.9	–
MW 2	A	11.73	847.1	835.37	833.1	822.1	–
	B	11.73	847.1	835.37	812.1	797.1	0
	C	NT	847.1	NT	789.1	772.1	–
MW 3	A	13.65	849.02	835.37	839.02	824.02	–
	B	13.54	849.02	835.48	816.02	801.02	0.01375
	C	13.29	849.02	835.73	791.02	773.02	0.025
MW 4	A	13	846.08	833.08	836.08	821.08	–
	B	13.4	846.08	832.68	814.08	799.08	–0.057
	C	13.6	846.08	832.48	789.08	771.08	–0.02
MW 5	A	NT	846.09	NT	826.09	821.09	–
	B	NT	846.09	NT	806.09	801.09	–
	C	NT	846.09	NT	782.09	772.09	–
MW 6	A	13.64	846.91	833.27	836.91	821.91	–
	B	13.62	846.91	833.29	811.91	796.91	0.002
	C	12.68	846.91	834.23	788.91	771.91	0.1175
MW 7	A	13.6	846.33	832.73	836.33	821.33	–
	B	13.35	846.33	832.98	811.33	796.33	0.025
	C	13.32	846.33	833.01	788.33	771.33	0.00375
MW 8	A	14.55	845.32	830.77	835.32	820.32	–
	B	13.34	845.32	831.98	810.32	795.32	0.121
	C	13.78	845.32	831.54	787.32	770.32	–0.055
MW 9	A	13.42	845.29	831.87	845.29	825.29	–
MW 10	A	3.9	832.07	828.17	832.07	817.07	–
MW 11	A	8.58	843.49	834.91	843.49	828.49	–
MW 12	A	6.2	838.68	832.48	838.68	823.68	–

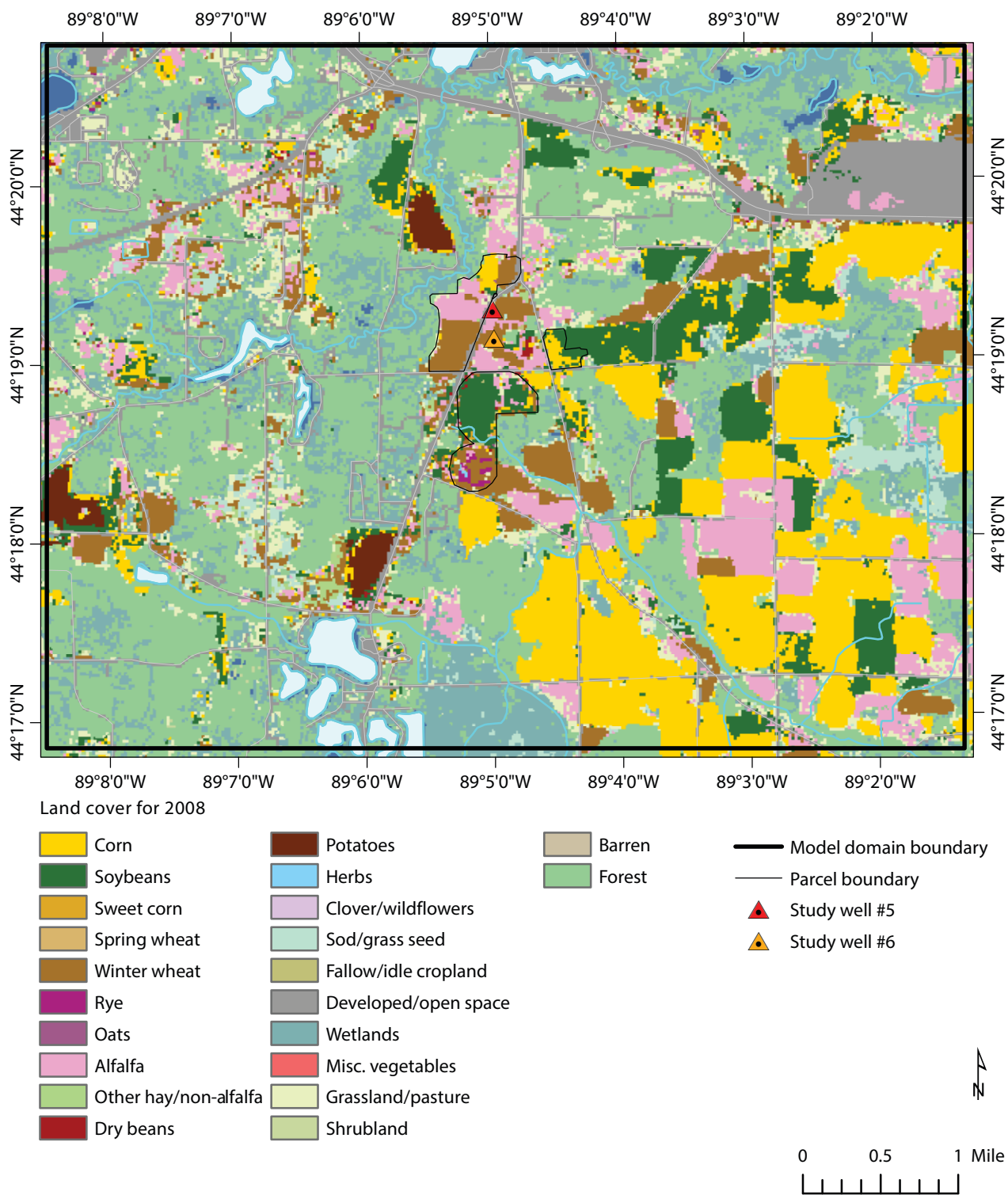
Abbreviations: ft = feet; ID = identification; MW = monitoring well; NT = measurement not taken; TOC = top of casing; USGS = U.S. Geological Survey; WGNHS = Wisconsin Geological and Natural History Survey.

¹A = shallow well; B = intermediate-depth piezometer; C = deep piezometer.

²Where values are positive, vertical gradients are upward.

Appendix B: Historical land-cover maps

Figure B.1. CropScape Data Layer covering the model domain for 2008 (National Agricultural Statistics Service, 2020).



Roads from U.S. Census Bureau, 2015. Hydrography from U.S. Geological Survey National Hydrography Dataset, 2016. Wisconsin Transverse Mercator projection, 1991 Adjustment to the North American Datum of 1983 (NAD 83/91); EPSG 3071.

Figure B.2. CropScape Data Layer covering the model domain for 2009 (National Agricultural Statistics Service, 2020).

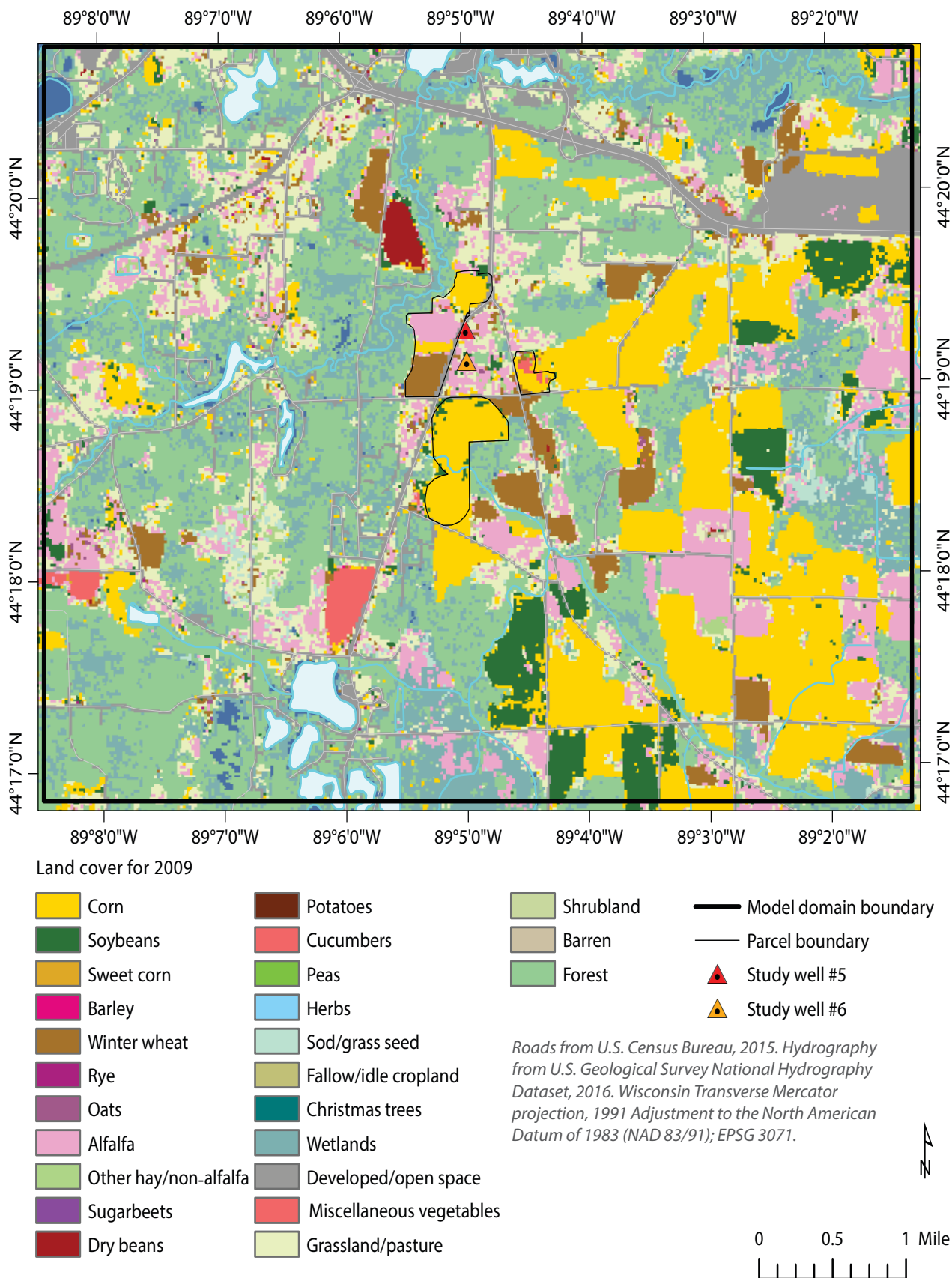
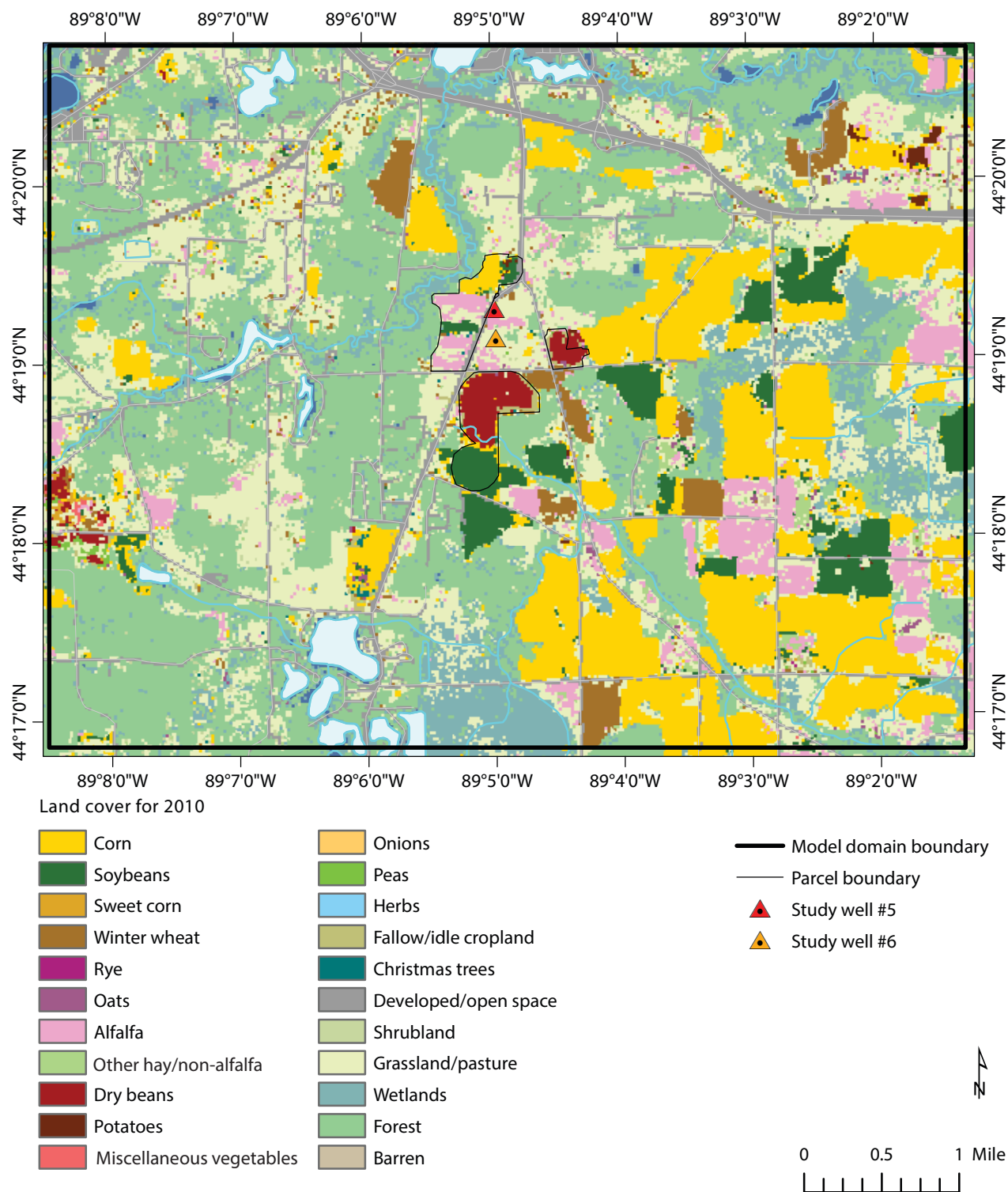
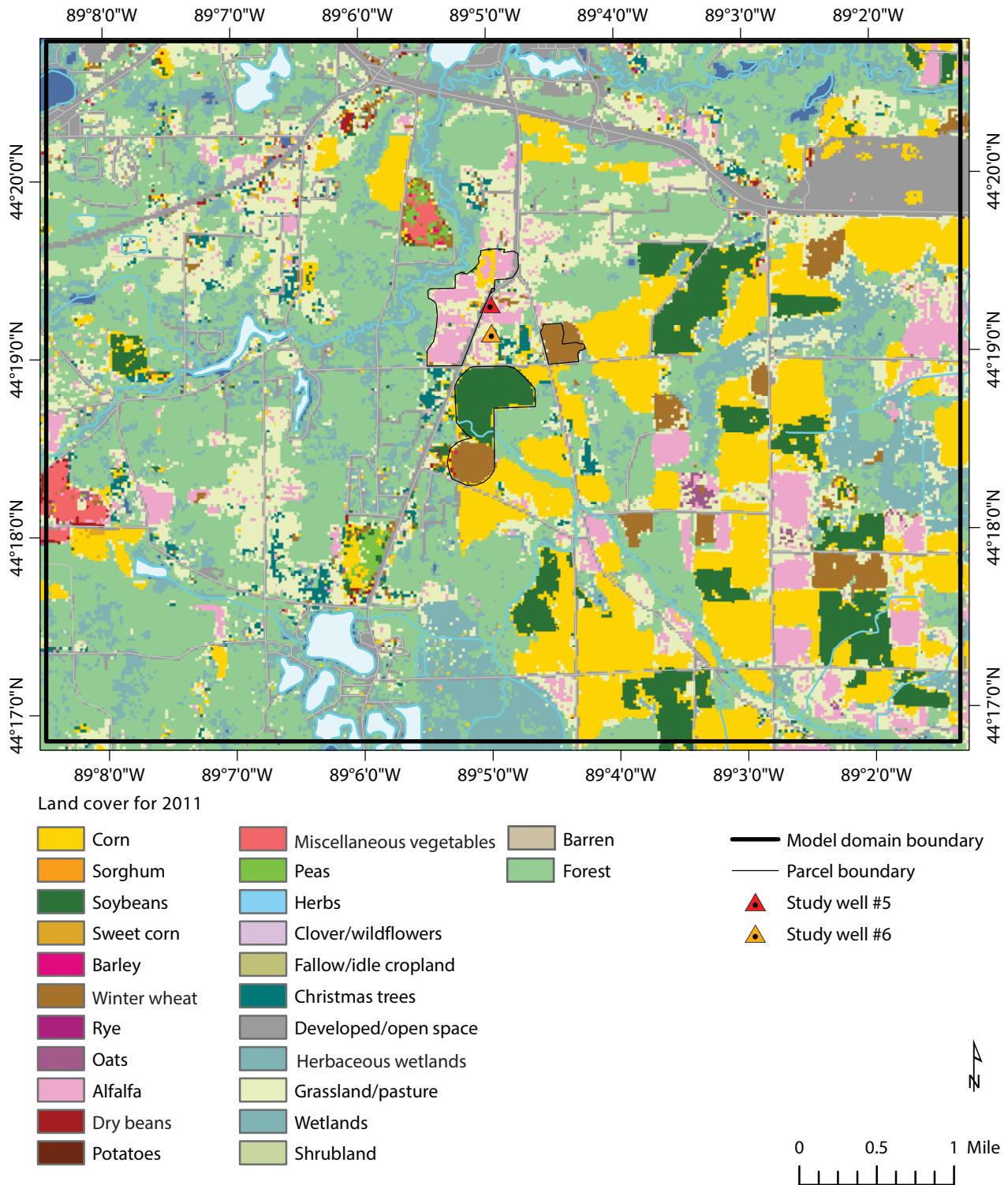


Figure B.3. CropScape Data Layer covering the model domain for 2010 (National Agricultural Statistics Service, 2020).



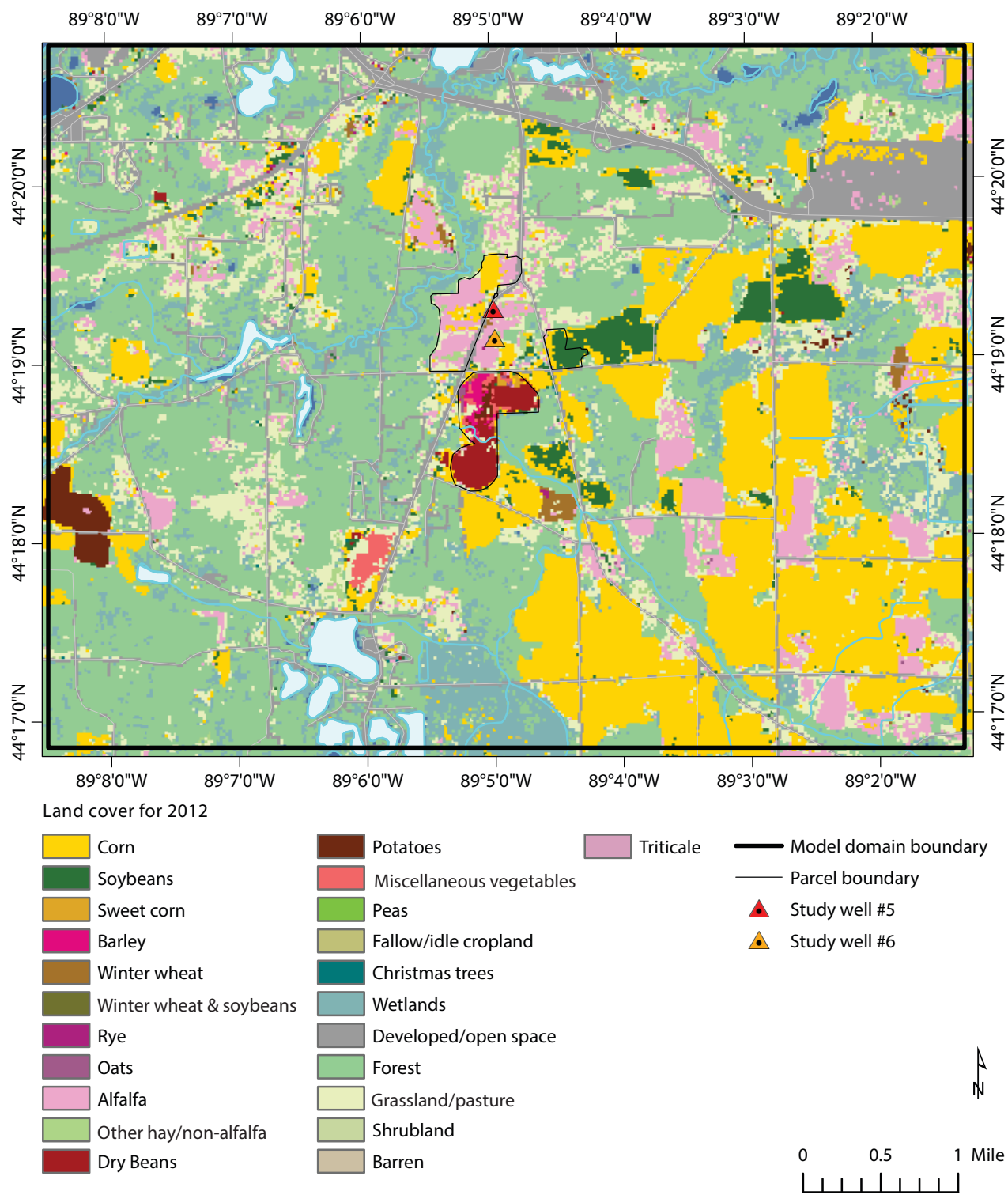
Roads from U.S. Census Bureau, 2015. Hydrography from U.S. Geological Survey National Hydrography Dataset, 2016. Wisconsin Transverse Mercator projection, 1991 Adjustment to the North American Datum of 1983 (NAD 83/91); EPSG 3071.

Figure B.4. CropScape Data Layer covering the model domain for 2011 (National Agricultural Statistics Service, 2020).



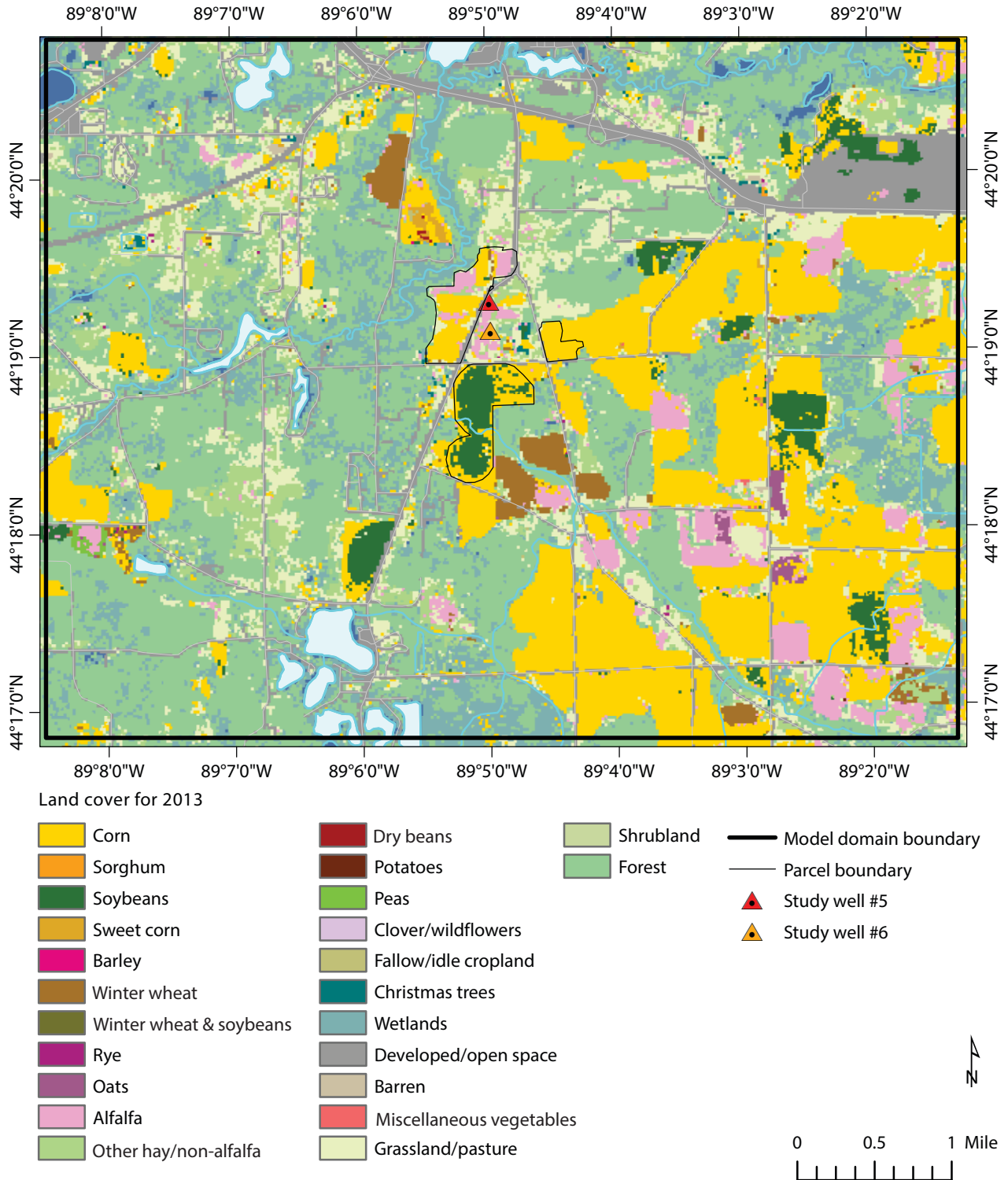
Roads from U.S. Census Bureau, 2015. Hydrography from U.S. Geological Survey National Hydrography Dataset, 2016. Wisconsin Transverse Mercator projection, 1991 Adjustment to the North American Datum of 1983 (NAD 83/91); EPSG 3071.

Figure B.5. CropScope Data Layer covering the model domain for 2012 (National Agricultural Statistics Service, 2020).



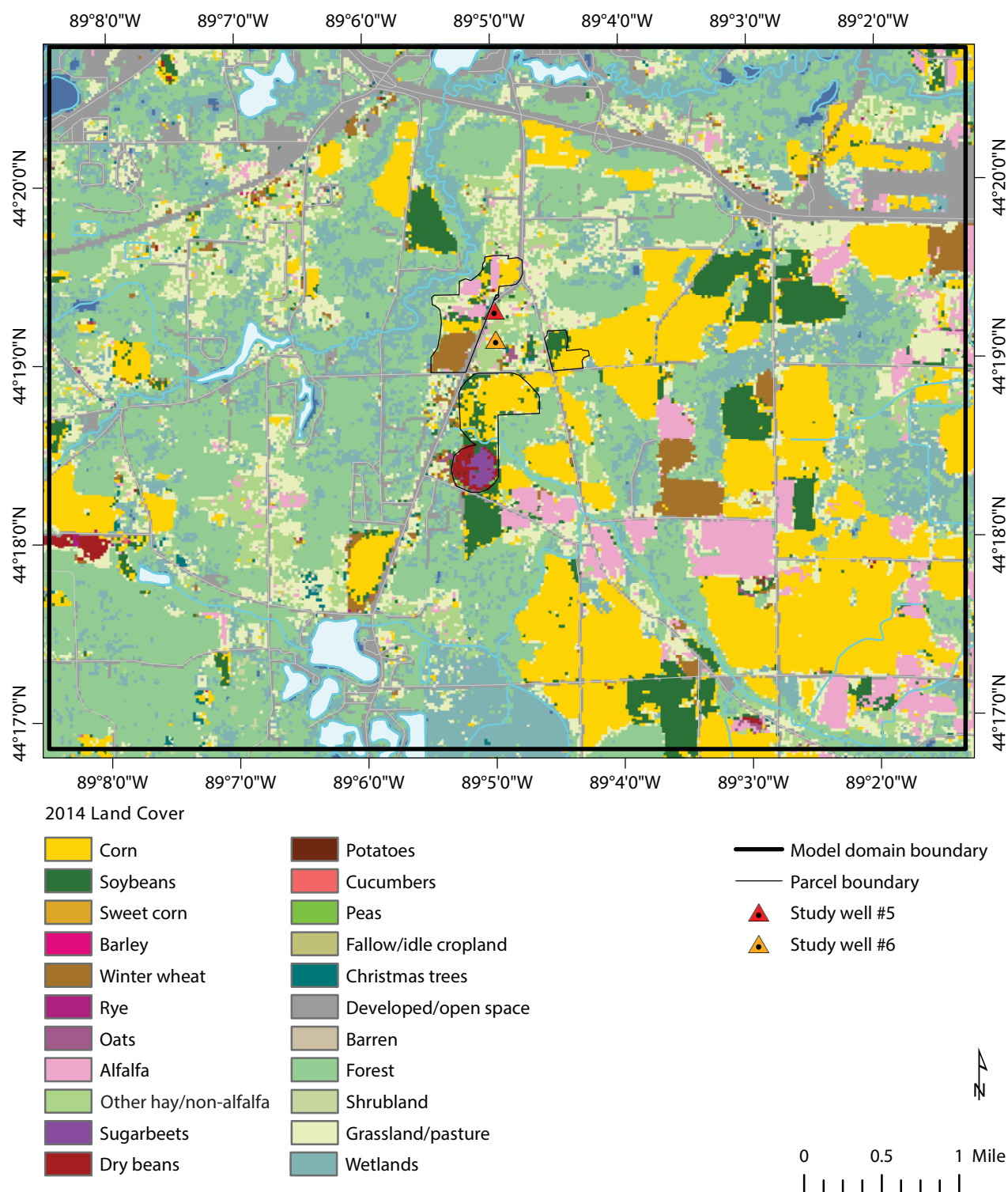
Projection: NAD83(HARN)/Wisconsin Transverse Mercator. Roads from U.S. Census Bureau, 2015. Hydrography from National Hydrography Dataset (U.S. Geological Survey, 2016).

Figure B.6. CropScape Data Layer covering the model domain for 2013 (National Agricultural Statistics Service, 2020).



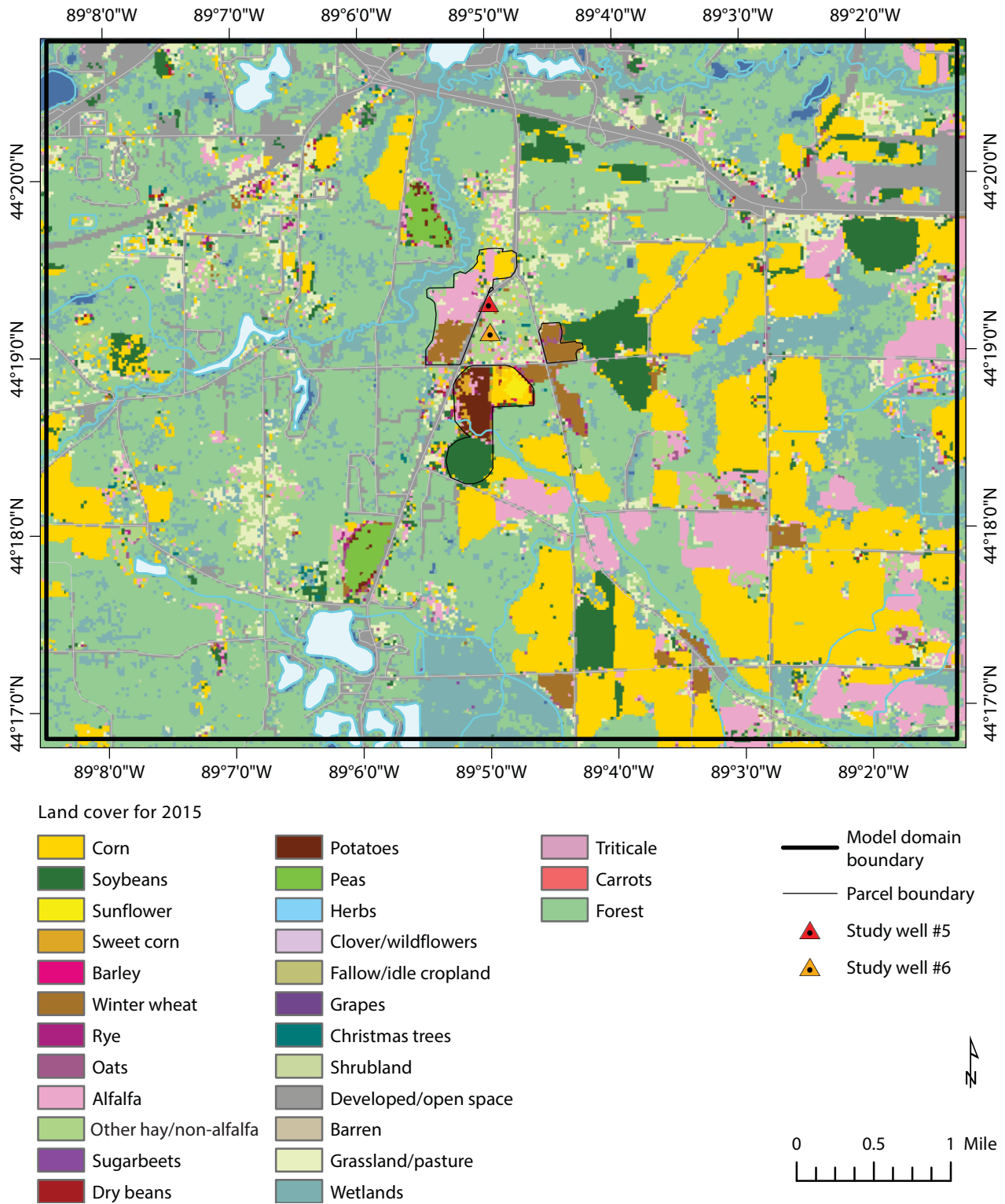
Roads from U.S. Census Bureau, 2015. Hydrography from U.S. Geological Survey National Hydrography Dataset, 2016. Wisconsin Transverse Mercator projection, 1991 Adjustment to the North American Datum of 1983 (NAD 83/91); EPSG 3071.

Figure B.7. CropScape Data Layer covering the model domain for 2014 (National Agricultural Statistics Service, 2020).



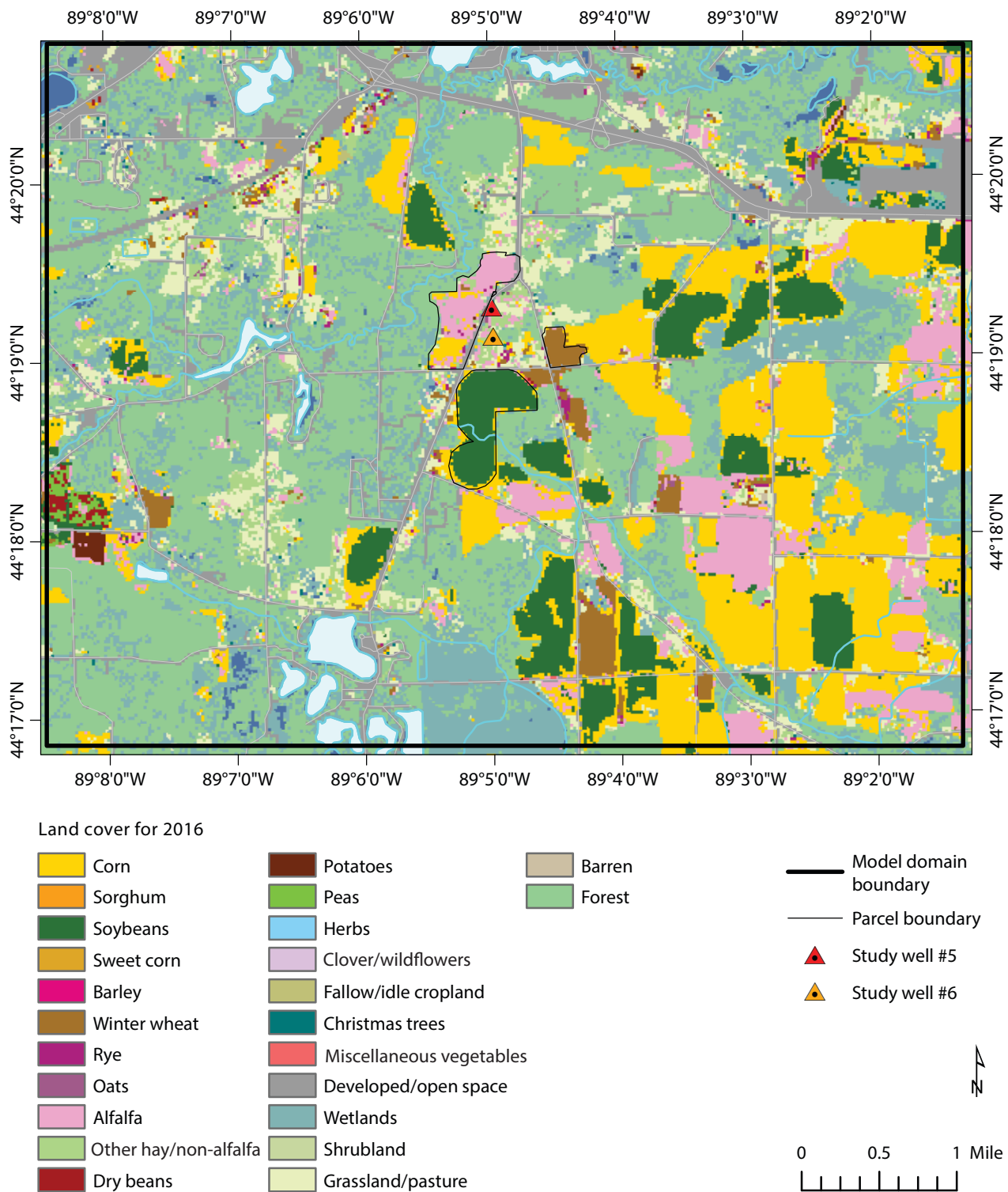
Roads from U.S. Census Bureau, 2015. Hydrography from U.S. Geological Survey National Hydrography Dataset, 2016. Wisconsin Transverse Mercator projection, 1991 Adjustment to the North American Datum of 1983 (NAD 83/91); EPSG 3071.

Figure B.8. CropScape Data Layer covering the model domain for 2015 (National Agricultural Statistics Service, 2020).



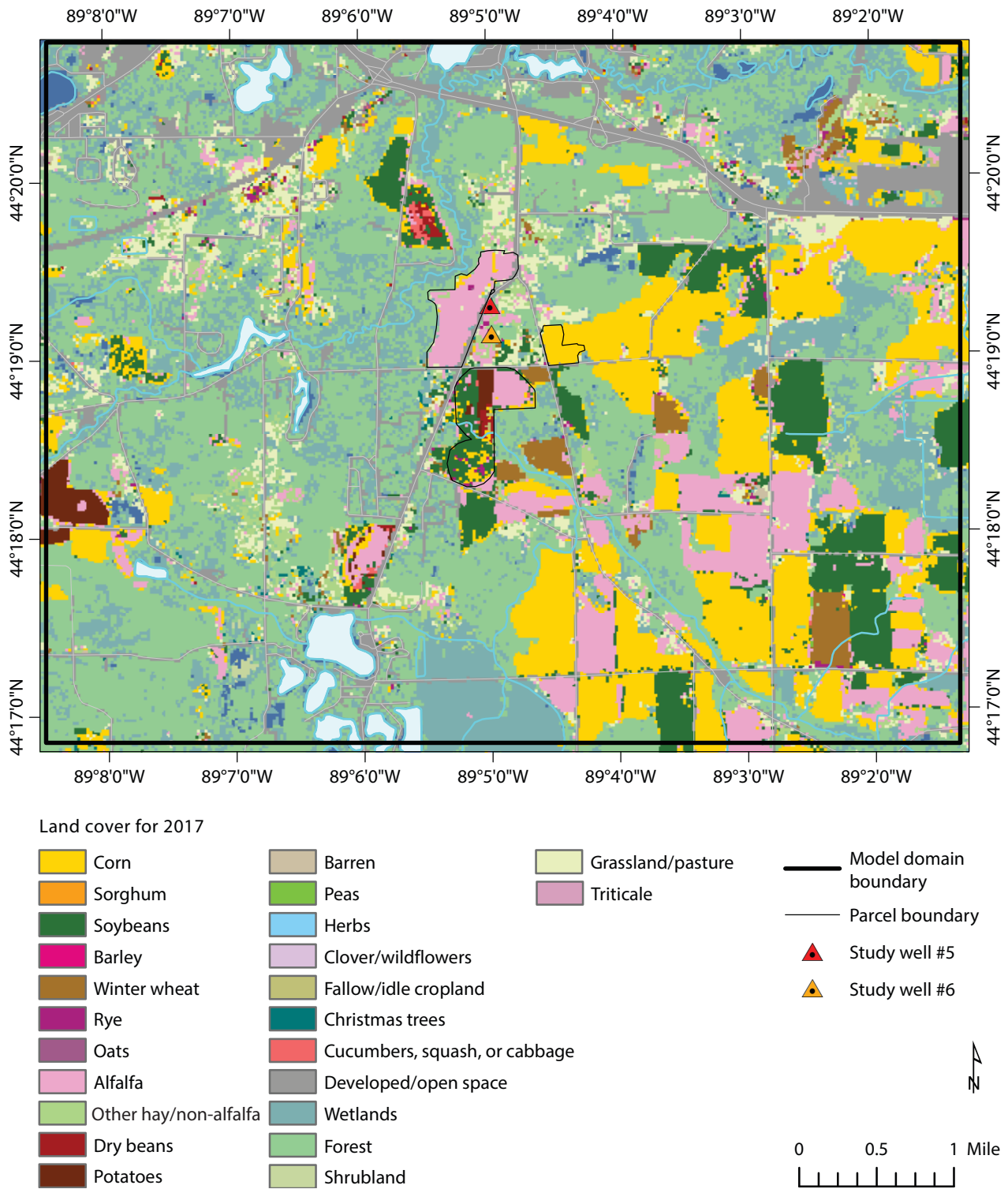
Roads from U.S. Census Bureau, 2015. Hydrography from U.S. Geological Survey National Hydrography Dataset, 2016. Wisconsin Transverse Mercator projection, 1991 Adjustment to the North American Datum of 1983 (NAD 83/91); EPSG 3071.

Figure B.9. CropScope Data Layer covering the model domain for 2016 (National Agricultural Statistics Service, 2020).



Roads from U.S. Census Bureau, 2015. Hydrography from U.S. Geological Survey National Hydrography Dataset, 2016. Wisconsin Transverse Mercator projection, 1991 Adjustment to the North American Datum of 1983 (NAD 83/91); EPSG 3071.

Figure B.10. CropScape Data Layer covering the model domain for 2017 (National Agricultural Statistics Service, 2020).



Roads from U.S. Census Bureau, 2015. Hydrography from U.S. Geological Survey National Hydrography Dataset, 2016. Wisconsin Transverse Mercator projection, 1991 Adjustment to the North American Datum of 1983 (NAD 83/91); EPSG 3071.

Appendix C: Streamflow data

Table C.1. Streamflow calibration targets for GFLOW.

Stream	Location	Source ¹	Streamflow (ft ³ /d)
Crystal River	Shadow Road (north), Waupaca, Wisc.	Field-measured	10,891,610
Crystal River	Shadow Road (south), Waupaca, Wisc.	Field-measured	10,368,648
Walla Walla Creek	Spencer Lake, Waupaca, Wisc.	Field-measured	157,524
Walla Walla Creek	Lind Center Road, Waupaca, Wisc.	Field-measured	157,524
Little Wolf River	Royalton, Wisc.	USGS 04080000	47,010,240
Wolf River	London, Wisc.	USGS 04079000	155,265,535
Waupaca River	Waupaca, Wisc.	USGS 04081000	20,752,848
Tomorrow River	Nelsonville, Wisc.	USGS 04080798	2,673,216

Abbreviations: ft³/d = cubic feet per day; USGS = U.S. Geological Survey.

¹USGS stream-gage numbers are provided.

Appendix D: Input data for monitoring-well method

Table D.1. Nitrate concentrations assigned to each parcel from 1994 to 2018 using a monitoring-well-based approach.

Year	Nitrate concentration (milligrams per liter)		
	Parcel 1	Parcel 2	Parcel 3
2018	11.2	14.2	14.2
2017	20.8	23.4	23.4
2016	15.5	22.9	22.9
2015	9.8	17.0	17.0
2014	4.0	11.0	11.0
2013	9.7	12.0	12.0
2012	6.6	9.1	9.1
2011	11.5	12.3	12.3
2010	13.0	19.0	19.0
2009	20.0	18.0	18.0
2008	16.0	12.0	12.0
2007	24.0	11.0	11.0
2006	23.0	14.0	14.0
2005	19.6	14.9	14.9
2004	19.6	14.9	14.9
2003	16.1	15.7	15.7
2002	16.5	16.1	16.1
2001	17.1	14.6	14.6
2000	24.7	9.7	9.7
1999	11.9	9.0	9.0
1998	11.8	9.5	9.5
1997	7.9	9.8	9.8
1996	12.1	14.6	14.6
1995	14.4	15.2	15.2
1994	NA	7.2	7.2

Abbreviation: NA = Not available.

Appendix E: Input data for land-cover method

Table E.1. Land cover and area-weighted nitrate concentrations for parcel 1 from 2008 to 2018.

Year	Parcel 1 land-cover (percent of total area)						
	Alfalfa	Corn	Dry beans	Soybeans	Pasture	Residential	Total
2008	73	13	0	0	11	3	100
2009	61	25	0	0	11	3	100
2010	55	31	0	0	11	3	100
2011	73	13	0	0	11	3	100
2012	73	13	0	0	11	3	100
2013	18	68	0	0	11	3	100
2014	41	45	0	0	11	3	100
2015	66	20	0	0	11	3	100
2016	56	30	0	0	11	3	100
2017	75	11	0	0	11	3	100
2018	50	36	0	0	11	3	100

Year	Parcel 1 area-weighted nitrate concentration (milligrams per liter)						
	Alfalfa	Corn	Dry beans	Soybeans	Pasture	Residential	Total
2008	7.32	3.09	0.00	0.00	3.90	0.05	14.36
2009	6.11	5.99	0.00	0.00	3.90	0.05	16.06
2010	5.48	7.50	0.00	0.00	3.90	0.05	16.94
2011	7.32	3.09	0.00	0.00	3.90	0.05	14.36
2012	7.32	3.09	0.00	0.00	3.90	0.05	14.36
2013	1.84	16.25	0.00	0.00	3.90	0.05	22.04
2014	4.12	10.78	0.00	0.00	3.90	0.05	18.85
2015	6.62	4.77	0.00	0.00	3.90	0.05	15.34
2016	5.63	7.15	0.00	0.00	3.90	0.05	16.73
2017	7.47	2.74	0.00	0.00	3.90	0.05	14.16
2018	4.96	8.75	0.00	0.00	3.90	0.05	17.67

Table E.2. Land cover and area-weighted nitrate concentrations for parcel 2 from 2008 to 2018.

Year	Parcel 2 land cover (percent of total area)						
	Alfalfa	Corn	Dry beans	Soybeans	Pasture	Residential	Total
2008	30	0	0	70	0	0	100
2009	0	100	0	0	0	0	100
2010	0	0	70	30	0	0	100
2011	0	30	0	70	0	0	100
2012	0	0	100	0	0	0	100
2013	0	25	0	75	0	0	100
2014	0	70	30	0	0	0	100
2015	45	25	0	30	0	0	100
2016	0	0	0	100	0	0	100
2017	0	0	0	100	0	0	100
2018	0	0	0	100	0	0	100

Year	Parcel 2 area-weighted nitrate concentration (milligrams per liter)						
	Alfalfa	Corn	Dry beans	Soybeans	Pasture	Residential	Total
2008	1.21	0.00	0.00	14.22	0.00	0.00	15.44
2009	0.00	20.00	0.00	0.00	0.00	0.00	20.00
2010	0.00	0.00	6.35	6.18	0.00	0.00	12.52
2011	0.00	6.05	0.00	14.22	0.00	0.00	20.28
2012	0.00	0.00	9.10	0.00	0.00	0.00	9.10
2013	0.00	5.00	0.00	15.30	0.00	0.00	20.30
2014	0.00	13.95	2.75	0.00	0.00	0.00	16.70
2015	1.79	5.00	0.00	6.18	0.00	0.00	12.96
2016	0.00	0.00	0.00	20.40	0.00	0.00	20.40
2017	0.00	0.00	0.00	20.40	0.00	0.00	20.40
2018	0.00	0.00	0.00	20.40	0.00	0.00	20.40

Table E.3. Land cover and area-weighted nitrate concentrations for parcel 3 from 2008 to 2018.

Year	Parcel 3 land cover (percent of total area)						Total
	Alfalfa	Corn	Dry beans	Soybeans	Pasture	Residential	
2008	0	100	0	0	0	0	100
2009	0	100	0	0	0	0	100
2010	0	0	100	0	0	0	100
2011	0	100	0	0	0	0	100
2012	0	0	0	100	0	0	100
2013	0	100	0	0	0	0	100
2014	0	100	0	0	0	0	100
2015	100	0	0	0	0	0	100
2016	0	100	0	0	0	0	100
2017	0	0	0	100	0	0	100
2018	0	0	0	100	0	0	100

Year	Parcel 3 weighted nitrate concentration (milligrams per liter)						Total
	Alfalfa	Corn	Dry beans	Soybeans	Pasture	Residential	
2008	0.00	20.00	0.00	0.00	0.00	0.00	20.00
2009	0.00	20.00	0.00	0.00	0.00	0.00	20.00
2010	0.00	0.00	9.10	0.00	0.00	0.00	9.10
2011	0.00	20.00	0.00	0.00	0.00	0.00	20.00
2012	0.00	0.00	0.00	20.40	0.00	0.00	20.40
2013	0.00	20.00	0.00	0.00	0.00	0.00	20.00
2014	0.00	20.00	0.00	0.00	0.00	0.00	20.00
2015	4.00	0.00	0.00	0.00	0.00	0.00	4.00
2016	0.00	20.00	0.00	0.00	0.00	0.00	20.00
2017	0.00	0.00	0.00	20.40	0.00	0.00	20.40
2018	0.00	0.00	0.00	20.40	0.00	0.00	20.40

Table E.4. Nitrate concentrations assigned to each parcel from 1994 to 2018 using a land-use approach.

Year ¹	Nitrate concentration (milligrams per liter)		
	Parcel 1	Parcel 2	Parcel 3
2018	17.7	20.4	20.4
2017	14.2	20.4	20.4
2016	16.7	20.4	20.0
2015	15.3	13.0	4.0
2014	18.9	16.7	20.0
2013	22.0	20.3	20.0
2012	14.4	9.1	9.1
2011	14.4	20.3	20.0
2010	16.9	12.5	9.1
2009	16.1	20.0	20.0
2008	14.4	15.4	20.0
2007	24.0	11.0	11.0
2006	23.0	14.0	14.0
2005	19.6	14.9	14.9
2004	19.6	14.9	14.9
2003	16.1	15.7	15.7
2002	16.5	16.1	16.1
2001	17.1	14.6	14.6
2000	24.7	9.7	9.7
1999	11.9	9.0	9.0
1998	11.8	9.5	9.5
1997	7.9	9.8	9.8
1996	12.1	14.6	14.6
1995	14.4	15.2	15.2
1994	NA	7.2	7.2

Abbreviation: NA = not available.

¹Land-cover data were not available before 2008, so monitoring-well values were substituted for earlier water years.



Published by and available from:

Wisconsin Geological and Natural History Survey

3817 Mineral Point Road ■ Madison, Wisconsin 53705-5100

608.263.7389 ■ www.WisconsinGeologicalSurvey.org

Kenneth R. Bradbury, Director and State Geologist



**Wisconsin Geological
and Natural History Survey**

DIVISION OF EXTENSION

UNIVERSITY OF WISCONSIN-MADISON

This report is an interpretation of the data available at the time of preparation. Every reasonable effort has been made to ensure that this interpretation conforms to sound scientific principles; however, the report should not be used to guide site-specific decisions without verification. Proper use of the report is the sole responsibility of the user.

The use of company names in this document does not imply endorsement by the Wisconsin Geological and Natural History Survey.

ISSN: 2159-9351

University of Wisconsin–Madison Division of Extension, in cooperation with the U.S. Department of Agriculture and Wisconsin counties, publishes this information to further the purpose of the May 8 and June 30, 1914, Acts of Congress. An EEO/AA employer, the University of Wisconsin–Madison provides equal opportunities in employment and programming, including Title VI, Title IX, and ADA requirements. If you have a disability and require this information in an alternative format, contact the Wisconsin Geological and Natural History Survey at 608-262-1705 (711 for Wisconsin Relay).

Our Mission

The Survey conducts earth-science surveys, field studies, and research. We provide objective scientific information about the geology, mineral resources, water resources, soil, and biology of Wisconsin. We collect, interpret, disseminate, and archive natural resource information. We communicate the results of our activities through publications, technical talks, and responses to inquiries from the public. These activities support informed decision making by government, industry, business, and individual citizens of Wisconsin.